AD-A257 330

②

# NAVAL POSTGRADUATE SCHOOL
## Monterey, California

# THESIS

ANALYSIS OF SHIP TRACKS
IN CLOUDINESS TRANSITION REGIONS

by

Michael E. Evans

September, 1992

Thesis Advisor:                                        Philip A. Durkee

92-29898

92 11 20 004

# REPORT DOCUMENTATION PAGE

| 1a. REPORT SECURITY CLASSIFICATION<br>Unclassified | 1b. RESTRICTIVE MARKINGS |
|---|---|
| 2a. SECURITY CLASSIFICATION AUTHORITY | 3. DISTRIBUTION/AVAILABILITY OF REPORT<br>Approved for public release; distribution is unlimited. |
| 2b. DECLASSIFICATION/DOWNGRADING SCHEDULE | |

| 4. PERFORMING ORGANIZATION REPORT NUMBER(S) | 5. MONITORING ORGANIZATION REPORT NUMBER(S) |
|---|---|

| 6a. NAME OF PERFORMING ORGANIZATION<br>Naval Postgraduate School | 6b. OFFICE SYMBOL<br>(If applicable)<br>35 | 7a. NAME OF MONITORING ORGANIZATION<br>Naval Postgraduate School |
|---|---|---|
| 6c. ADDRESS (City, State, and ZIP Code)<br>Monterey, CA 93943-5000 | | 7b. ADDRESS (City, State, and ZIP Code)<br>Monterey, CA 93943-5000 |
| 8a. NAME OF FUNDING/SPONSORING<br>ORGANIZATION | 8b. OFFICE SYMBOL<br>(If applicable) | 9. PROCUREMENT INSTRUMENT IDENTIFICATION NUMBER |

| 8c. ADDRESS (City, State, and ZIP Code) | 10. SOURCE OF FUNDING NUMBERS | | | |
|---|---|---|---|---|
| | Program Element No. | Project No. | Task No. | Work Unit Accession Number |

11. TITLE (Include Security Classification)
Analysis of Ship Tracks in Cloudiness Transition Regions

12. PERSONAL AUTHOR(S)  Michael E. Evans

| 13a. TYPE OF REPORT<br>Master's Thesis | 13b. TIME COVERED<br>From       To | 14. DATE OF REPORT (year, month, day)<br>September 1992 | 15. PAGE COUNT<br>102 |
|---|---|---|---|

16. SUPPLEMENTARY NOTATION
The views expressed in this thesis are those of the author and do not reflect the official policy or position of the Department of Defense or the U.S. Government.

| 17. COSATI CODES | | | 18. SUBJECT TERMS (continue on reverse if necessary and identify by block number) |
|---|---|---|---|
| FIELD | GROUP | SUBGROUP | ship track, algorithm, AVHRR, albedo |
| | | | |

19. ABSTRACT (continue on reverse if necessary and identify by block number)

The radiative and spatial characteristics of 63 ship tracks are analyzed in cloudiness transition regions using AVHRR satellite data. Channels 1, 2, 3, 4 and 5 are utilized to determine the variations in ship track albedo and temperature in three distinct cloud environments: stratus, broken stratus, and cumulus. Stratus Tracks in a stratus environment are brightest with respect to broken stratus and cumulus tracks. Cumulus tracks have the highest percentage increase in albedo over their environment in Channel 1, while broken stratus tracks have the highest percentage change over their environment in Channel 3. There is little temperature difference between the ambient cloud and ship track in all three environments. Stratus tracks tend to be longer than either broken stratus or cumulus tracks. No significant variation in track width was observed between environments.

| 20. DISTRIBUTION/AVAILABILITY OF ABSTRACT<br>☐ UNCLASSIFIED/UNLIMITED ☐ SAME AS REPORT ☐ DTIC USERS | 21. ABSTRACT SECURITY CLASSIFICATION<br>Unclassified | |
|---|---|---|
| 22a. NAME OF RESPONSIBLE INDIVIDUAL<br>Philip A. Durkee | 22b. TELEPHONE (Include Area code)<br>(408) 646-3465 | 22c. OFFICE SYMBOL<br>MR/De |

**DD FORM 1473, 84 MAR**   83 APR edition may be used until exhausted   SECURITY CLASSIFICATION OF THIS PAGE
All other editions are obsolete   Unclassified

Analysis of Ship Tracks
in Cloudiness Transition Regions

by

Michael E. Evans
Lieutenant, United States Navy
B.A., Memphis State University, 1982

Submitted in partial fulfillment
of the requirements for the degree of

MASTER OF SCIENCE IN METEOROLOGY AND PHYSICAL OCEANOGRAPHY

from the

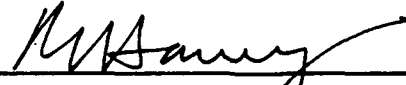NAVAL POSTGRADUATE SCHOOL
September, 1992

Author: _____
Michael E. Evans

Approved by: _____
Philip A. Durkee, Thesis Advisor

_____
Carlyle H. Wash, Second Reader

_____
Robert L. Haney, Chairman
Department of Meteorology

ii

# ABSTRACT

The radiative and spatial characteristics of 63 ship tracks are analyzed in cloudiness transition regions using AVHRR satellite data. Channels 1, 2, 3, 4 and 5 are utilized to determine the variations in ship track albebo and temperature in three distinct cloud environments: stratus, broken stratus and cumulus. Stratus Tracks in a stratus environment are brightest with respect to broken stratus and cumulus tracks. Cumulus tracks have the highest percentage increase in albedo over their environment in Channel 1, while broken stratus tracks have the highest percentage change over their environment in Channel 3. There is little temperature difference between the ambient cloud and ship track in all three environments. Stratus track tend to be longer than either broken stratus or cumulus tracks. No significant difference in the width of the track was observed between the environments.

DTIC QUALITY INSPECTED 4

| Accession For | | |
|---|---|---|
| NTIS CRA&I | | ☒ |
| DTIC TAB | | ☐ |
| Unannounced | | ☐ |
| Justification | | |
| By | | |
| Distribution / | | |
| Availability Codes | | |
| Dist | Avail and / or Special | |
| A-1 | | |

iii

# TABLE OF CONTENTS

## LIST OF TABLES

## ACKNOWLEDGEMENTS

# I.  INTRODUCTION

## A.  OVERVIEW

Ship tracks have been observed in satellite imagery for many years. In the mid 1960's Conover (1966) described "anomalous cloud lines" and attributed their formation to passing ships. However, it is only in recent years that research efforts have been directed towards explaining the atmospheric conditions responsible and cloud physics required for ship track formation. These research results have many applications ranging from the effect of anthropogenic aerosols clouds, which contributes to our understanding of the global climate, to intelligence applications, which focus on tracking and classifying ships based their signature in the ambient cloud field. Ship tracks form in a wide variety of marine stratiform clouds, transitioning from uniform solid stratus, broken stratus to open-celled cumulus. Each of these cloud types have unique formation processes, micro-physical properties and radiative characteristics.  Since ship tracks have not been observed in completely clear air regions it is apparent that a link exists between the formation conditions necessary for stratiform clouds and those of ship tracks. This link will be investigated by describing the spatial and

1

radiative characteristics of the ship tracks which form in marine stratiform clouds, specifically the cloud forms associated with transitional regions between broken or partial cloud and solid stratiform cloud decks. The purpose of this study is to determine if the observed variations in the cloud forms found in these transition regions are reflected in the ship tracks which form in them.

## B. BACKGROUND

### 1. Ship Tracks

Ship tracks are formed primarily during the summer months in the low stratus and stratocumulus clouds of eastern ocean basins. Current theory suggests they are the direct result of a ship passing under a stratiform cloud and either modifying the existing cloud or creating new cloud by expelling exhaust gases into the saturated marine boundary layer. These gases contain heat, moisture and combustion particles, the last of which serve as cloud condensation nuclei (CCN) for water droplets. The injection of additional CCN into the stratiform cloud deck, by direct means or by gas-to-particle conversion of the exhaust gases (Hobbs, et al,1980), creates cloud droplets with much smaller radii than those found in the adjacent cloud. Since the concentration and size of cloud droplets is determined primarily by the

2

concentration of CCN in the air (Radke, et al 1989), any increase in the number of CCN or decrease in cloud drop radii, changes the micro-physical characteristics of the cloud. This shift in cloud drop properties changes the reflectivity of the modified cloud making it readily discernable at certain wavelengths in satellite imagery. A comparison of the radiance in the NOAA-10 Advanced Very High Resolution Radiometer (AVHRR) near infrared channel 3, centered at 3.7 $\mu$m, with the visible channel 1, centered at .63 $\mu$m, clearly reveals these features, Figure 1.

Additionally, the buoyancy flux generated by the temperature difference between the exhaust gases and atmosphere enhances mixing. This buoyancy flux induced mixing in concert with the small-scale vortex created by the ship motion may initiate and further amplify the ship track cloud formation process by introducing marine aerosols from the surface of the ocean into the well mixed marine boundary layer (Figure 2). Continuing gas-to-particle conversion of the exhaust plume coupled with the tendency for smaller droplets to remain in the cloud longer helps explain the longevity of these tracks. A more detailed discussion of proposed formation mechanisms and the radiative signature of ship tracks is provided by Hindman, 1990 and Coakley, et al., 1987, respectively.
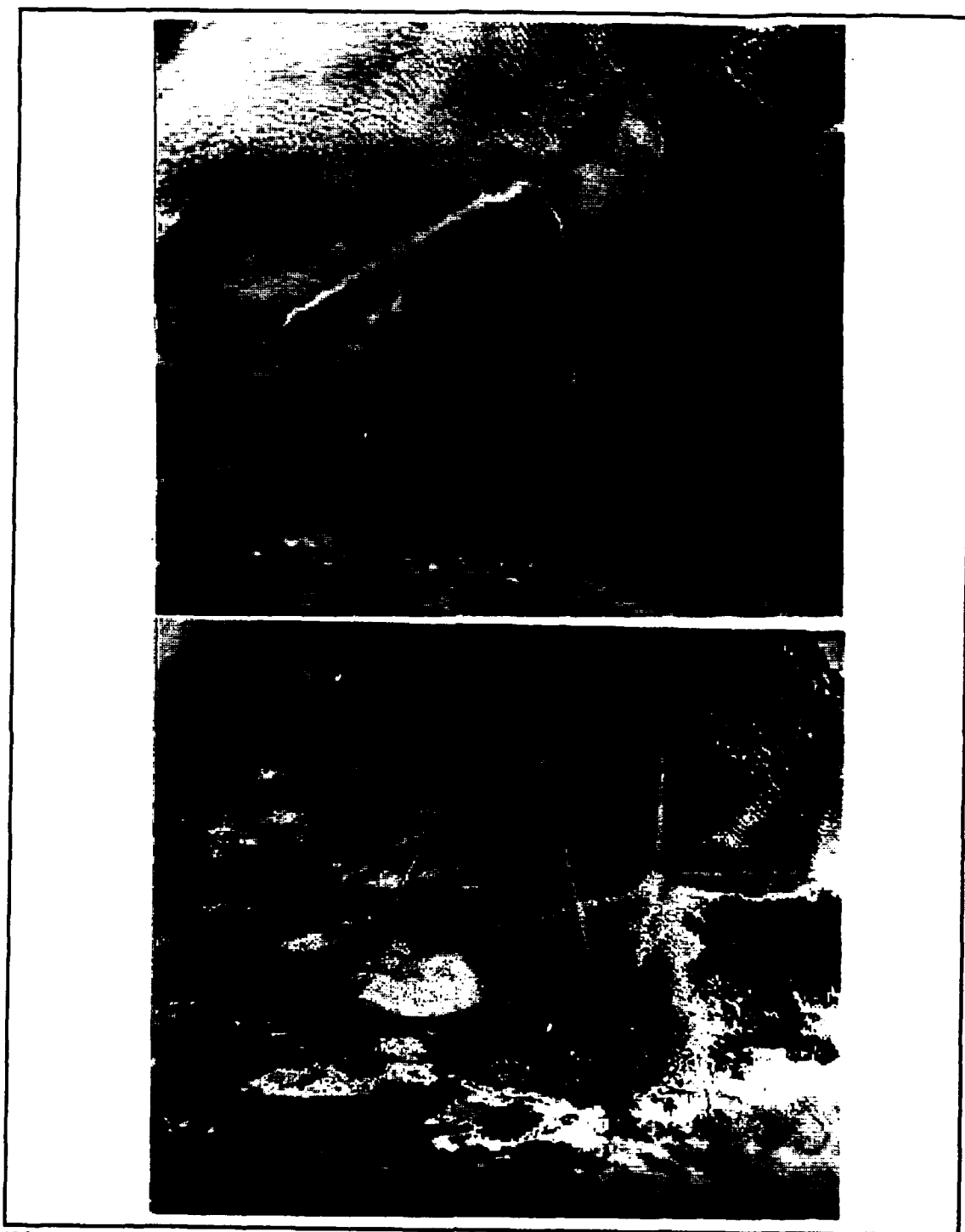
3

Figure 1. Ship Tracks in Satellite Imagery at .63 μm, (top), and 3.7 μm, (bottom).
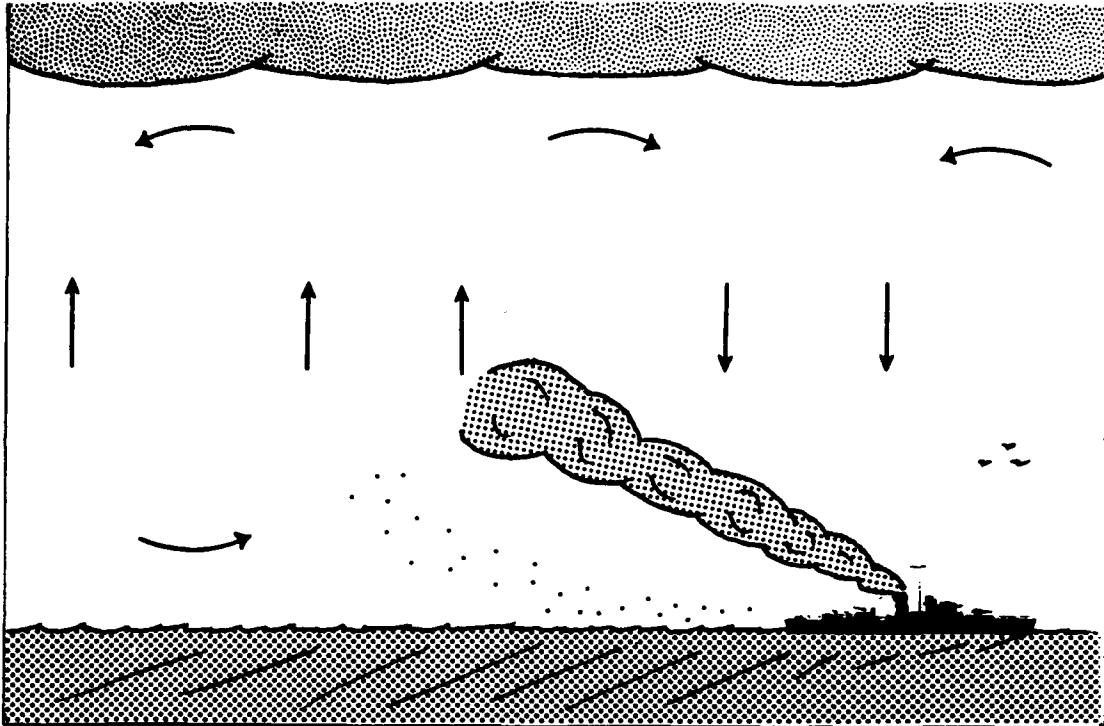
**Figure 2.** Introduction of Anthropogenic and Marine Aerosols into the Well-mixed Marine Boundary Layer by Small-scale Ship-passage Induced Mixing.

## 2. Marine Stratiform Clouds

Marine stratiform clouds and their associated environments have been the focus of numerous research efforts in recent years because of their impact on the planet's albedo and global climate. The physical mechanisms which control the formation of these clouds are generally explained, but the in-

cloud mechanisms responsible for their modification, breakup and dissipation are not as well understood.

Certain atmospheric conditions must be present for stratiform clouds to develop. In general, stratus and stratocumulus clouds form in the summer in the eastern oceans when the subtropical high is fully developed. Strong subsidence, associated with the subtropical high creates a strong temperature inversion over the entire region which keeps the moisture confined near the surface (Brost et al, 1982). Northerly winds along the coast cause the upwelling of deeper, colder ocean water that cools the marine boundary layer to saturation. This provides an ideal environment for the formation of statiform clouds.

Synoptically, this inversion slopes from east to west with the strong, low inversion in the east near the coast and the weak, higher inversion to the west. This occurs on a scale comparable to the region between California and Hawaii in the eastern Pacific Ocean. Associated with this sloping and weakening inversion is a corresponding transition in the cloud types from low stratiform clouds in the east to cumuliform clouds in the west.

On the mesoscale, the reverse has been observed. Betts and Boers (1990) and Paluch and Lenschow (1991) observed that cloudiness transition regions exist in the marine boundary layer off the west coast of southern California. They are characterized by a gradual change from a clear boundary layer through small cumulus and broken stratocumulus to a deck of solid stratocumulus (Betts and Boers, 1990). Within these cloudiness transition regions the inversion height changes from weaker and somewhat lower (950 mb) in the cloud free region to relatively stronger and higher (935 mb) in the solid stratus clouds (Figure 3).

Both Cahalan and Snider (1989) and Paluch and Lenschow (1991) noted increases in the liquid water content (LWC), mixing ratio and vertical motion moving from clear air to solid stratiform clouds in similar transition regions. These variations manifest themselves as changes in the radiative signatures of the clouds.

The structure of the clouds depends largely on the environment in which they form. Uniform stratus is characterized by a fairly flat top surface which reflects the presence of a very strong inversion which suppresses vertical motion at the cloud top. A fairly new cloud will have a nearly
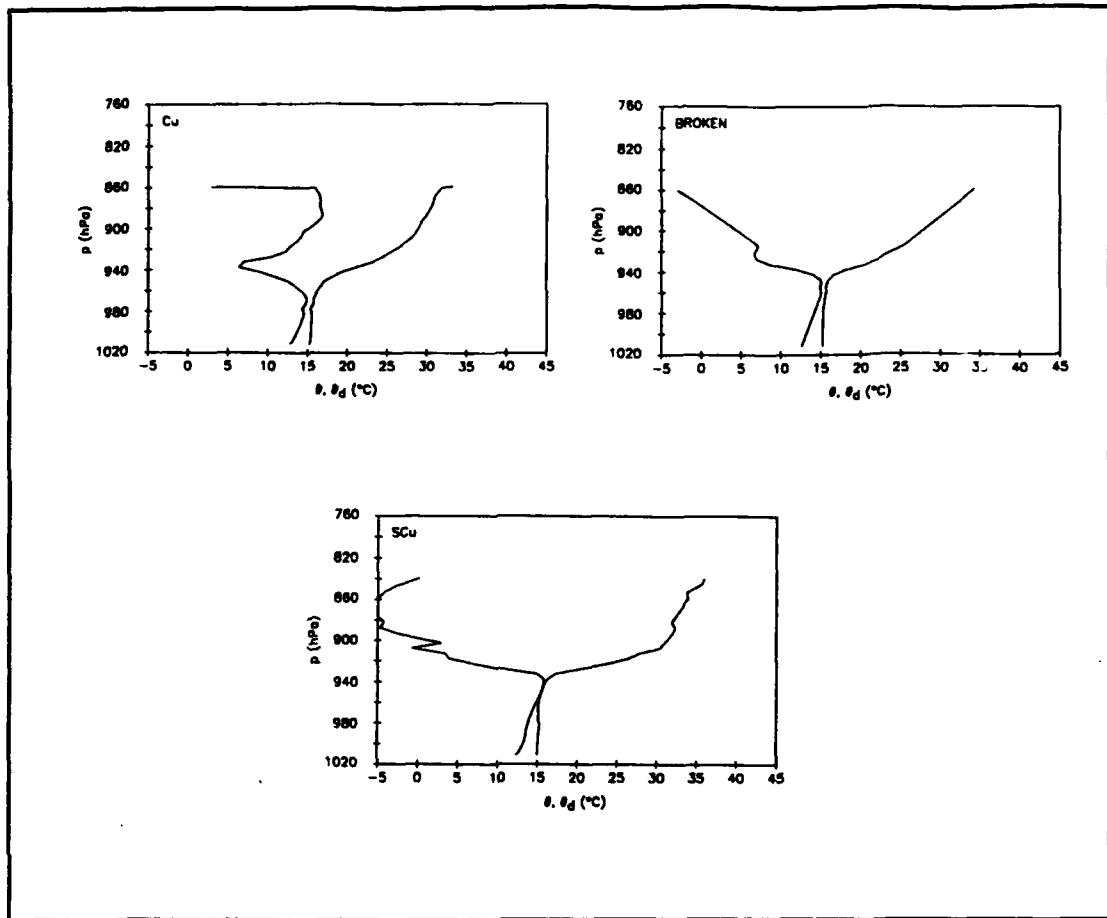
**Figure 3.** Mean Profiles for Three Regimes: Cumulus, Broken, and Stratus Clouds (Betts and Boers, 1990).

homogenous internal structure having not been subjected to differential heat fluxes from both the surface and from above. As the cloud gets older and thicker through mixing, entrainment and a variety of heat fluxes, its texture changes. Differential heating allows vertical plumes to penetrate the inversion and distort the top of the cloud. As a result it is transformed into a solid field of symmetric cellular clouds. In the presence of surface winds speeds greater than 10 ms$^{-1}$

this same cloud field can be modified into cloud streets which align themselves parallel to the wind direction. These cloud streets consist of the same cellular cloud field but they are elongated by the wind. A secondary roll circulation can form within the cloud. In between the cloud streets subsidence from the secondary circulation creates a variegated cloud top appearance. Further entrainment and heat fluxes can cause the solid cloud deck to break up producing a cloud field with a broken or patchy appearance. If the cloud layer reaches the precipitation stage, evaporation of the precipitation moistens and cools the air below. Eventually this causes cumuli to form below the stratus deck. In time the stratus clouds can dissipate due to further entrainment leaving behind only the cumulus clouds (Paluch and Lenschow, 1991). This cloud type can be modified by the ship or provide a suitable environment for the production of new cloud line.

## C. THESIS OBJECTIVE

The objective of this study is to observe and describe the spatial and radiative variations of ship tracks that form in the clouds associated with transition regions. Chapter II will outline the approach of the study and describe the data collection and analysis. Chapter III will discuss the results

and Chapter IV will present the conclusions and make recommendations for future study.

## II. APPROACH

### A. OVERVIEW

The studies noted earlier clearly indicate variations in the liquid water content, vertical velocity, and inversion height in the ambient clouds associated with cloudiness transition regions (CTR). The focus of this study is to locate ship tracks that transit these regions and describe their radiative and spatial characteristics as a function of the surrounding regime. For the purpose of this study the ambient clouds associated with CTR's are divided into cumulus, broken stratocumulus, and solid stratus similar to the method utilized by Betts and Boers, 1990. Since in situ measurements of liquid water content, vertical velocity and inversion height are not available for study, mean quantities for each cloud type will be based on the data collected in previous studies of marine stratiform clouds by Brost et al, 1982. These values will be utilized to characterize the CTR environments and provide some insight into the physical mechanisms responsible for ship track formation.

## B. DATA

The data utilized in this study are from the Advanced Very High Resolution Radiometer (AVHRR) onboard the NOAA-9/10 satellites. These satellites are in a polar orbit approximately 850 kilometers above the earth's surface. The instrument continuously records 2048 samples per scan line centered on the nadir. It scans upwelling radiation, both emitted and reflected energy, over five wavelength channels centered at 0.63, 0.86, 3.7, 11, and 12 $\mu$m. This scanning geometry produces a pixel resolution of 1 km by 1 km at nadir.

The primary data source utilized in this study come from the First ISSP Regional Experiment (FIRE) which was conducted from 28 June to 14 July 1987 off the coast of southern California. Both morning and afternoon passes were collected, copies of which are archived in the Naval Postgraduate School IDEA Laboratory. Using the IDEA Lab VAX computer system, the AVIAN software package was employed to glean and navigate the magnetic tapes containing these data. This allowed the production of an overview of the entire satellite pass. This overview is visually scanned for the presence of ship tracks. When ship tracks are found in CTR's or cloud regimes associated with them, a 512 km x 512 km channel 3 subscene is extracted from the overview for further analysis and ship

12

track digitization. After the track is digitized, five additional image products are also extracted from the overview. A brief description of the characteristics of these image products is provided below:

LOW1 - channel 1 albedo scaled by the solar zenith angle and low cloud asymmetric reflectance factor (in percent).

LOW3 - channel 3 albedo scaled by the solar zenith angle and low cloud anisotropic reflectance factor (in percent).

S12A - a ratio of channel 1 albedo to channel 2 albedo (1.0 to 3.0).

TMP4 - channel 4 brightness temperature (°K)

T45 - difference between channel 4 and channel 5 brightness temperatures (°K).

These 512 X 512 image products subscenes become input parameters into the ship track data extraction algorithm to be described next.

## C. SHIP TRACK DATA EXTRACTION ALGORITHM

Following on the approach of Coakley et al. (1987) and Morehead (1988), a ship track detection algorithm was developed at the Naval Postgraduate School. A description of the algorithm is contained in Nielsen and Durkee, (1992). The algorithm divides the subscene into 16 km x 16 km subareas and computes the mean and standard deviation for each subarea. Next, it performs a brightness "neighborhood" test to determine which local pixels show some relation to other local pixels. Then the algorithm determines which brightness neighborhoods belong to ship tracks and constructs a linear pathway connecting the neighborhoods.

The algorithm was designed to automate the ship track detection process by independently identifying ship tracks with a minimum of manual intervention. In this study the algorithm was modified to allow the user to manually select the ship track(s) of interest, digitize a series of points to define the track and input the points into the algorithm. This greatly speeds up the extraction process since the algorithm only scans the subscene for the specified track and ignores other tracks and anomalous linear features.

Once the track is selected, digitized, and inputted into the algorithm, it extracts a 31 km swath of data along the entire length of the track. This swath of data contain the radiative signature of both the ship track and the ambient cloud field surrounding it. A file is created for each of the subscenes previously described. It is these data which will be analyzed to determine the variation in the spatial and radiative characteristics of ship tracks in CTR's.

## D. DATA ANALYSIS

Before any averaging technique or statistical analysis can be performed, the data contained in the linerized ship track records file must be transferred to 1 km x 1 km grid to ensure that the size of a pixel is constant throughout the width and length of the track. This adjustment is necessary because the combined effect of the AVHRR's scan geometry and the earth's curvature causes a degradation in resolution. Additionally, the distance between data points increases away from the nadir of the satellite, particularly near the edges. So the extracted swath of data contain some holes particularly when curved tracks are straightened out. The best resolution is obtained directly below the satellite, at nadir, resulting in a pixel size of approximately 1.1 km x 1.1 km spaced approximately .9 km apart. This resolution decreases toward

15

either end of the scan line where the pixels measure about 2.4 km along-track and about 14.7 km across-track. Basically, the algorithm takes the linerized records file, determines its location in the overview, and applies a scaling correction to each pixel based on the angular distortion present at that point. Then the records file is mapped onto a 1 km grid. Each data point of the records file is assigned an x-y coordinate in the grid. Values are assigned to the grid points based on a weighting function which assigns a $1/r^2$ weight to each data point within a user defined radius of 2-5 km around each grid point. This variable radius is necessary because the distance between data points varies as a function of the tracks' location on the overview. It also allows the user some control over the number of data points used in computing each grid point value. The procedure results in some smoothing but the ship track/ambient cloud swath essentially retains its radiative signature and spatial characteristics. A raw satellite image and a linerized, weighted-average version of the same ship track are shown in Figure 4.

## E. AVERAGING METHODS

The procedure employed in the previous section allows ship tracks to be averaged and statistically analyzed. Sample pixels are extracted from the records file for each subscene.
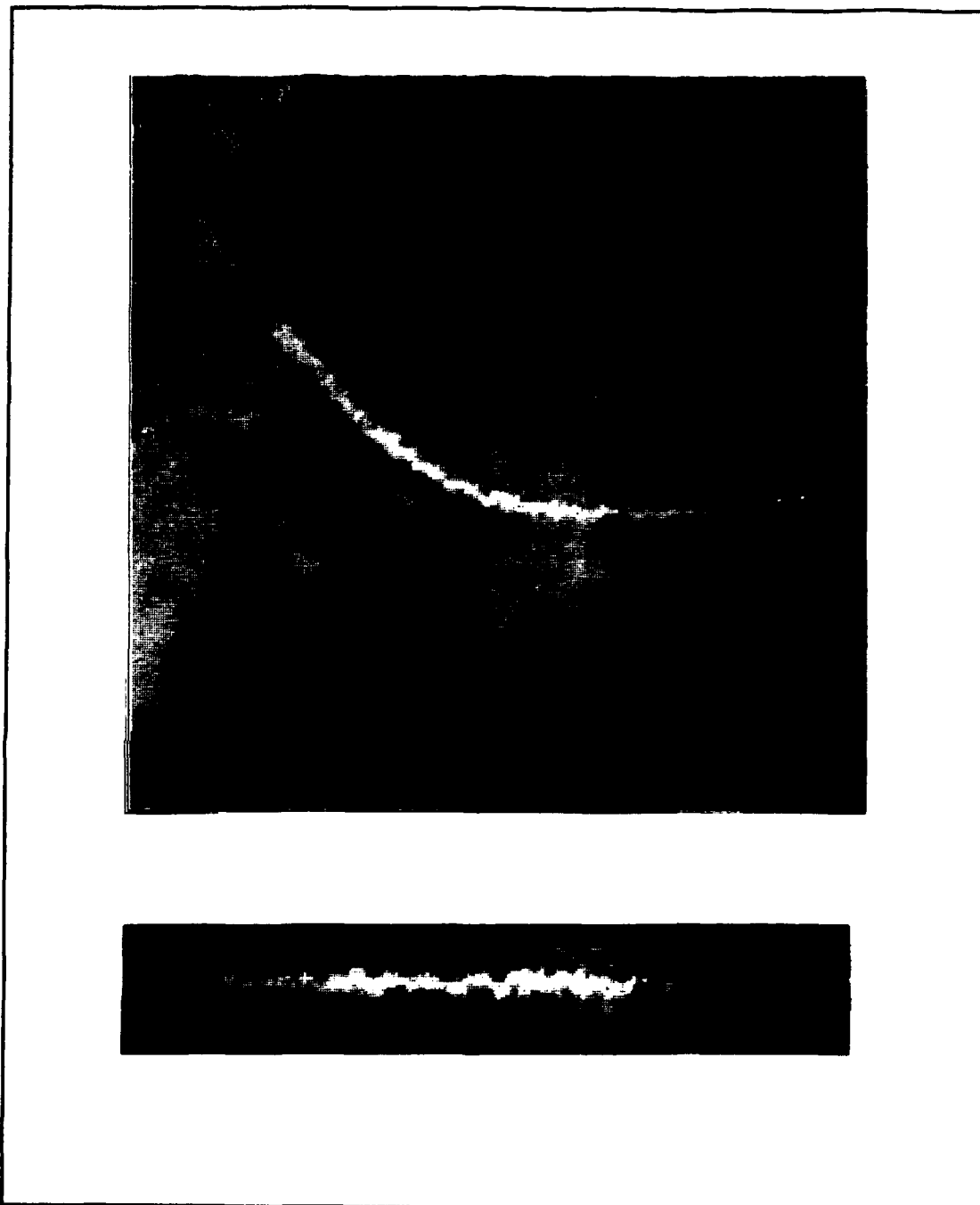
**Figure 4.** Raw and Linearized, Weighted Average Versions of the Same Ship Track.

The extraction algorithm takes the pixel at the center ship track and one pixel on either side. Then, using a brightness gradient to find the edge of the ship track, it extracts six pixels from the uncontaminated cloud, three from either side of the track. A distance of 15 km from the edge is utilized as a separation distance. The track pixels are averaged together and the six cloud pixels are averaged together for each line of data along the track. This operation is performed for each line of data in the records file. Figure 5, which is an enlargement of the previous weight-averaged ship track, depicts pixel scale data points utilized for the ambient cloud and ship track data sets. Combining records files for similar track/cloud types allows class averages and comparisons to be produced for each ship track/cloud pair.

Once the tracks for each cloud type are averaged, the spatial and radiative variations are examined. A summary of the statistics utilized in the study for each ship track/cloud pair are summarized in Table I.
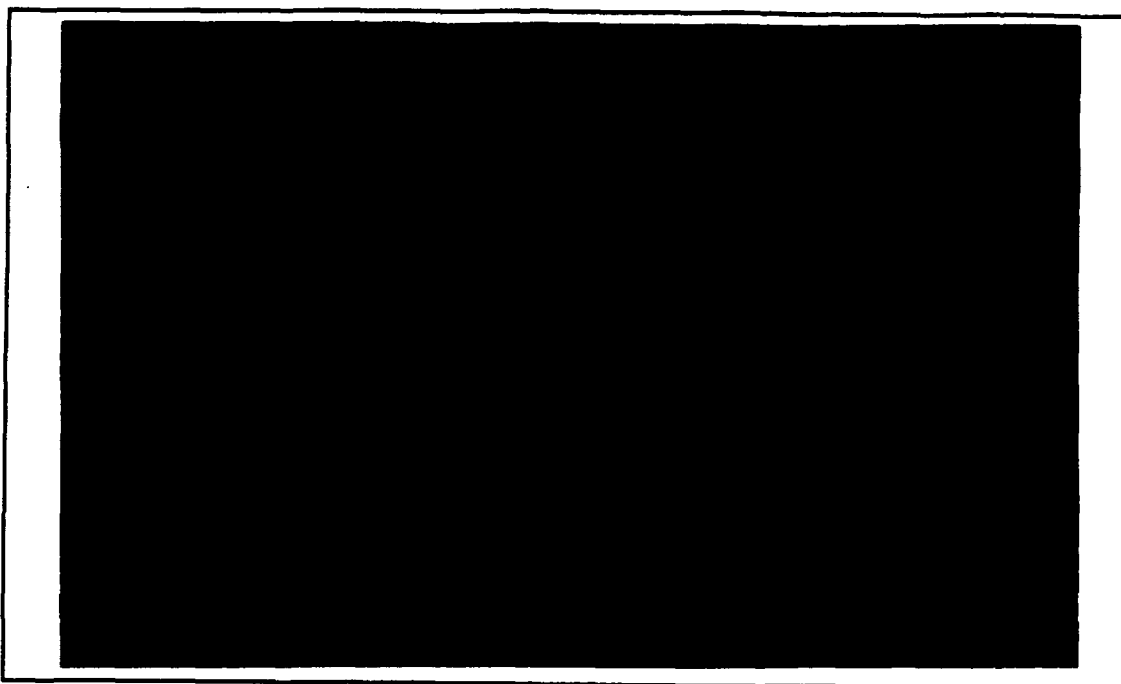
**Figure 5.** Typical Ship Track and Ambient Cloud Pixels Utilized in Averaging Scheme.

The results of the analysis of the radiative and spatial variations of ship tracks, with respect to the environment in which the form, are detailed in Chapter III.

**Table I**   SUMMARY OF STATISTICAL DATA COLLECTED ON SHIP
TRACKS AND AMBIENT CLOUD FIELDS.

LOW1 AVERAGE AMBIENT CLOUD ALBEDO
LOW1 AVERAGE TRACK ALBEDO
LOW3 AVERAGE AMBIENT CLOUD ALBEDO
LOW3 AVERAGE TRACK ALBEDO
S12A AVERAGE AMBIENT CLOUD ALBEDO
S12A AVERAGE TRACK ALBEDO
TMP4 AVERAGE AMBIENT CLOUD TEMPERATURE
TMP4 AVERAGE TRACK TEMPERATURE
T45 AVERAGE AMBIENT CLOUD TEMPERATURE DIFFERENCE
T45 AVERAGE TRACK TEMPERATURE DIFFERENCE
DELTA PERCENT CHANGE LOW1 CLOUD/TRACK
DELTA PERCENT CHANGE LOW3 CLOUD/TRACK
DELTA PERCENT CHANGE S12A CLOUD/TRACK
DELTA PERCENT CHANGE TMP4 CLOUD/TRACK
DELTA PERCENT CHANGE T45 CLOUD/TRACK
WIDTH OF TRACK VS. LENGTH

# III. RESULTS

## A. OVERVIEW

A total of 63 ship tracks were collected and analyzed in this study. They were collected from both morning and afternoon satellite passes. They had a latitudinal range from approximately 20°N to 45°N and a longitudinal range from 118°W to 138°W. Throughout the period of the study the entire region was under the influence of the semi-permanent subtropical high. Surface pressures ranged from 1012 mb to 1024 mb. Surface winds were generally north-northwesterly varying from 5 to 30 kt throughout the period.

Ship tracks were observed in a wide range of cloud types, textures and patterns. These were analyzed and classified into three broad categories: solid stratiform, broken stratiform and cumulus. The observed radiative and spatial variation by satellite image product and cloud type are described by analyzing the class averages for the statistical data described previously. The results of this analysis are summarized in the following sections.

## B.  STATISTICAL METHODS AND TESTS

The analysis of these data required the determination of the mean and standard deviation for the track and ambient cloud for each cloud type and image product. The means of the track and cloud values were compared and a percentage assigned based on the differences observed between the means. An additional statistic was computed by subtracting the value of each ambient cloud pixel from the value of its corresponding track pixel. This difference was divided by the value of the ambient cloud pixel to produce a delta percent change (DPC) between the track and cloud. The mean and standard deviation of average of the differences were also computed.

The Mann-Whitney (MW) ranking scheme for two independent samples, Snedecor and Cochran (1967), was utilized to test the significance of the difference between the means of the track and cloud values. The null hypothesis that both samples come from the same population is rejected if the MW statistic gives a probability value that produces a significance level greater than 95 percent. In each of the following cases the MW test results will be reported to estimate the probability that the the differences observed between two means is significant and not the result of chance.

## C. DATA DISPLAY METHOD

Prior to any discussion of the results of this study, a description of data display methods is necessary. The data collected for each cloud/track pair within a particular cloud regime are displayed in both scatterplot and histogram form. Both displays depict the cloud regime or track with the head of the track to the left of the graph. Figure 6 illustrates scatterplots for a single ship track in both LOW1 and LOW3. Combining a number of tracks produces the plots contained in the following section. Although there is considerable variability in one ship track, most of the variation present is from track to track.

## D. OBSERVATIONS OF RADIATIVE CHARACTERISTICS

### 1. Stratus Clouds and Associated Tracks

#### a. *LOW1*

The LOW1 mean for the albedo of stratus clouds is 34.672 with a standard deviation of 13.919 while the mean for the tracks which form in them is 38.652 with a standard deviation of 14.512. This indicates that, on the average, tracks that form the stratus cloud are 11% brighter than the ambient cloud. Utilizing the MW test, the probability that the means are from different populations is 100%. The mean of the DPC between track and cloud is 15.128 with a standard

23

## LOW1 ST TRACK ALBEDO



## LOW3 ST TRACK ALBEDO
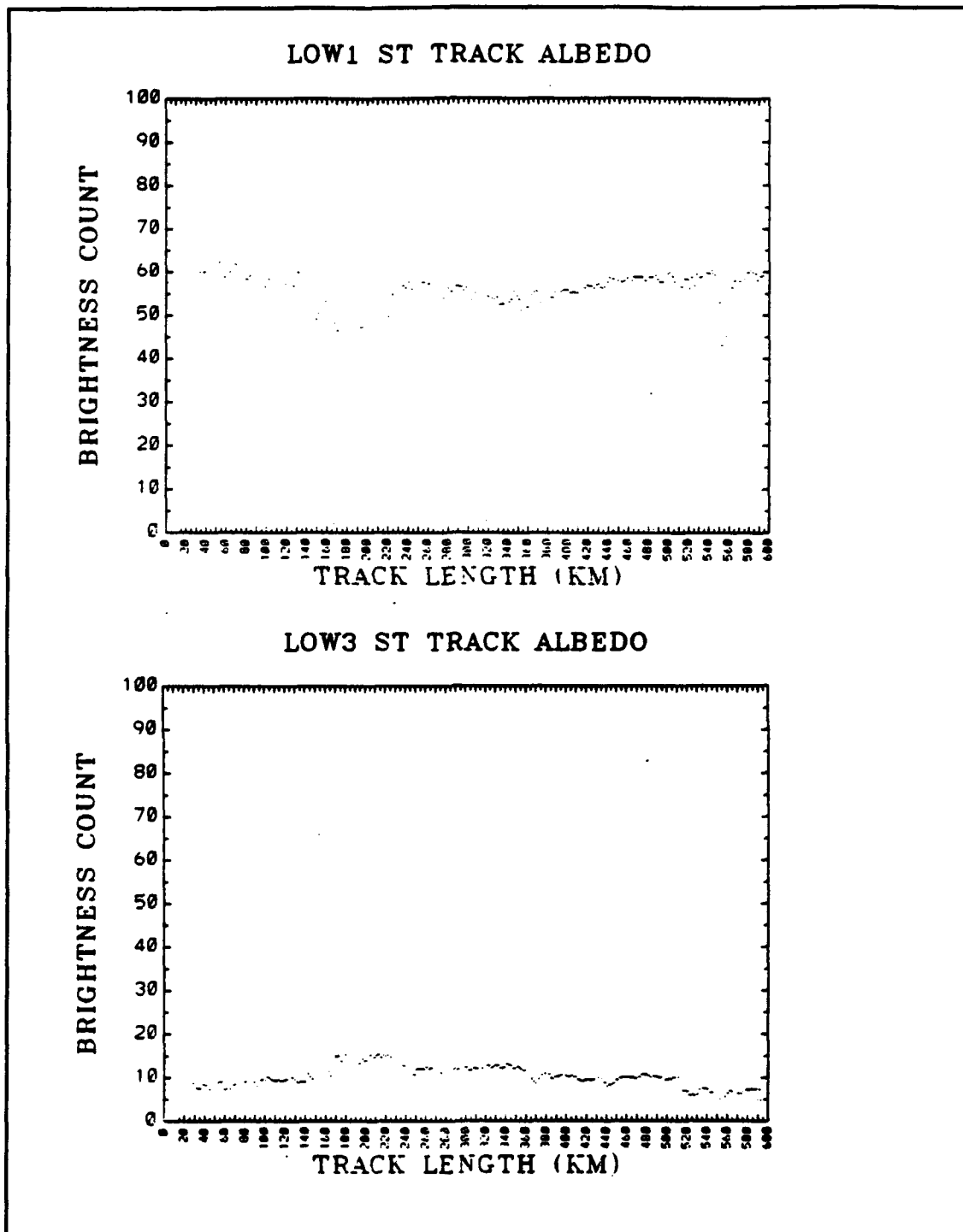


**Figure 6.** LOW1 and LOW3 Scatterplots Depicting a Single Ship Track.

24

deviation of 31.004. Figure 7 shows the raw data utilized to compute the means. The LOW1 albedo value for stratus range from 8 to 77 with 23.1 being the most frequently occurring value. The cloud brightness for individual track is fairly constant along each track but varies considerably between tracks. Figure 8 shows the albedo values for ship tracks in stratus. The values vary from 10 to 78 with a value of 23.8 occurring most frequently. The delta percent change (DPC) shown in Figure 9 fluctuates between -30% and 60% with a maximum occurring value of 6%. These means values are consistent with, but higher than, the observations reported by Coakley et al., 1987, who noted that the change was caused by an increase in cloud droplets numbers. A larger concentration of cloud droplets causes the cloud to be more reflective.

### b. LOW3

The LOW3 mean for the albedo of stratus clouds is 8.191 with a standard deviation of 5.105. The mean for the ship tracks in them is 10.397 with a standard deviation of 5.643. The percent change in reflectivity on the average between the track and the cloud is 27%. The MW shows a 100% probability the difference is significant. The mean of the DPC is 35.631 with a standard deviation of 40.55. Figure 10 displays the plots for LOW3 stratus clouds. The values vary from 2 to 25 with maximum occurring near 4.1. The ship track

25
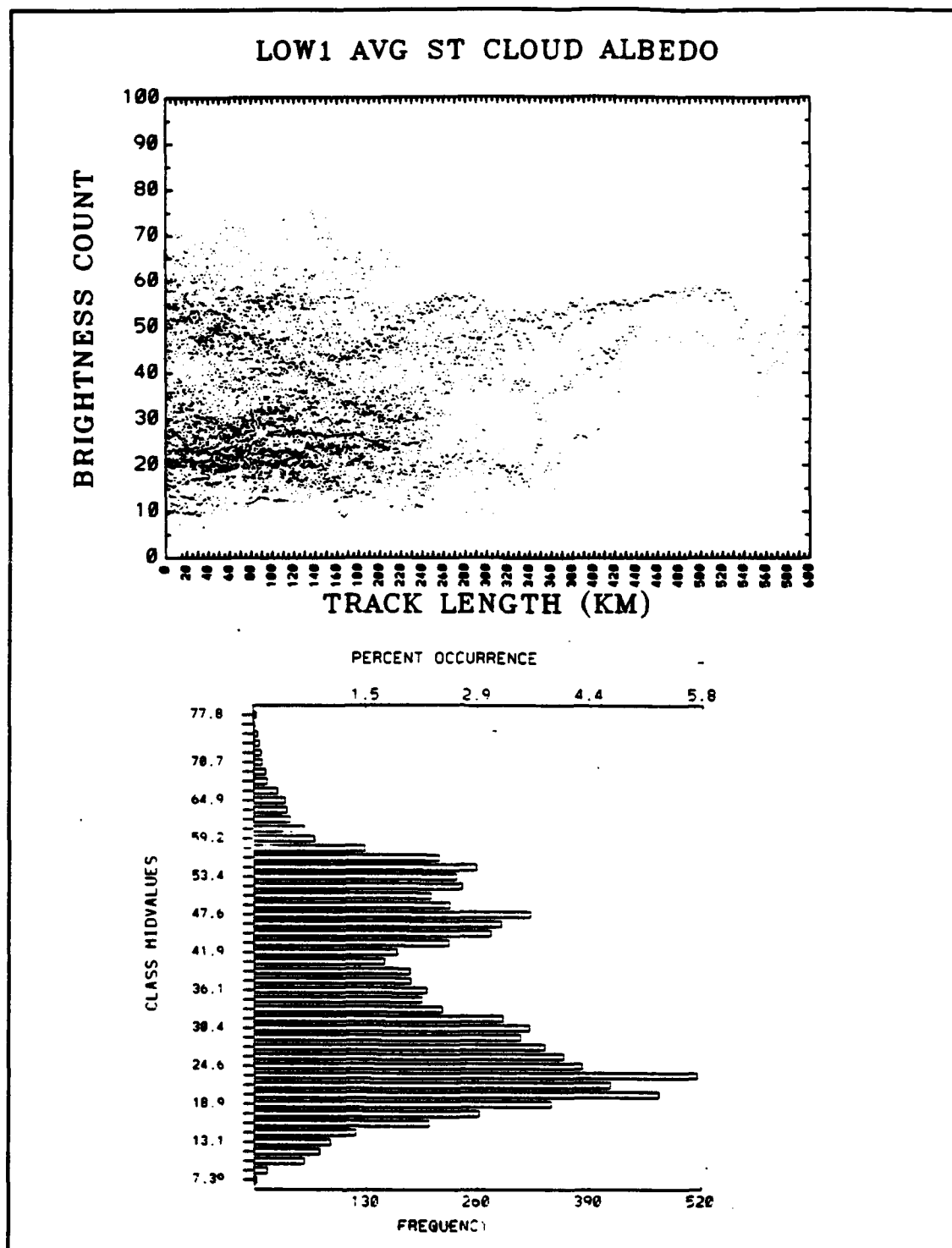
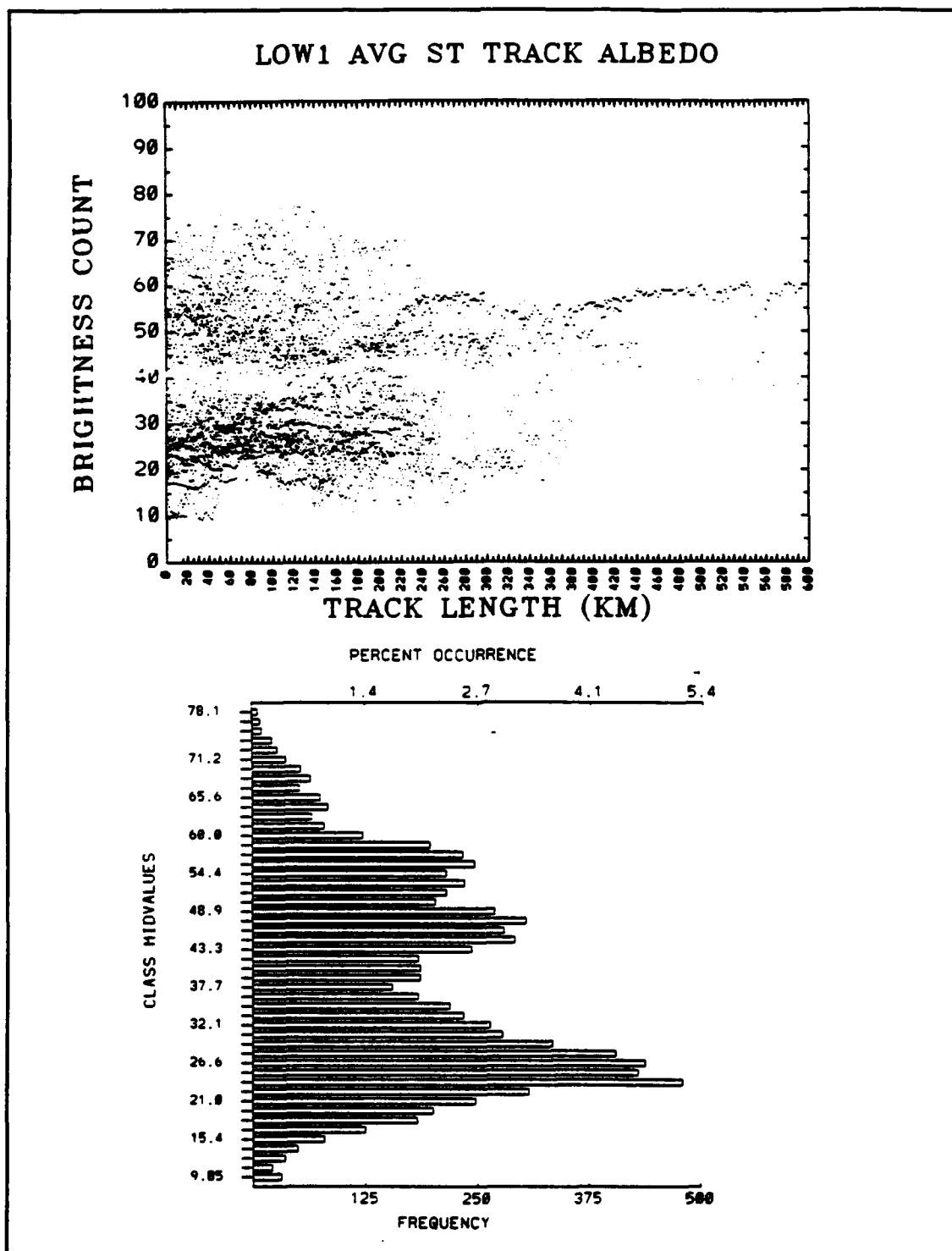**Figure 7.** Scatterplot and Histogram for LOW1 Stratus Regime.

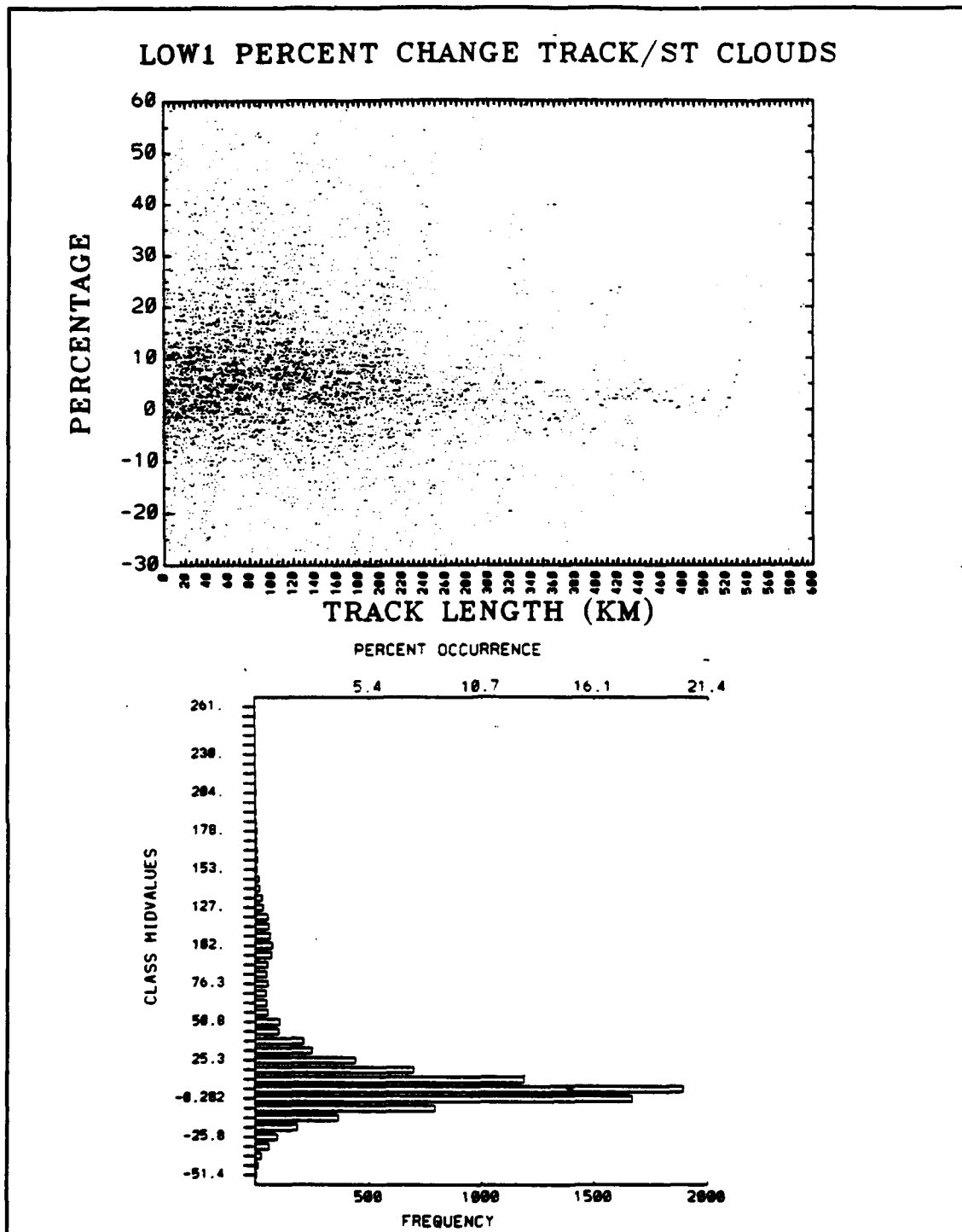**Figure 8.** Scatterplot and Histogram for LOW1 Stratus Tracks.

**Figure 9.** Scatterplot and Histogram for DPC LOW1 Cloud/Track.

data points are displayed in Figure 11. They range from 4 to 30 with a most frequent value at 5.1. The DPC, shown in Figure 12, ranges between -30% and 260% but the most frequently occurring value is 16.8%. The injection of additional CCN into the cloud by a passing ship causes smaller water droplets to form. Since the smaller in-track water droplets are more efficient scatters of energy than the neighboring larger ambient cloud droplets, ship tracks tend to be more reflective at 3.7 $\mu$m (Coakley et al., 1987).

### c. S12A

The mean of the S12A ratio for stratus clouds is 1.175 with a standard deviation of 0.008. The ship track class average is 1.174 with a standard deviation of 0.008. This states that both cloud and track are brighter in channel 1 than channel 2. On the average the percent change between cloud and track is slightly negative at -0.004. The MW shows a 79% probability the difference is significant. The mean of the DPC is -0.003 with a standard deviation of 2.210. These observations are consistent with the different channel 1 and 2 wavelengths. Both the ambient cloud and the ship track are brighter in Channel 2. However, because of the shift to smaller, more reflective water droplets in the track, ship tracks gets brighter faster than the ambient clouds. This same effect is observed at 3.7 $\mu$m where ship tracks are
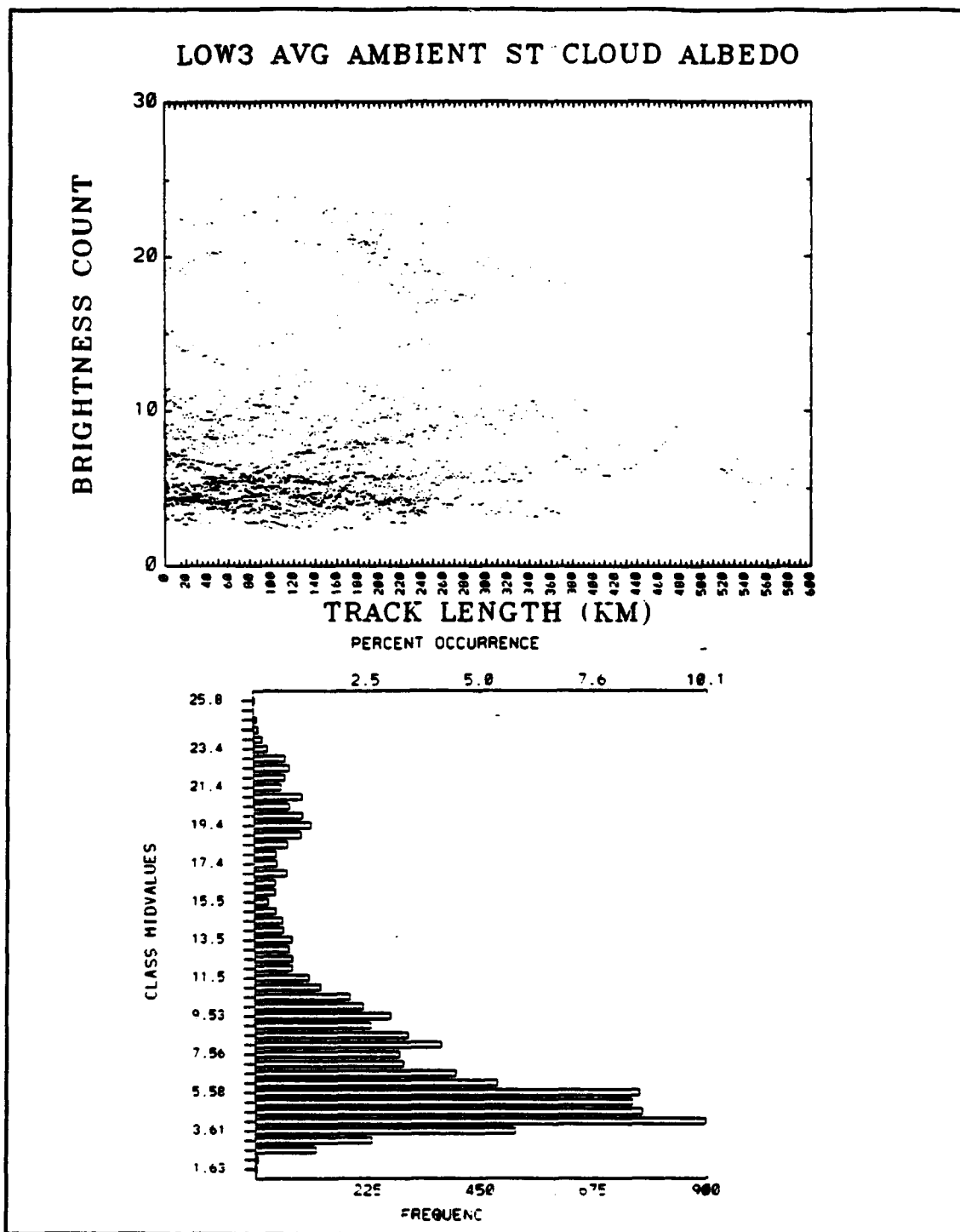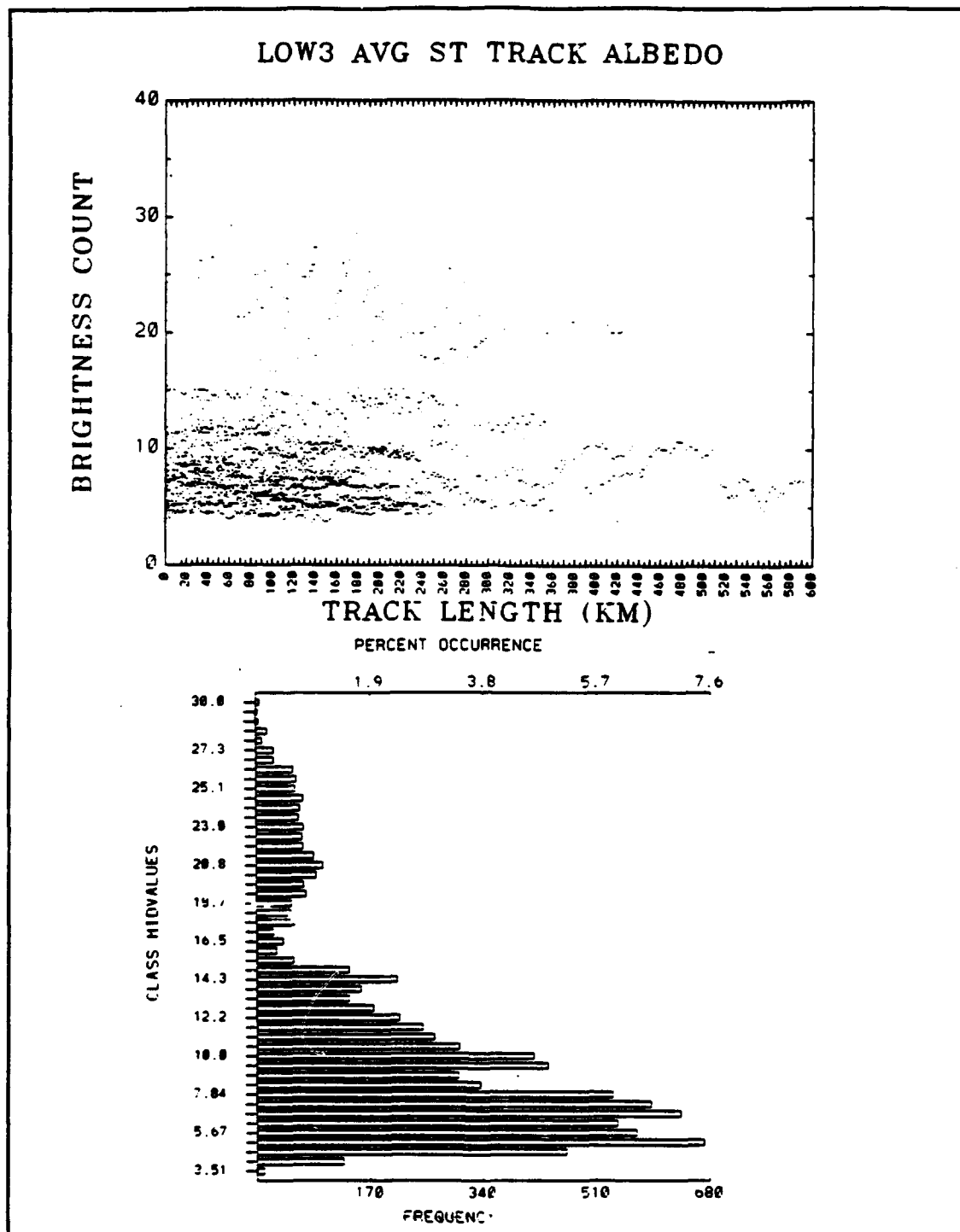
29

# LOW3 AVG AMBIENT ST CLOUD ALBEDO



**Figure 10.** Scatterplot and Histogram for LOW3 Stratus Regime.

**Figure 11.** Scatterplot and Histogram for LOW3 Stratus Tracks.
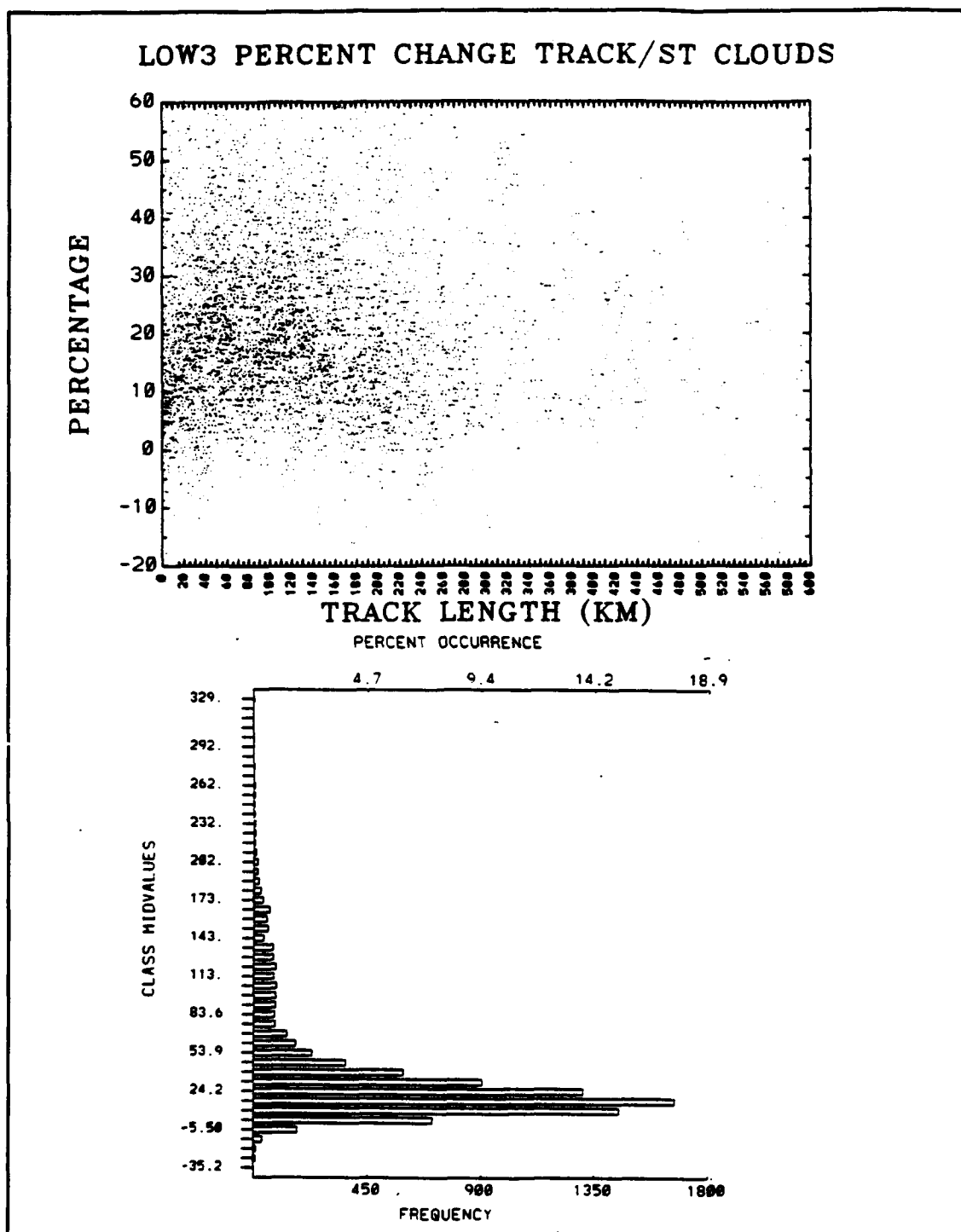
## LOW3 PERCENT CHANGE TRACK/ST CLOUDS

**Figure 12.** Scatterplot and Histogram for DPC LOW3 Cloud/Track.

significantly brighter than the ambient cloud. The resultant
ratio of the S12A for the ship track and cloud is therefore
negative. The scatterplots and histograms for the data show
little variation. For completeness, the S12A plots for
stratus, broken stratus and cumulus are included in the
Appendix.

### d. TMP4

The mean for TMP4 temperature in both stratus
cloud and the ship track is 285.2 °K. The standard deviations
were 2.358 °K and 2.412 °K, respectively. The MW shows a 56%
probability the difference is significant. The mean of the DPC
is -0.001 with a standard deviation of 0.173. These means are
identical indicating that both the cloud and track emit
equally as well at 11 $\mu$m. It also suggests that ships cause no
appreciable change in the cloud top height or a temperature
difference would be observed. The scatterplots and histograms
for the data show little variation between cloud and track.
The TMP4 plots for stratus, broken stratus and cumulus are
also presented in the Appendix.

### e. T45

The mean for the T45 temperature difference is
-.395 °K with and standard deviation of 1.306 °K while the
mean for ship tracks is 0.001 °K with a standard deviation of
.306 °K. This translates to a large percent change from track

33

to cloud but represents the differences between numbers on the order 1E-02 and 1E-03. The sensor can only resolve temperature differences on the order of 1E-01. So, although a weak signature appears to exist no real significance is attached to the large percent change observed. The scatterplots and histograms for this data, broken stratus and cumulus are provided in the Appendix.

A summary of the statistics change for each of the image products described above for stratus clouds is contained in Table II.

## 2. Broken Clouds and Associated Tracks

### a. *LOW1*

The LOW1 mean albedo of broken stratus clouds and ship tracks is 23.422 and 27.770 respectively. The standard deviation for the cloud average is 8.535 and versus 9.039 for the track. On the average, the total increase in albedo between the track and the cloud is 18%. The MW test shows this to be significant to 100%. The mean of the DPC is 26.016 with a standard deviation of 44.854. The average percent change and the DPC are both higher than that observed in the stratus case. In broken clouds the ship track is contrasted against a background clouds that have gaps. The radiative signature of these clouds is influenced the less reflective sea surface.

34

**Table II.** SUMMARY OF STATISTICS FOR STRATUS CLOUDS/TRACKS.

| PRODUCT | MEAN | STD DEV | % CHANGE |
|---|---|---|---|
| LOW1 ST | 34.652 (A) | 13.919 | |
| LOW1 TRACK | 38.341 (A) | 14.512 | |
| LOW1 TRK/ST | | | 0.11 |
| LOW1 DPC | 15.128 (A) | 31.004 | |
| LOW3 ST | 8.191 (A) | 5.105 | |
| LOW3 TRACK | 10.397 (A) | 5.643 | |
| LOW3 TRK/ST | | | 0.27 |
| LOW3 DPC | 35.631 (A) | 40.55 | |
| S12A ST | 1.176 (R) | 0.008 | |
| S12A TRACK | 1.174 (R) | 0.008 | |
| S12A TRK/ST | | | -0.001 |
| S12A DPC | -0.003 (R) | 2.210 | |
| TMP4 ST | 282.2 (T) | 2.358 | |
| TMP4 TRACK | 282.2 (T) | 2.412 | |
| TMP4 TRK/ST | | | 0.000 |
| TMP4 DPC | -0.001 (T) | 0.173 | |
| T45 ST | -0.396 (D) | 1.306 | |
| T45 TRACK | 0.000 (D) | 0.306 | |
| T45 TRK/ST | | | -100.00 |
| T45 DPC | -9.280 (D) | 195.47 | |
| A=ALBEDO, R=RATIO, T=TEMPERATURE (°K), D=DIFFERENCE | | | |

35

This makes ship tracks which form in broken clouds appear brighter relative to their environment. The albedo values for LOW 1 broken stratus vary from 7 to 58 with a most frequently occurring value of 20 as shown in Figure 13. For the track, Figure 14 shows the values fluctuate between 9 and 64 the maximum occurring near 24. Figure 15 illustrates the DPC between track and cloud. It ranges from -60% to 237% with a maximum at 8%. As noted the tracks in broken cloud have a lower albedo than in stratus. One possible explanation for this is that the ambient broken clouds have a lower liquid water content (LWC). The additional flux of CCN into the cloud causes a shift to smaller droplet size but because the LWC in broken clouds is less than that in stratus clouds, the total concentration of smaller radii water droplets is lower.

   *b. LOW3*

The mean for LOW3 broken cloud albedo is 5.842 with a standard deviation of 3.114. The track mean albedo is 8.210 with a standard deviation of 3.820. On the average there is a 40% increase in reflectivity between the track and the cloud. The MW test shows the significance of the differences in the means to be significant to 100%. The mean of the DPC is 53.911 with a standard deviation of 57.644. Figure 16 presents the LOW3 broken stratus cloud data. The values range from 8 to 15 with bimodal maximums occurring at 2.8 and 7.7. This

36
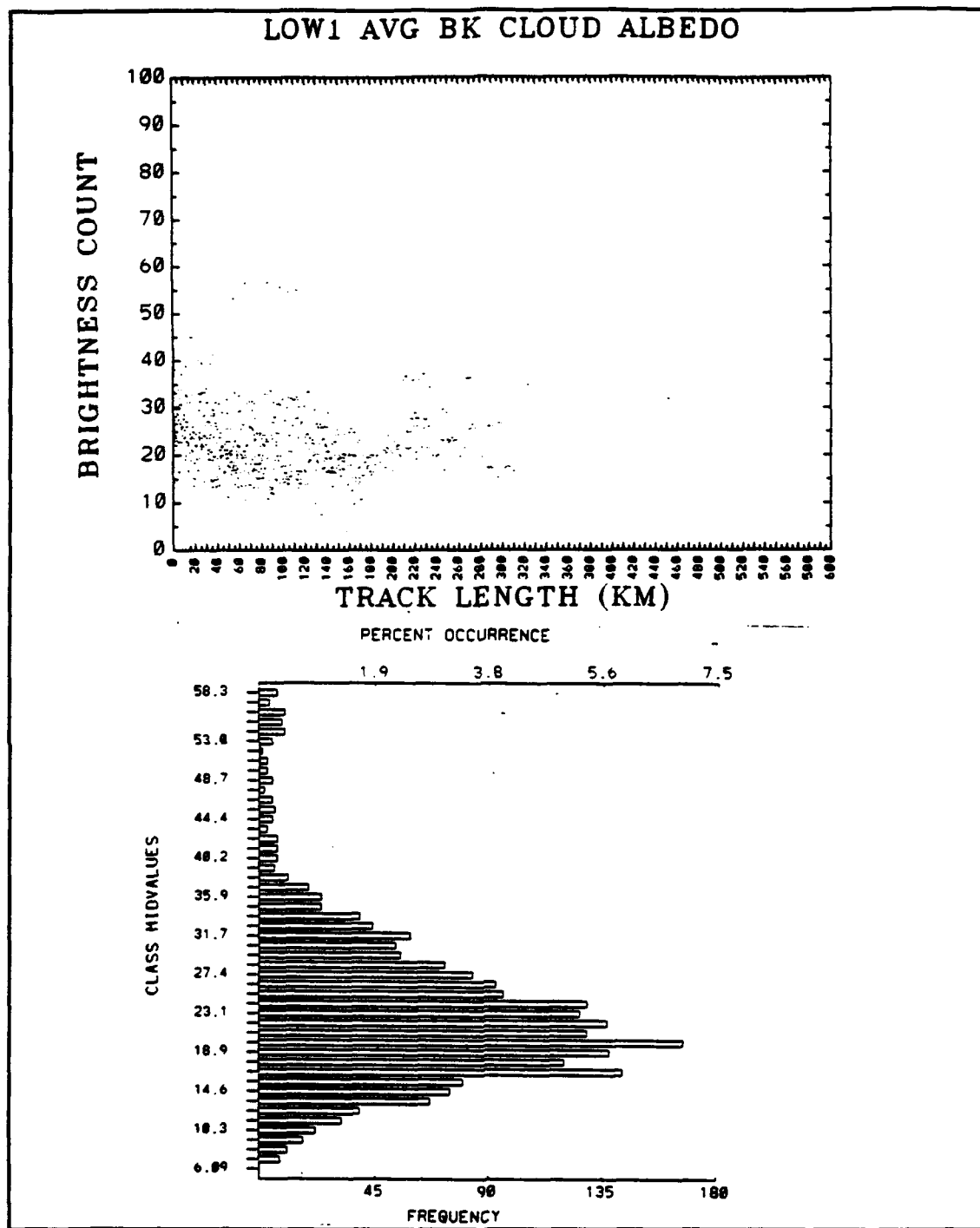
**Figure 13.** Scatterplot and Histogram for LOW1 Broken Stratus Regime.

37
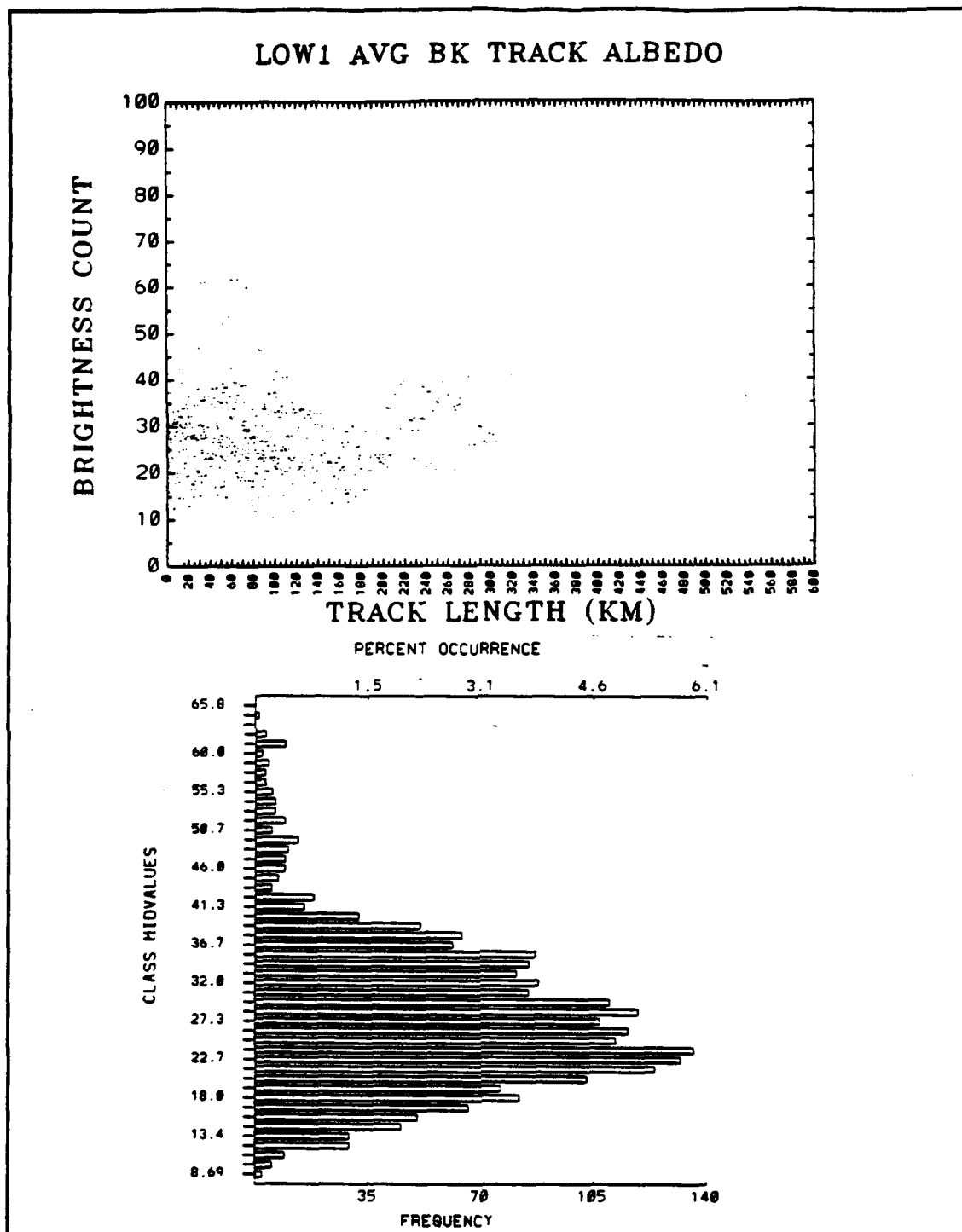
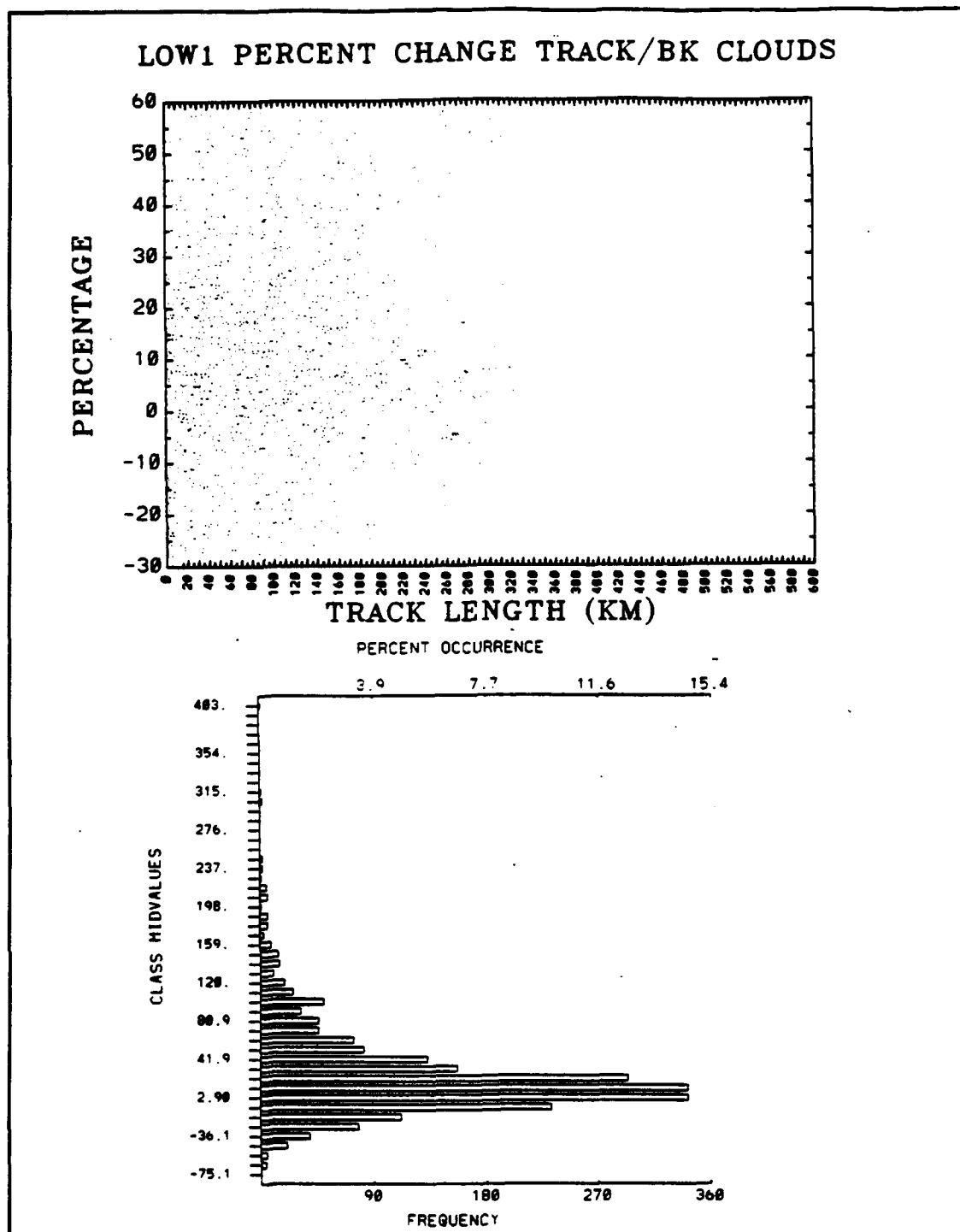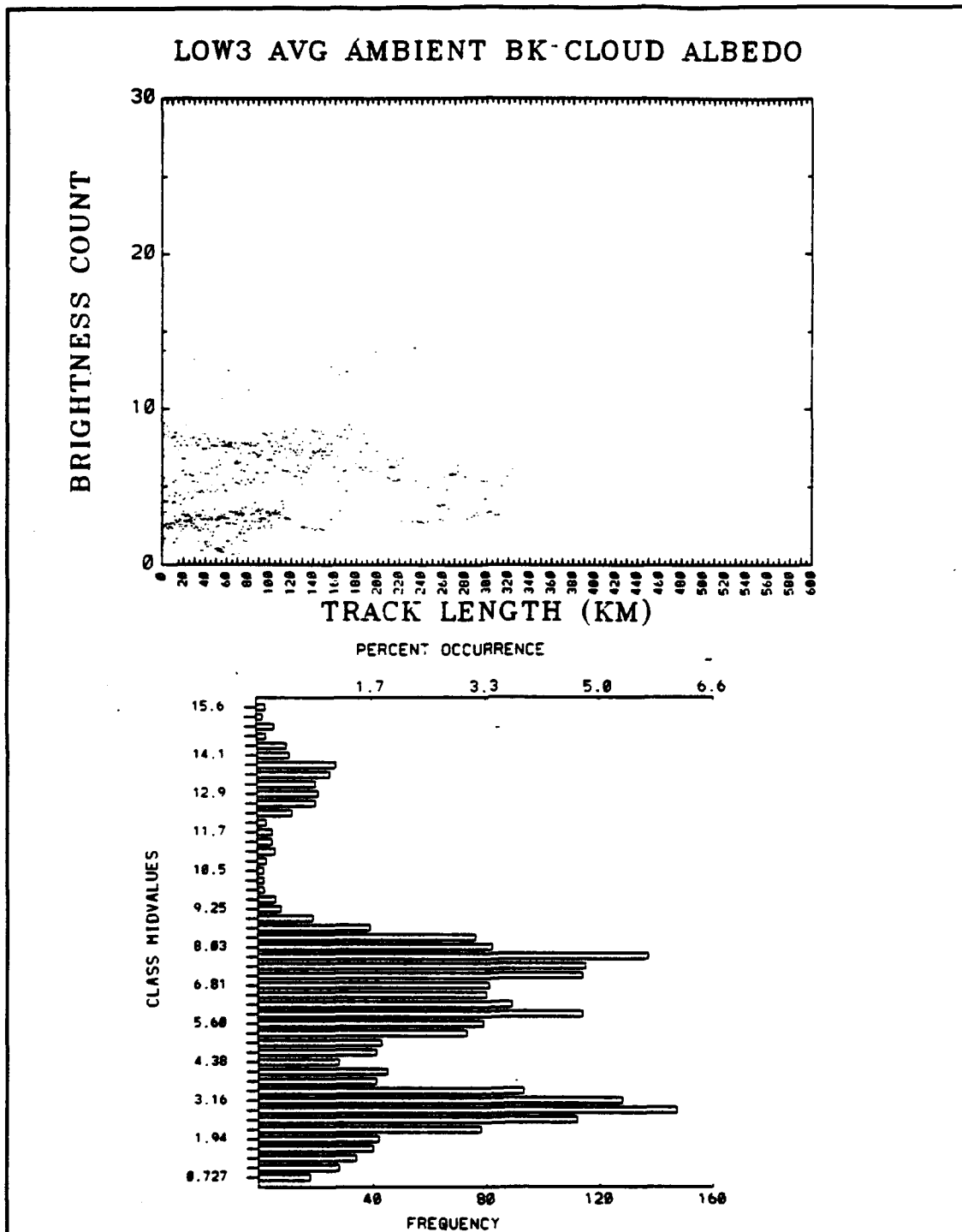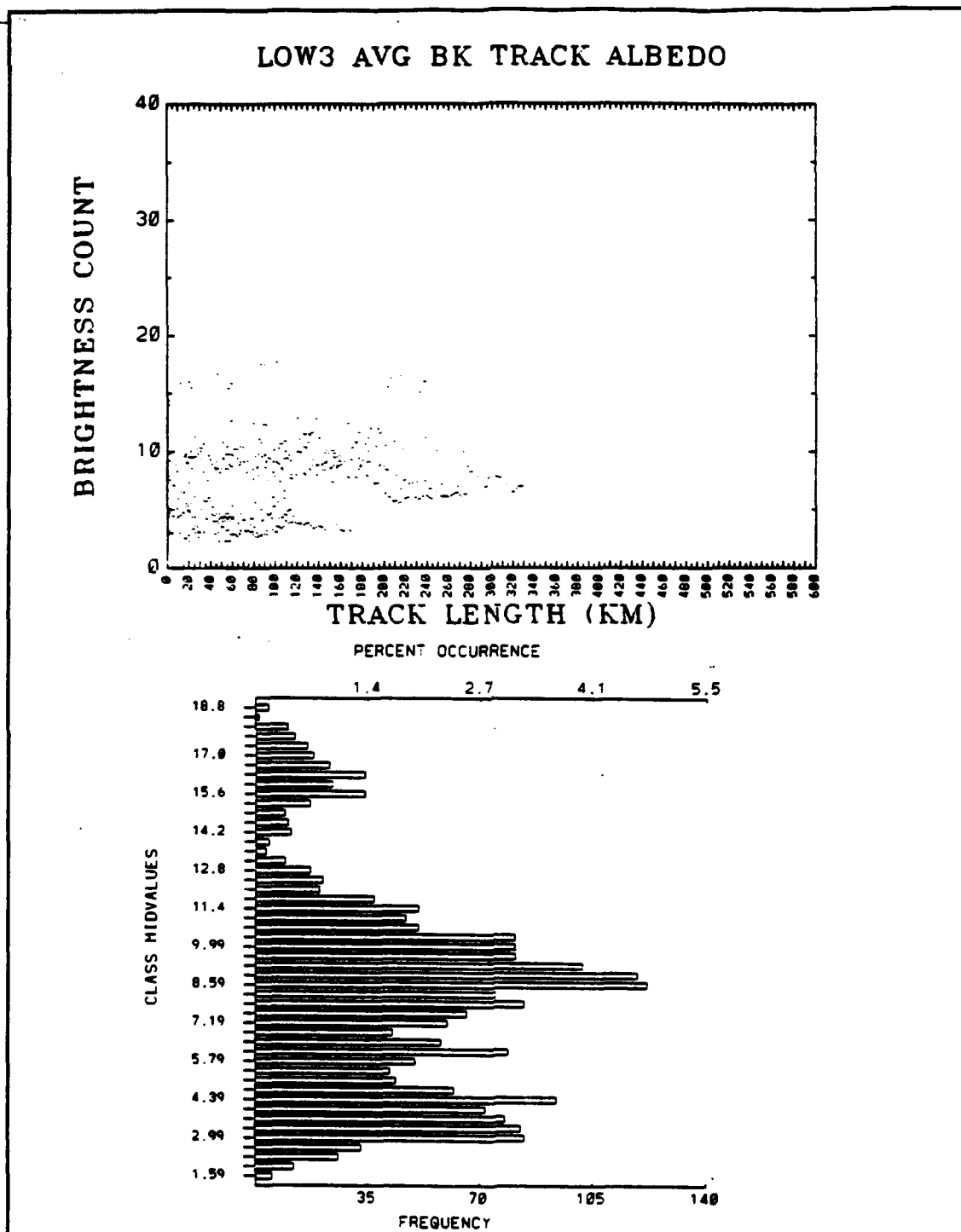**Figure 14.** Scatterplot and Histogram for LOW1 Broken Stratus Tracks.

**Figure 15.** Scatterplot and Histogram for DPC LOW1 Track/Cloud.

39

bimodal signature results from the variability observed between tracks. The track values, Figure 17, fluctuate between 1.6 and 18 with a most frequently occurring value at 8.6. The DPC, shown in Figure 18 has a wide range with a minimum near 14.3%. While this is substantial increase over the stratus case, it is consistent with smaller droplet radii and increased droplet concentration over the ambient cloud. It is also consistent with the comparable increase observed in LOW1.

### c. S12A

The S12A mean ratio is 1.145 with a standard deviation of .102 while the mean for the ship track is 1.136 with a standard deviation of 0.009. The average percent change between the track and the cloud is -0.008. The MW test places the significance of the difference at 100%. The mean of the DPC is -0.669 with a standard deviation of 3.285. The same effect previously discussed in stratus is present in broken clouds as well, albeit more pronounced. Since the contrast between broken clouds and ship tracks is greater the resultant S12A ratio of track to cloud is slightly more negative than that observed in stratus. Scatterplots and histograms from which these data are derived are in the Appendix.

40

**Figure 16.** Scatterplot and Histogram for LOW3 Broken Stratus Regime.

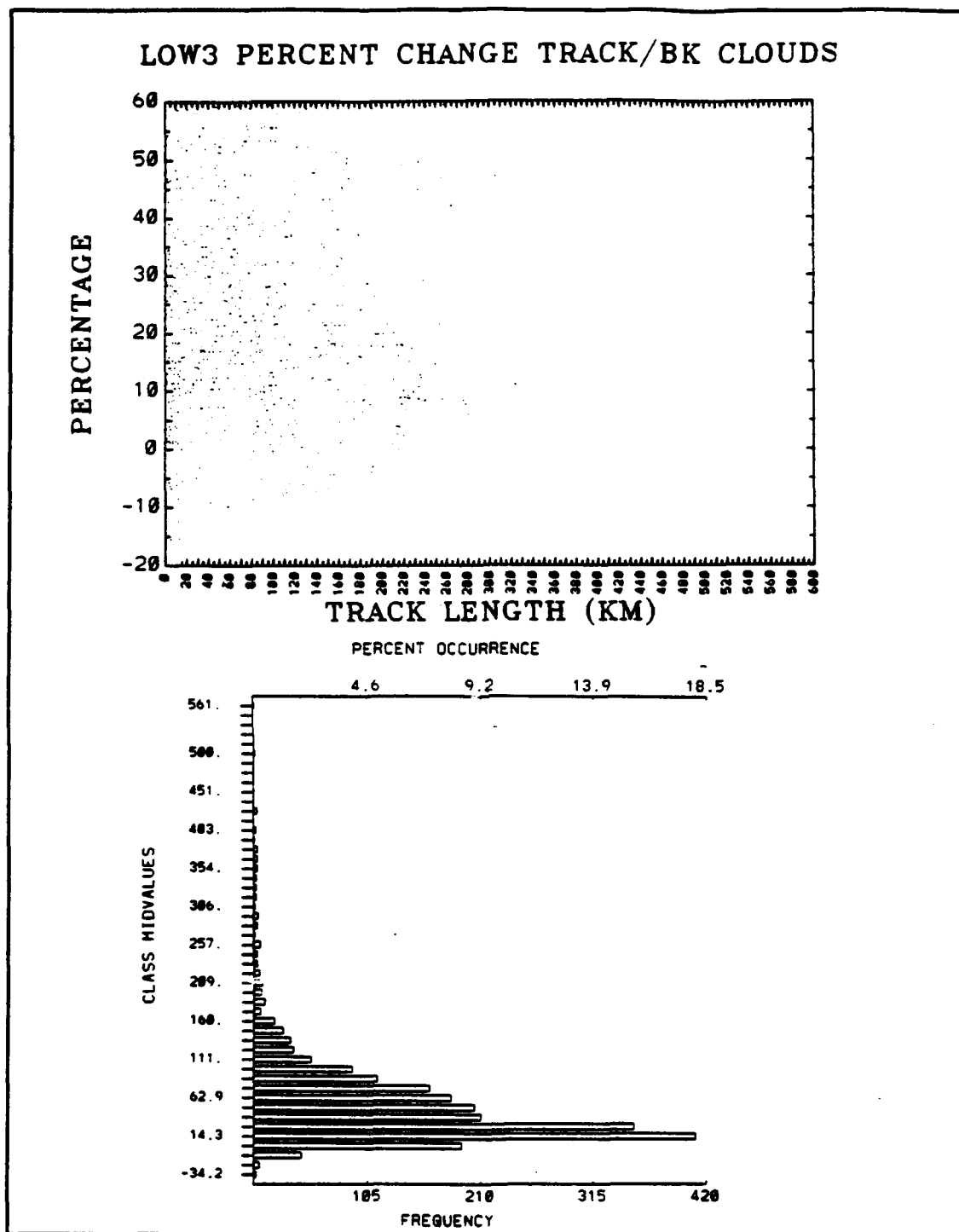**Figure 17.** Scatterplot and Histogram for LOW3 Broken Stratus
Tracks.

**Figure 18.** Scatterplot and Histogram for DPC LOW3 Track/Cloud.

43

### d. TMP4

The mean for TMP4 temperature in broken cloud is 284.4 °K with a standard deviation of 1.921 °K. The mean for the track is 284.3 °K with a standard deviation of 1.881 °K. The MW significance for the difference in the means is 99%, much higher that in the stratus case. The mean of the DPC is -0.005 with a standard deviation of 0.025. The influence of the sea surface temperature is perhaps one reason these statistics are different the stratus case. The statistics point to a difference in the means but is detectable difference exists in the ambient cloud and track temperature. The Appendix contains the scatterplots and histograms for the above data.

### e. T45

The mean T45 temperature difference is -0.261 °K for broken stratus with a standard deviation of 1.417 °K. The average difference for the track is 0.200 °K with a standard deviation of 0.343 °K. The percent change is again large but not considered significant. Scatterplots and histograms for this data are included in the Appendix.

A summary of the statistics each of the image products described above for broken stratus clouds is contained in Table III.

**Table III.** SUMMARY OF STATISTICS FOR BROKEN STRATUS CLOUD/TRACKS.

| PRODUCT | MEAN | STD DEV | % CHANGE |
|---|---|---|---|
| LOW1 BK | 23.422 (A) | 8.535 | |
| LOW1 TRACK | 27.770 (A) | 9.039 | |
| LOW1 TRK/BK | | | 0.18 |
| LOW1 DPC | 26.016 | 44.854 | |
| LOW3 BK | 5.842 (A) | 3.114 | |
| LOW3 TRACK | 8.210 (A) | 3.820 | |
| LOW3 TRK/BK | | | 0.40 |
| LOW3 DPC | 53.911 | 57.644 | |
| S12A BK | 1.145 (R) | 0.102 | |
| S12A TRACK | 1.136 (R) | 0.009 | |
| S12A TRK/BK | | | -0.008 |
| S12A DPC | -0.669 | 3.285 | |
| TMP4 BK | 284.4 (T) | 1.921 | |
| TMP4 TRACK | 284.2 (T) | 1.881 | |
| TMP4 TRK/BK | | | 0.000 |
| TMP4 DPC | -0.005 | 0.025 | |
| T45 BK | -0.261 (D) | 1.417 | |
| T45 TRACK | 0.200 (D) | 0.343 | |
| T45 TRK/BK | | | -176.00 |
| T45 DPC | -20.97 | 183.81 | |
| A=ALBEDO, R=RATIO, T=TEMPERATURE (°K), D=DIFFERENCE | | | |

### 3. Cumulus Clouds and Associated Tracks

#### a. *LOW1*

The mean of the albedo of cumulus clouds is 19.054 with a standard deviation of 8.210. The mean albedo of the ship tracks that form in them is 23.42 with a standard deviation of 9.464. On the average there is a 22% increase in albedo between the track and cloud which implies that cumulus tracks are much brighter than both stratus tracks and broken stratus tracks relative to their environment. The Mann-Whitney test gives a 100% probability the difference between these two means is significance. The mean of the DPC is 30.231 with a standard deviation of 46.975. Figure 19 shows the data distribution within the LOW1 cumulus cloud regime. There is a range of values from 5 to 47 with a maximum occuring at 13.5. The track albedo data points, shown in Figure 20, vary from 7 to 52 with the most frequently occurring value at 13.4. Figure 21 show the DPC for LOW1 between track and cloud. The values fluctuate over a wide range with a maximum occurring a 10.2%. The radiative signature of cumulus clouds is heavily influenced by the low reflectivity of the sea surface. This cloud type also has the lowest LWC of all three cases because the inversion is weaker and allows the cumulus clouds to penetrate and disperse

moisture. In this type of cloud the ship usually produces new cloud as it forms a track.

**b.  LOW3**

The mean for the LOW3 albedo in cumulus clouds is 5.748 with a standard deviation of 2.945. The mean for the tracks is 7.721 with a standard deviation of 2.864. The average percent change in albedo is 34%. The MW test assigns a significance of 100% to the difference between the means. The data for LOW3 ambient cumulus cloud regime is shown in Figure 22. They vary from 1.2 to 12 with a maximum value at 4.5. Figure 22, which displays the track data, has a range from 2 to 15 with a maximum of 6.6. The DPC for LOW3 cumulus track and cloud shows a large fluctuation with a maximum at 13.7%. This is a substantial increase in albedo over the ambient cloud but reverses an increasing trend from stratus to broken. This is consistent with a lower LWC in cumulus clouds due to vertical dispersion. That implies that there is less total water droplet to be affected by the injection of CCN so while a shift to smaller droplet size occurs it is not a dramatic as the shift in stratus and broken stratus clouds. The mean of the DPC is 51.778 with a standard deviation of 61.425.

47
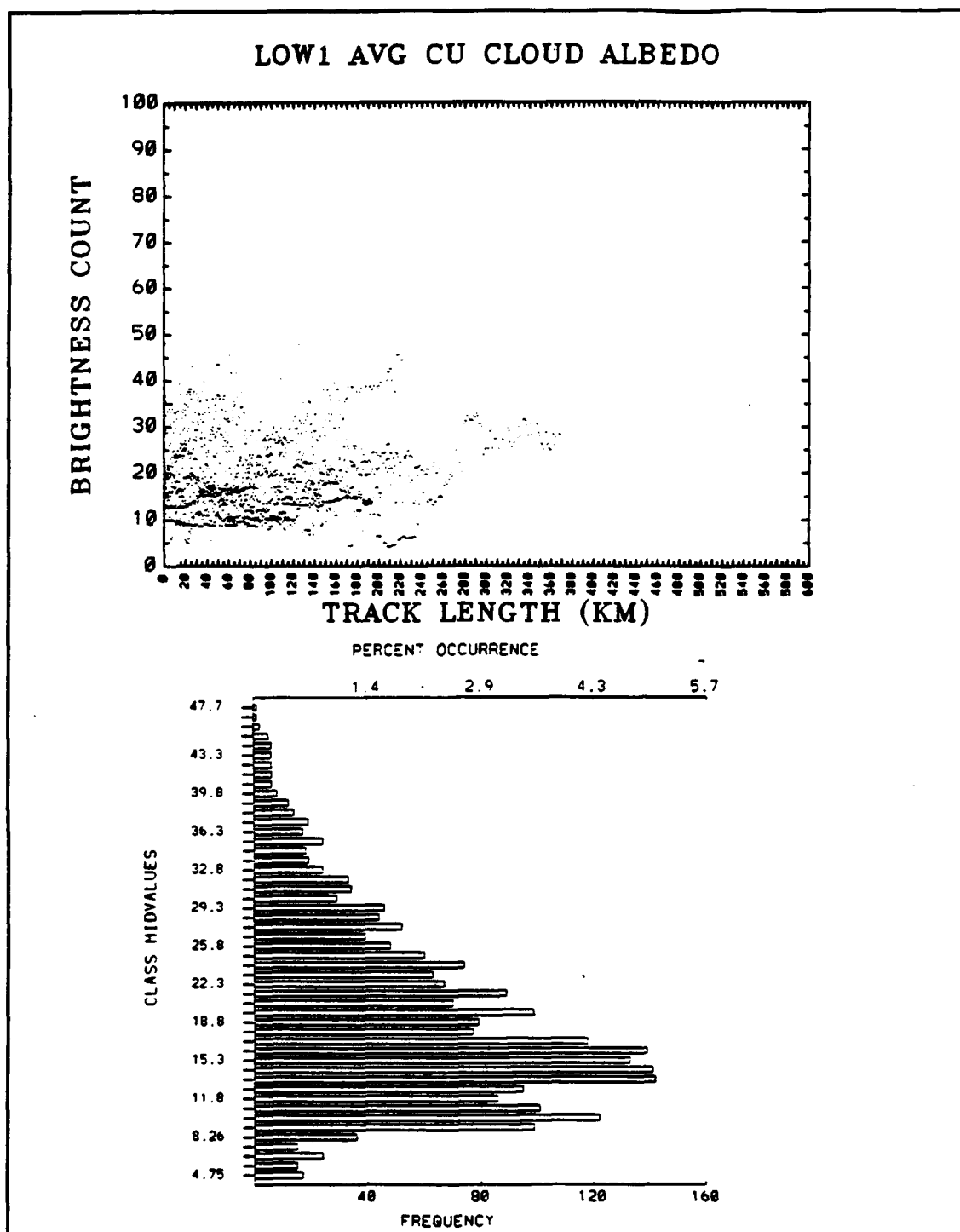
**Figure 19.** Scatterplot and Histogram for LOW1 Cumulus Cloud Regime.

# LOW1 AVG CU TRACK ALBEDO
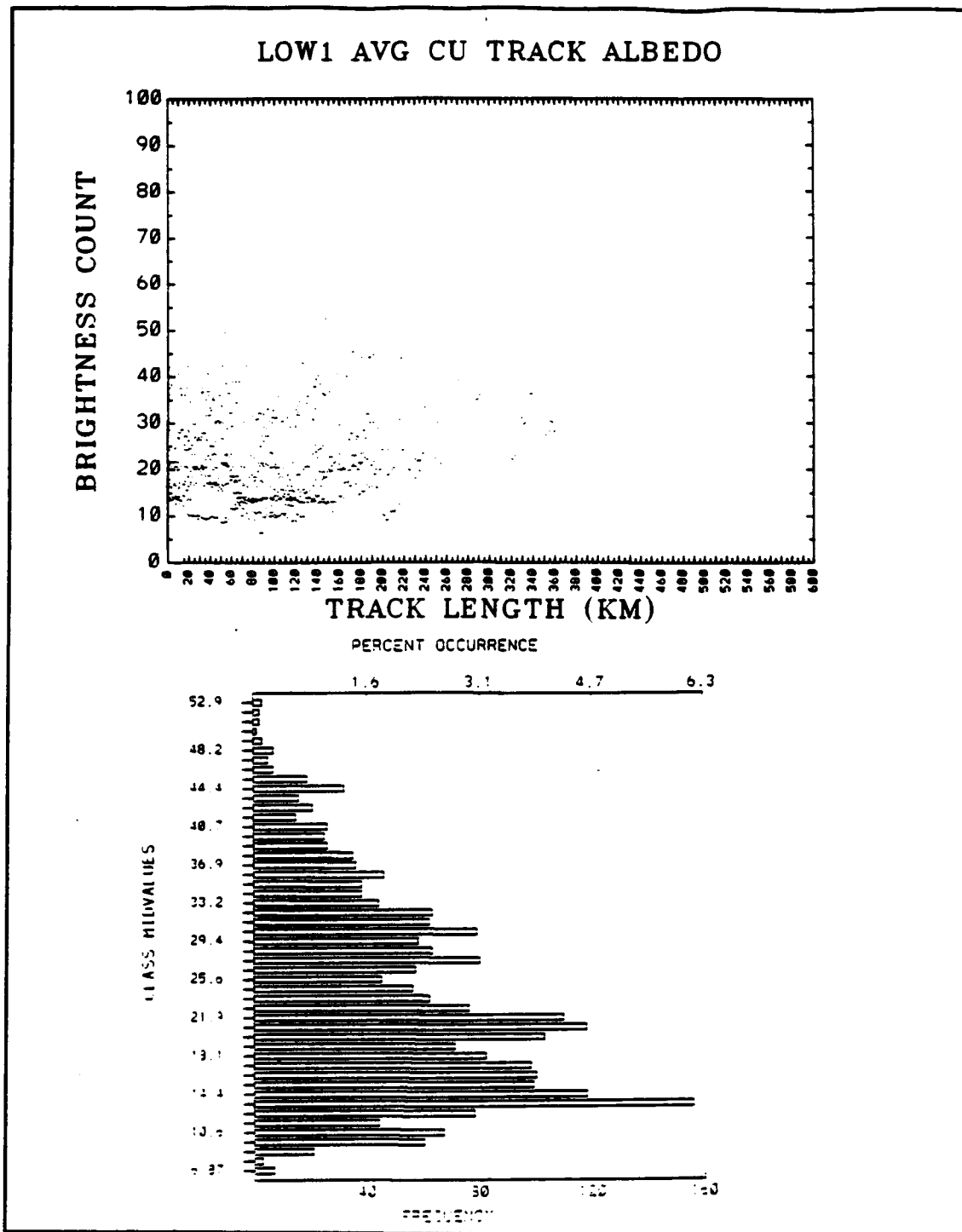


**Figure 20.** Scatterplot and Histogram for LOW1 Cumulus Tracks.

# LOW1 PERCENT CHANGE TRACK/CU CLOUDS
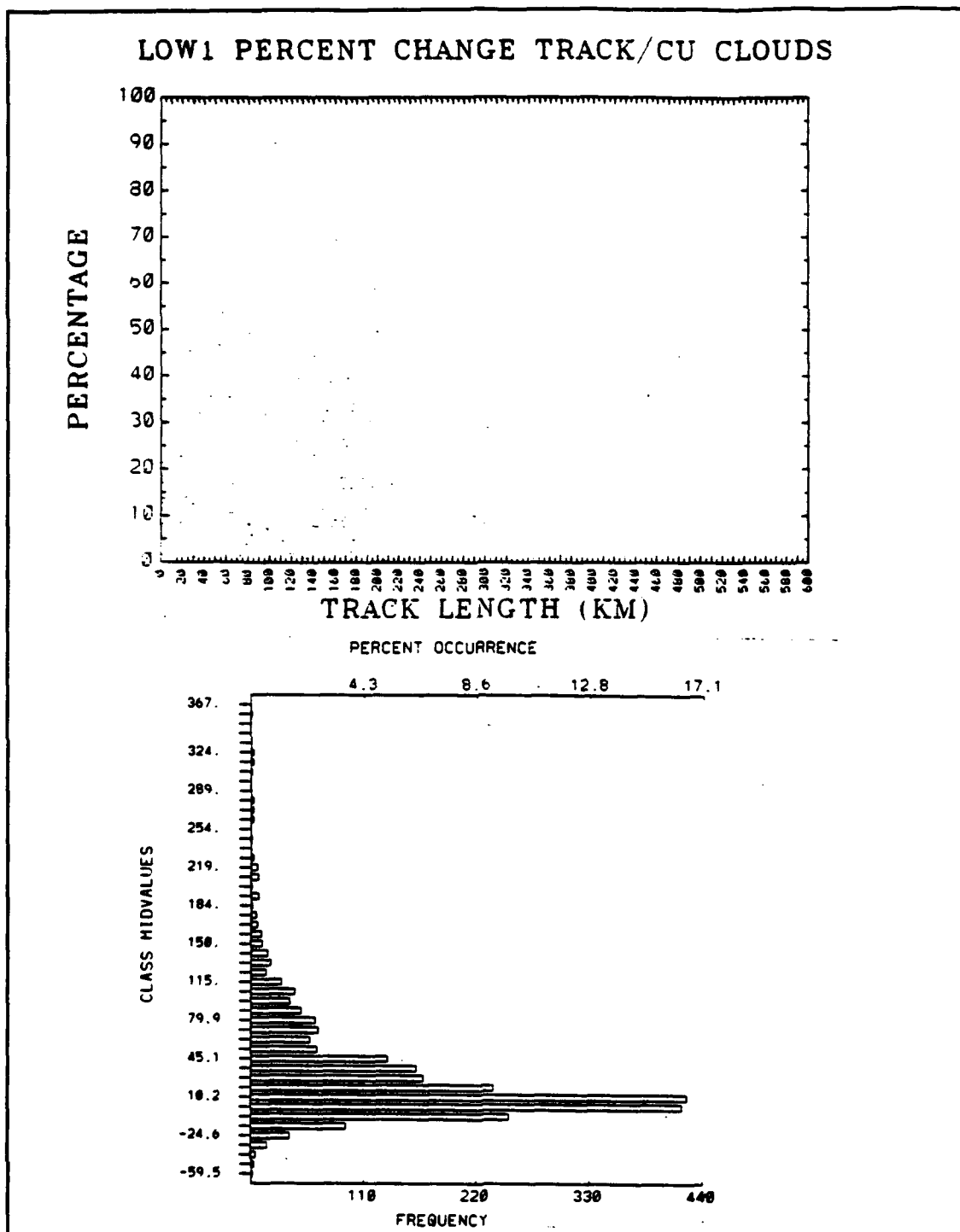


**Figure 21.** Scatterplot and Histogram for DPC LOW1 Track/Cloud.

### c. S12A

The S12A mean ratio is 1.172 in cumulus clouds with a standard deviation of 0.007 while the mean ratio of the track is 1.158 again with a standard deviation of 0.007. The average total percent change is -0.011 is larger than the previous two cases and establishes a trend that ship tracks gets brighter relative to their environment as the cloud fraction decreases. The MW test gives a significance of 100% to the differences in the means. The mean of the DPC is -1.088 with a standard deviation of 2.676. Scatterplots and histograms for the above data are contained in the Appendix.

### d. TMP4

The mean for the TMP4 for cumulus clouds is 286.5 °K and 286.4 °K in the track. There is no appreciable difference between the means of the cloud and track temperatures. However, the MW test gives a significance to the difference of 100%. The mean of the DPC is -0.005 with a standard deviation of 0.136. The cloud and track are both warmer than both the stratus and broken cases which is consistent with lower clouds. The Appendix includes the scatterplots and histograms for this data.

### e. T45

The mean of the T45 difference for cumulus clouds is -0.154 °K with a standard deviation of 1.236 °K. The track
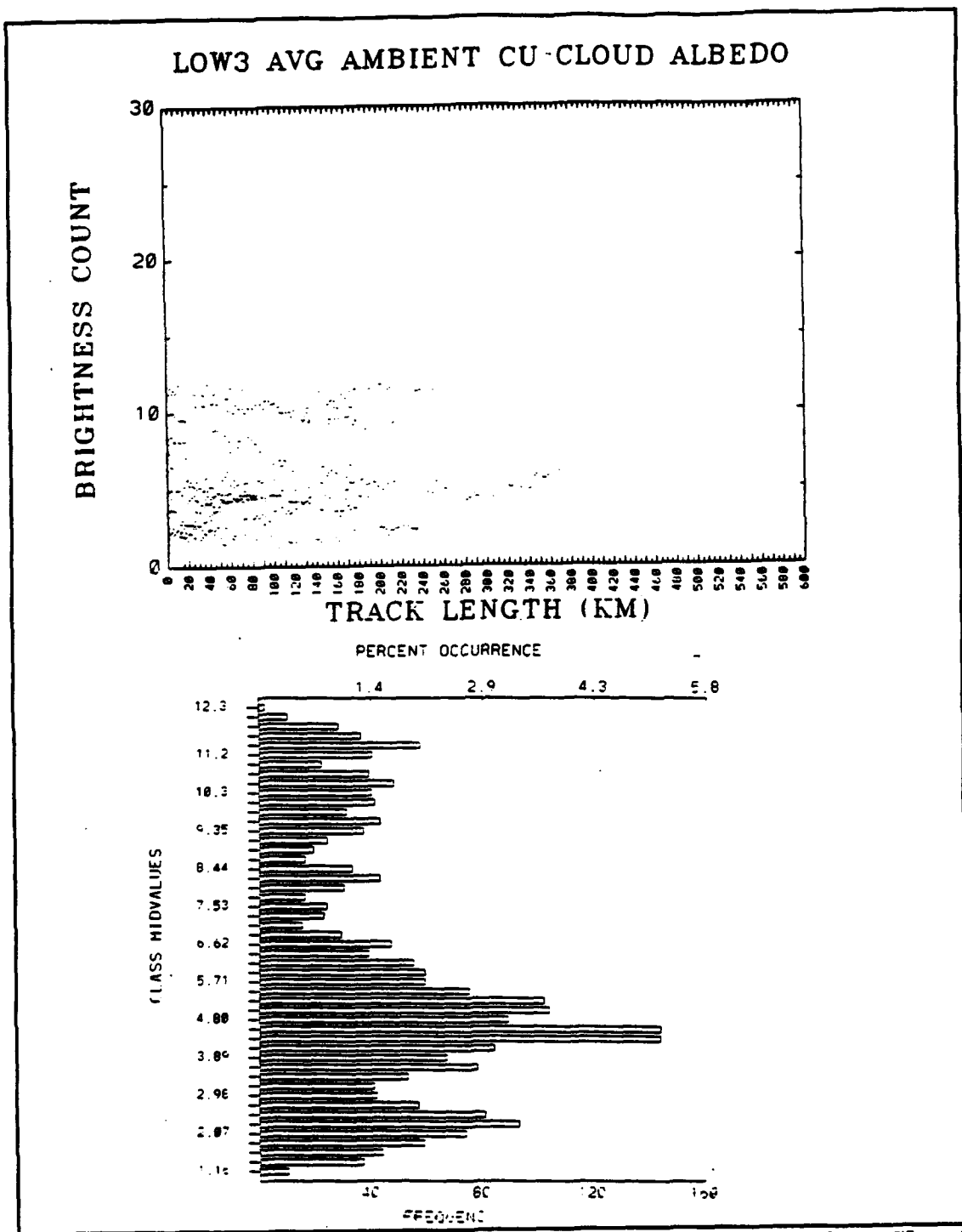
**Figure 22.** Scatterplot and Histogram for LOW3 Cumulus Cloud Regime.
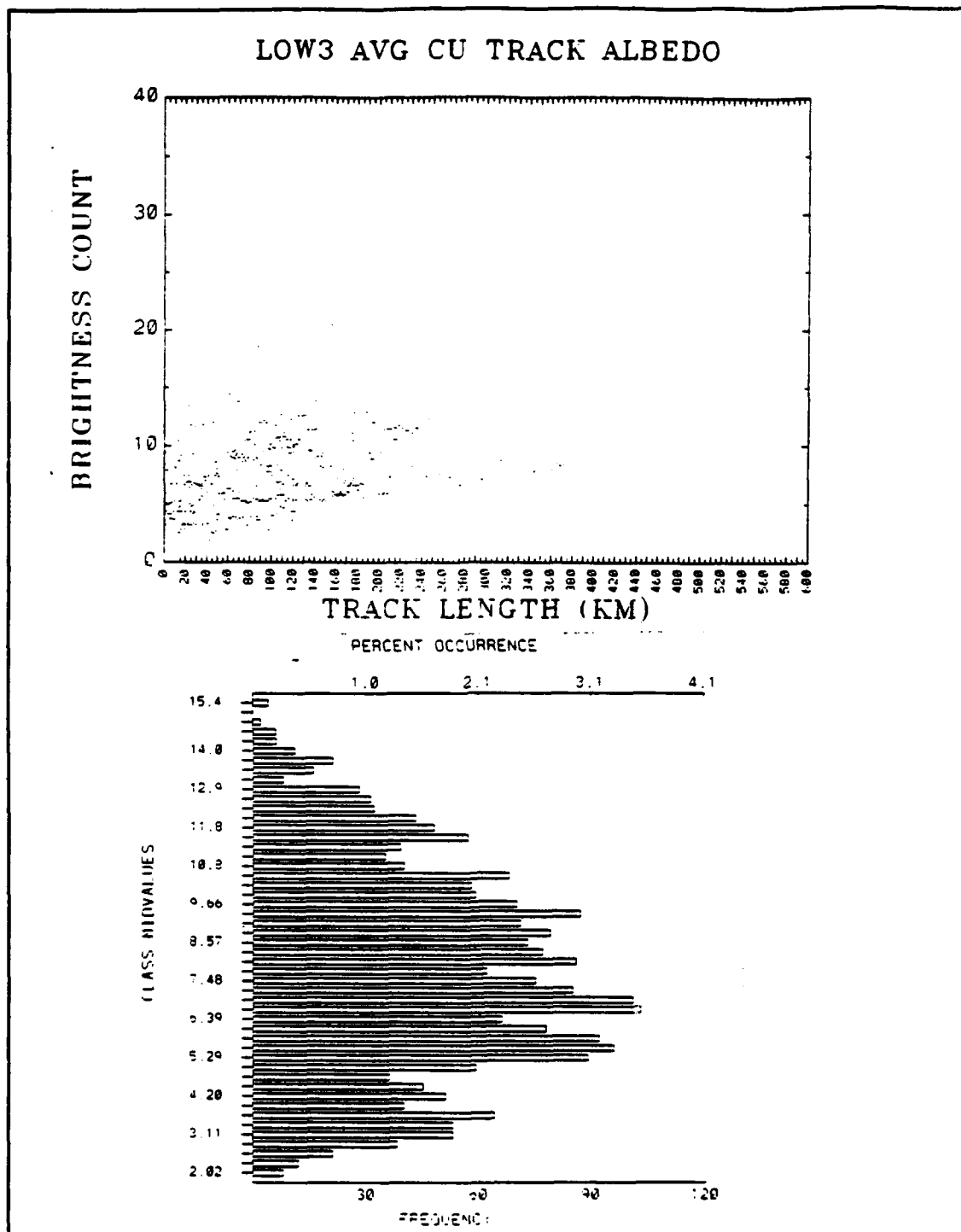
**Figure 23.** Scatterplot and Histogram for LOW3 Cumulus Tracks.

53
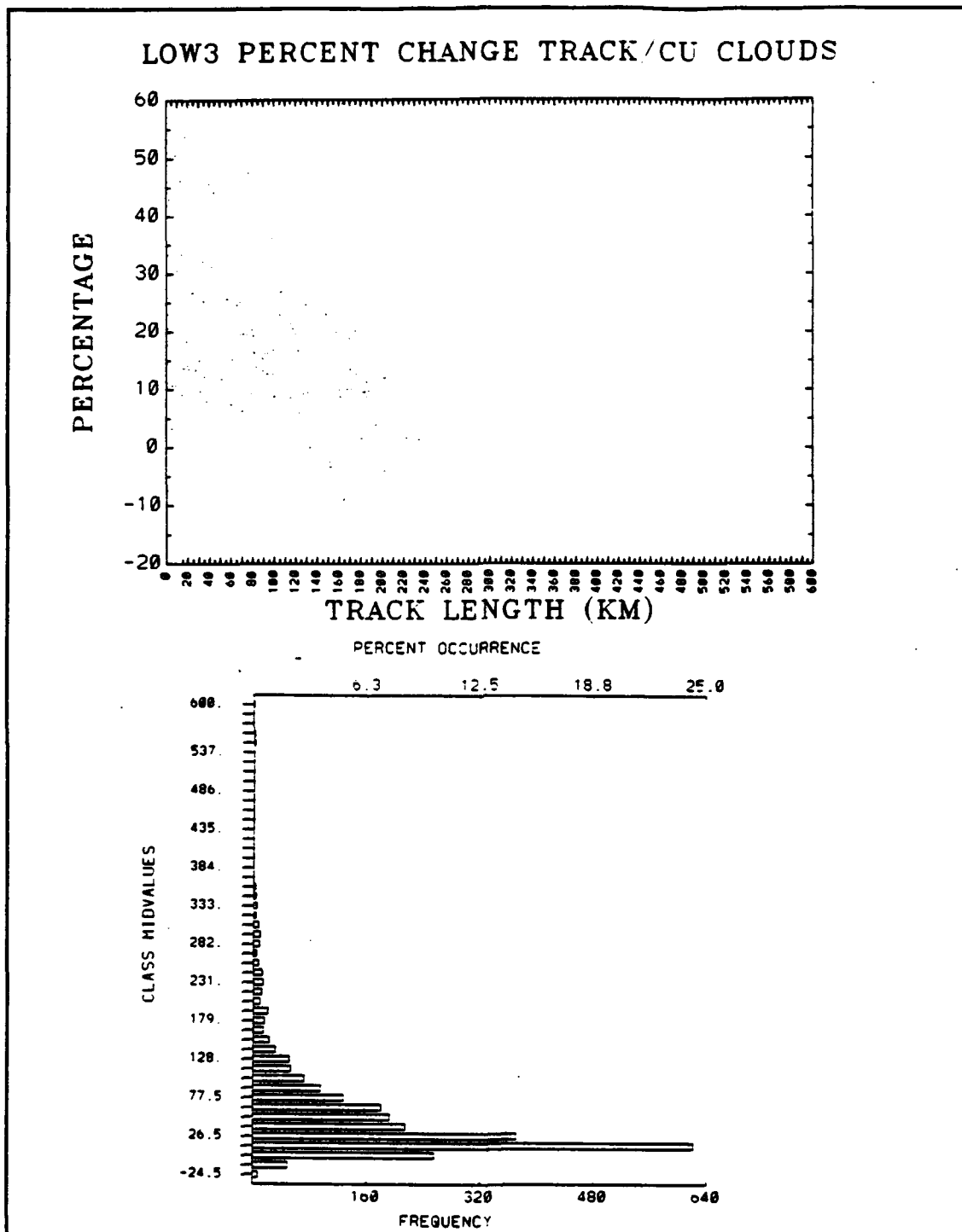
**Figure 24.** Scatterplot and Histogram for DPC LOW3 Cumulus Track/Cloud.

mean is 0.228 °K with a standard deviation of 0.233 °K. This again represents a large percentage change but no statistical significance is attached to this difference. Scatterplots and histograms for this data are in the Appendix.

A summary of the statistics for each of the image products described above for cumulus clouds is contained in Table IV. Table V contains a summary of the Mann-Whitney test results.

## E.  OBSERVATIONS OF SPATIAL CHARACTERISTICS

Each of the 63 ship tracks collected for the study was manually analyzed to determine the width of track as a function of length. The tracks ranged in length from tens to hundreds of kilometers. One ship track observed, but not analyzed in this study, was well over 1000 km long. If the ship was moving at 25 knots then this track was over two days old.

### 1.  Width of Tracks

The spatial variations between cloud types was not as dramatic as originally hypothesized. One hundred kilometers down the length of the track was used as a benchmark for the analysis of track width and dispersion. Tracks which form in stratus cloud were found to be 4-9 km wide. Broken stratus

**Table IV.** SUMMARY OF STATISTICS CUMULUS CLOUD/TRACK.

| PRODUCT | MEAN | STD DEV | % CHANGE |
|---|---|---|---|
| LOW1 CU | 19.054 (A) | 8.210 | |
| LOW1 TRACK | 23.427 (A) | 9.564 | |
| LOW1 TRK/CU | | | 0.22 |
| LOW1 DPC | 30.231 | 46.975 | |
| LOW3 CU | 5.748 (A) | 2.945 | |
| LOW3 TRACK | 7.721 (A) | 2.864 | |
| LOW3 TRK/CU | | | 0.34 |
| LOW3 DPC | 51.778 | 61.425 | |
| S12A CU | 1.172 (R) | 0.007 | |
| S12A TRACK | 1.158 (R) | 0.007 | |
| S12A TRK/CU | | | -0.011 |
| S12A DPC | -1.088 | 2.676 | |
| TMP4 CU | 286.5 (T) | 1.443 | |
| TMP4 TRACK | 286.4 (T) | 1.431 | |
| TMP4 TRK/CU | | | .000 |
| TMP4 DPC | -0.005 | 0.136 | |
| T45 CU | -0.154 (D) | 1.236 | |
| T45 TRACK | 0.228 (D) | 0.233 | |
| T45 TRK/CU | | | -248.00 |
| T45 DPC | -17.233 | 120.286 | |
| A=ALBEDO, R=RATIO, T=TEMPERATURE (°K), D=DIFFERENCE | | | |

**Table V.** SUMMARY OF MANN-WHITNEY TEST RESULTS.

| MEAN VALUES CLOUD/TRACK | PROBABILITY |
|---|---|
| LOW1 STRATUS/TRACK | 100% |
| LOW1 BROKEN/TRACK | 100% |
| LOW1 CUMULUS/TRACK | 100% |
| LOW3 STRATUS/TRACK | 100% |
| LOW3 BROKEN/TRACK | 100% |
| LOW3 CUMULUS/TRACK | 100% |
| S12A STRATUS/TRACK | >79% |
| S12A BROKEN/TRACK | 100% |
| S12A CUMULUS/TRACK | 100% |
| TMP4 STRATUS/TRACK | >56% |
| TMP4 BROKEN/TRACK | >99% |
| TMP4 CUMULUS/TRACK | >99% |
| T45 STRATUS/TRACK | 100% |
| T45 BROKEN/TRACK | >93% |
| T45 CUMULUS/TRACK | 100% |

cloud regime tracks ranged from 4-10 km. The width of tracks in cumulus clouds at 100 km also was between 4-9 km. This result was surprising since the weaker inversion, particularly in cumulus clouds, allows vertical motion to penetrate and disperse boundary constituents. It was expected ship tracks in the cumulus environment would be wider and more diffuse than was observed.

## 2. Length of Tracks

The length of ship tracks in each environment was difficult to quantify. Tracks were collected in each image product so as to include the head of the track and as much of the track as would fit in the 512 X 512 image. Some tracks were too long to be captured in one image. In addition, the ship track extraction algorithm limited extraction of tracks too near to the edges of the subscene to ensure a complete sample of the track and the ambient cloud. So any quantitative analysis of ship track length in this study would not be valid. Qualitatively however, observations throughout the collection and analysis process indicate that tracks which form in stratus clouds tend to be longer. This is consistent with the strong capping inversion associated with this environment. This cap would tend to limit vertical dispersion of the track and perhaps make it more long lived. Broken and cumulus tracks were generally the same, although exceptionally long tracks were observed in these environments as well.

58

# IV. CONCLUSIONS AND RECOMMENDATIONS

## A. CONCLUSIONS

The purpose of this thesis was to investigate and analyze the radiative and spatial variations of ship tracks in three distinct marine stratiform cloud environments: stratus, broken stratus and cumulus. The variations is ship tracks are consistent with the differences in inversion strength, liquid water content and vertical velocity present in each environment.

The results indicate that the radiative signature of ship tracks varies with respect to the environment in which it forms. Specifically:

- A comparison of the means of ship tracks and ambient clouds for each environment shows that the tracks are at least 11% brighter in LOW1 and at least 27% brighter in LOW3. Cumulus tracks have the highest average albedo relative to their environment in LOW1 at 22%. Broken stratus tracks are highest in their environment at 40% in LOW3.

- The delta percent change statistic indicates broken stratus tracks are 2% brighter than cumulus tracks and 18% brighter than stratus tracks relative to their environment in LOW3. In LOW1 cumulus tracks are 4% brighter than broken stratus tracks and 15% brighter than stratus tracks.

59

- There is a link between the albedo of the track and the liquid water content of the cloud. Cumulus tracks are generally brightest with respect to their environment but lowest in absolute albedo over stratus and broken stratus tracks. Ship do not appear to enhance the liquid water content of the clouds they pass beneath.

- The S12A signature observed supports the observations noted in LOW1 and LOW3.

- There was no temperature change observed between the track and its environment in all three cases.

- The T45 signature shows a large percentage change between the track and the ambient cloud but the differences are between very small numbers, so the percent change is greatly inflated.

- Spatial variations in the width of ship tracks between each environments was small but the lengths of tracks in solid stratus tended to be longer than in the other two environments.

## B.  RECOMMENDATIONS

This study represents the first attempt at identifying differences in the radiative and spatial characteristics of ship tracks with respect to the cloud type in which they form. In this approach cloud fields were classified into three broad categories. Many cloud sub-types were observed within each broad category. The physical mechanisms responsible for ship track formation are still not well understood so future ship track research should:

- Continue to refine the ship track detection algorithm.

60

· Automate the collection, extraction, classification and archiving of ship tracks.

· Continue to analyze ship tracks in a variety of cloud environments for clues to their formation mechanisms.

· Continue in-situ location of ships producing tracks

· Continue to investigate ship track formation mechanisms with respect to cloud liquid water content and CCN concentrations to better understand the environmental parameters necessary for ship track production.

Much work remains to be done on this subject. Collection and analysis of this data is important because of its applications to military intelligence, commerce, and climatology. Continuing investigation of these small cloud streaks could, perhaps, help unravel the effect man has on the global environment.

## APPENDIX. SCATTERPLOTS AND HISTOGRAMS

The scatterplots and histograms for S12A, TMP4 and T45 stratus, broken stratus and cumulus cloud regimes and ship tracks can be found in this Appendix. The S12A plots appear in Figures A1 to A9. The TMP4 plots appear in Figures A10 to A18 and the T45 plots appear in Figures A19 to A27.

62

# S12A AVG AMBIENT ST CLOUD ALBEDO
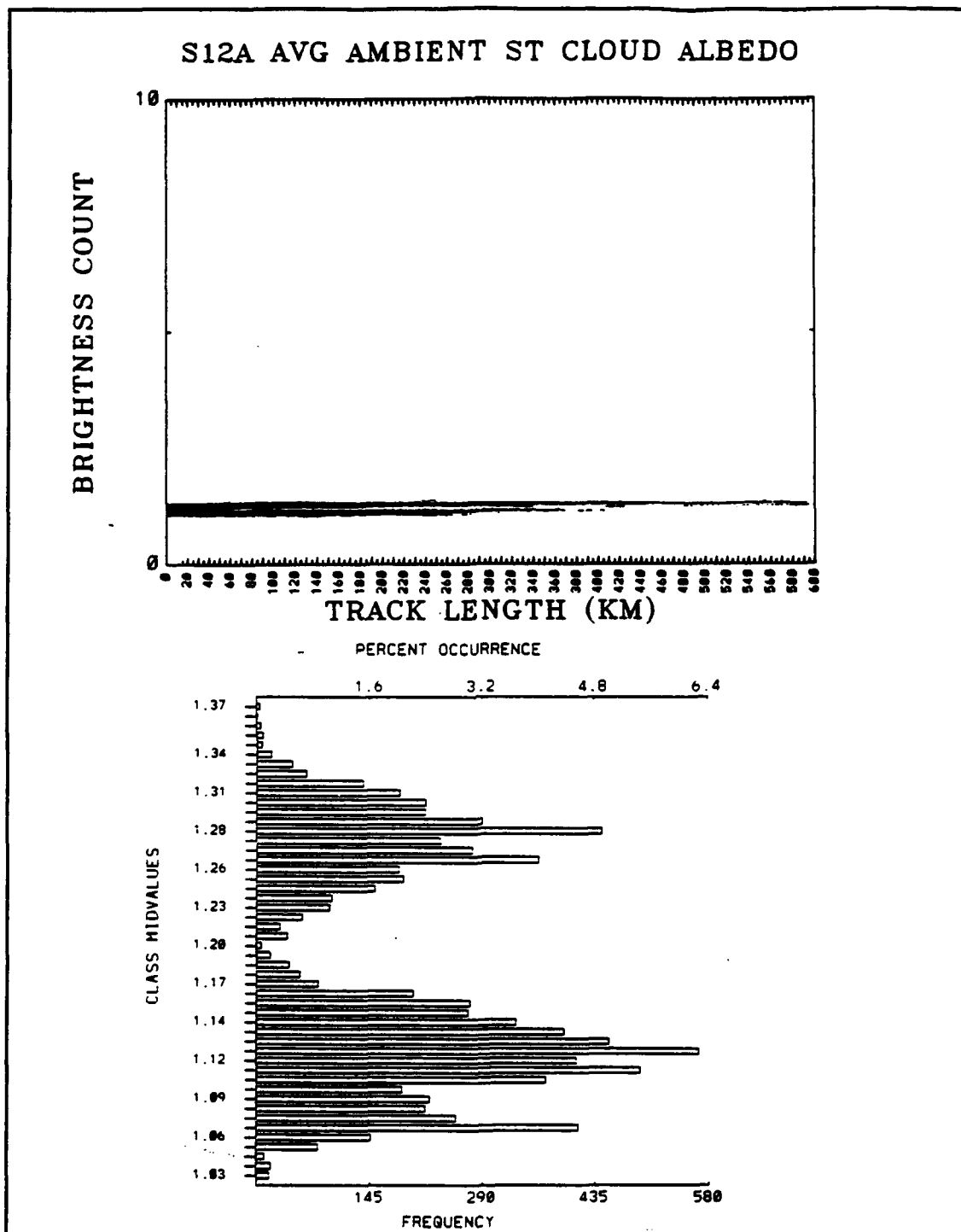


**Figure A1.** Scatterplot and Histogram for S12A Stratus Cloud Regime.
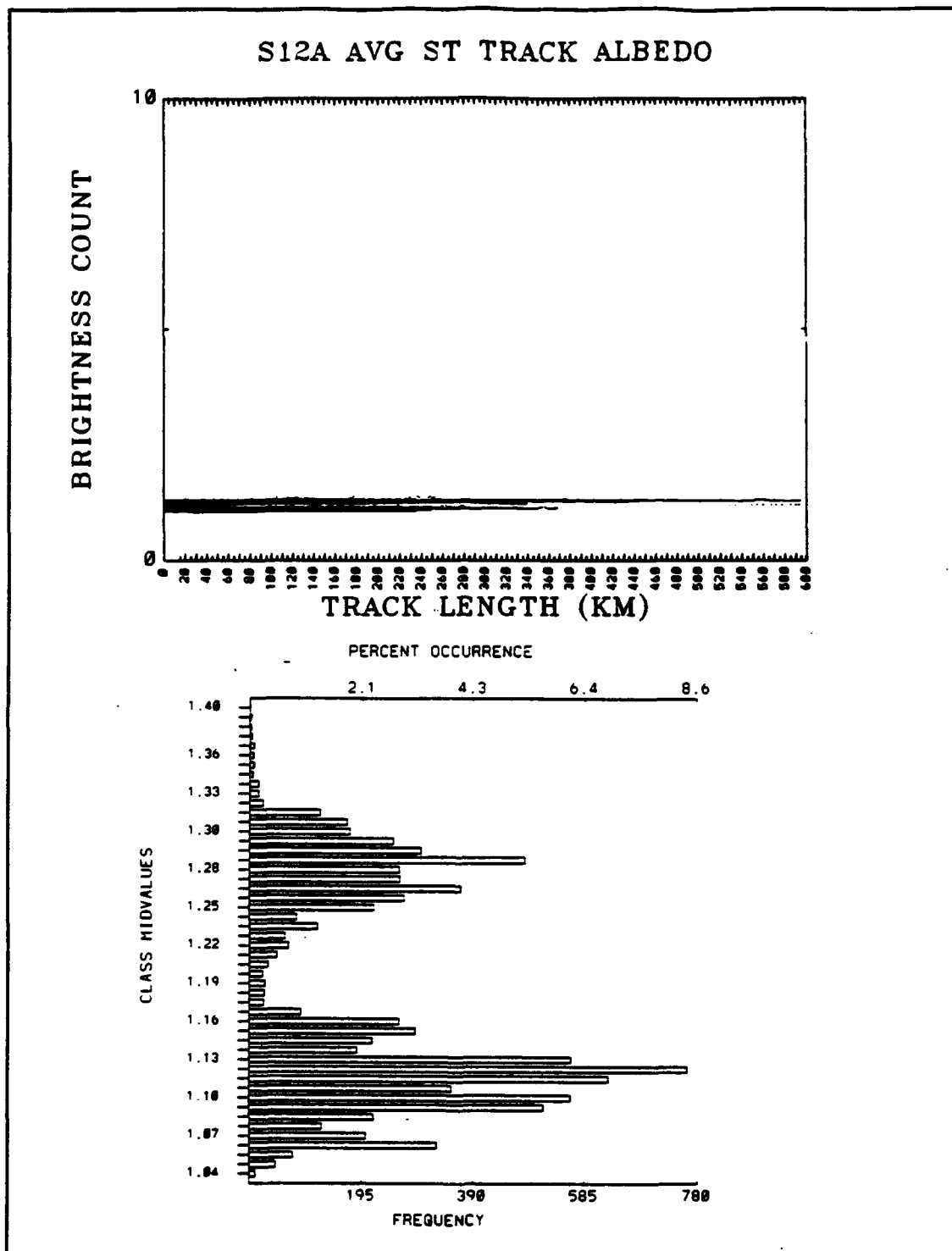
**Figure A2.** Scatterplot and Histogram for S12A Stratus Track.
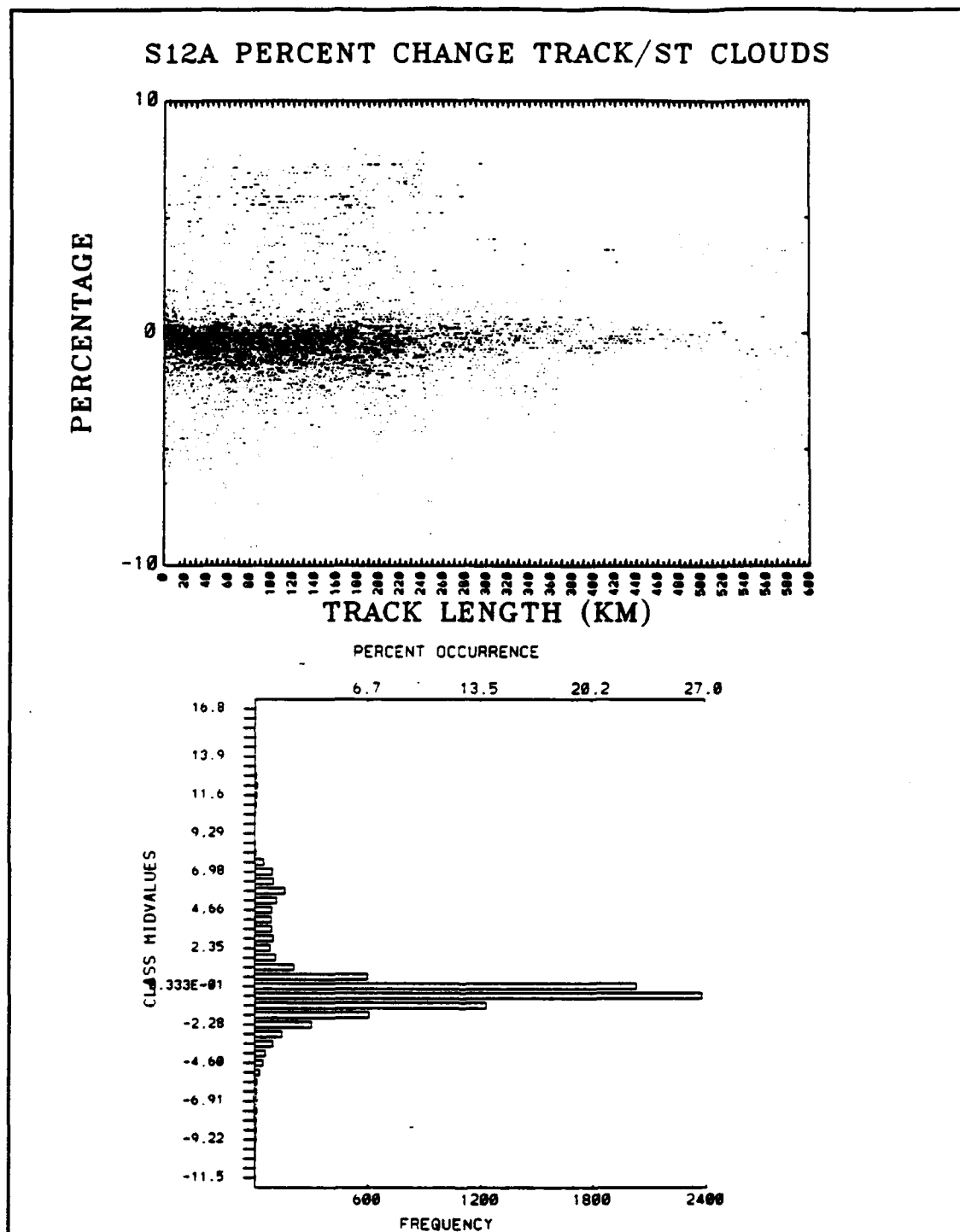
**Figure A3.** Scatterplot and Histogram for DPC S12A Stratus Track/Cloud.
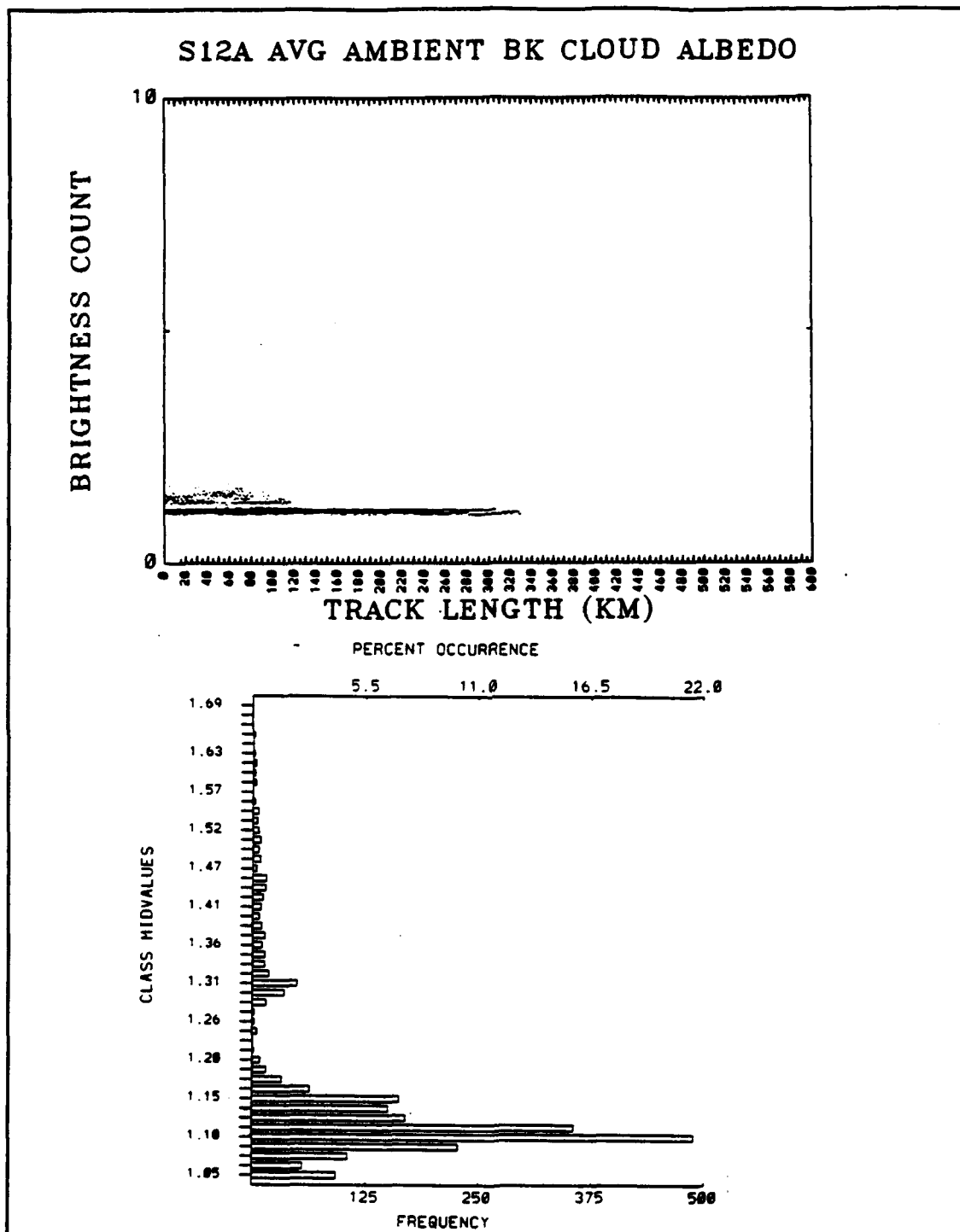
**Figure A4.** Scatterplot and Histogram for S12A Broken Stratus Cloud Regime.

## S12A AVG BK TRACK ALBEDO
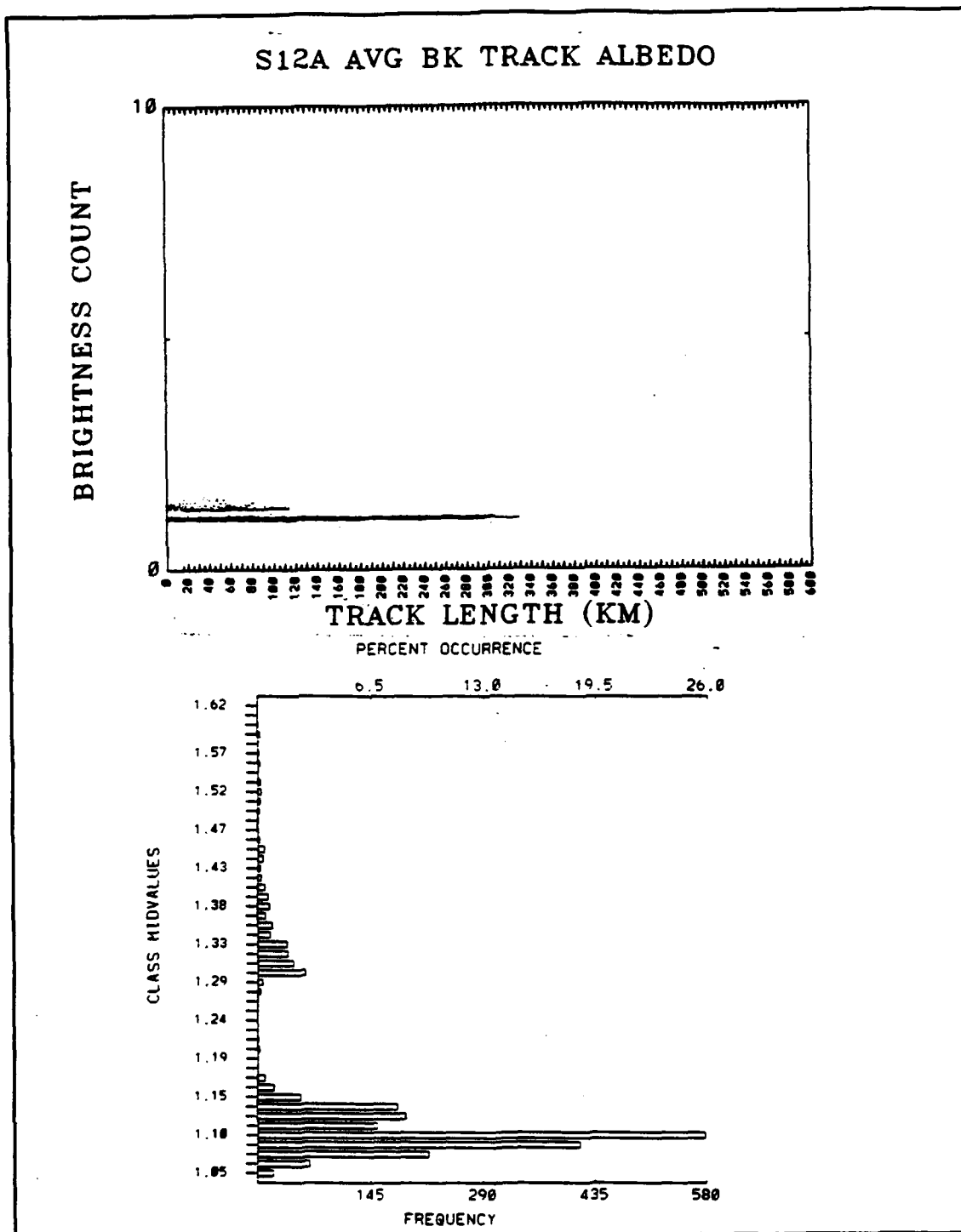


**Figure A5.** Scatterplot and Histogram for S12A Broken Stratus Tracks.

# S12A PERCENT CHANGE TRACK/BK CLOUDS
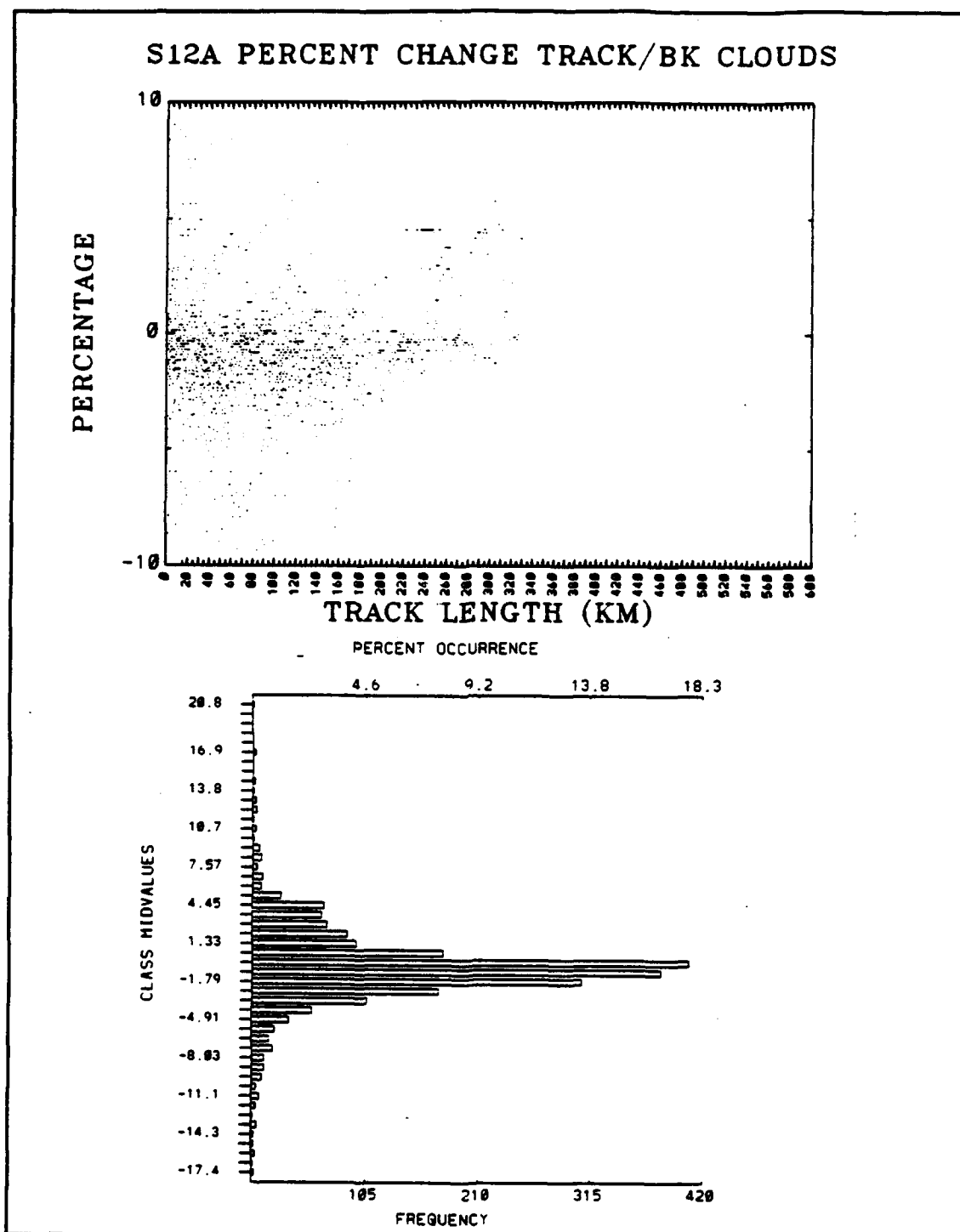


**Figure A6.** Scatterplot and Histogram for DPC S12A Broken Stratus Track/Cloud.

## S12A AVG AMBIENT CU CLOUD ALBEDO
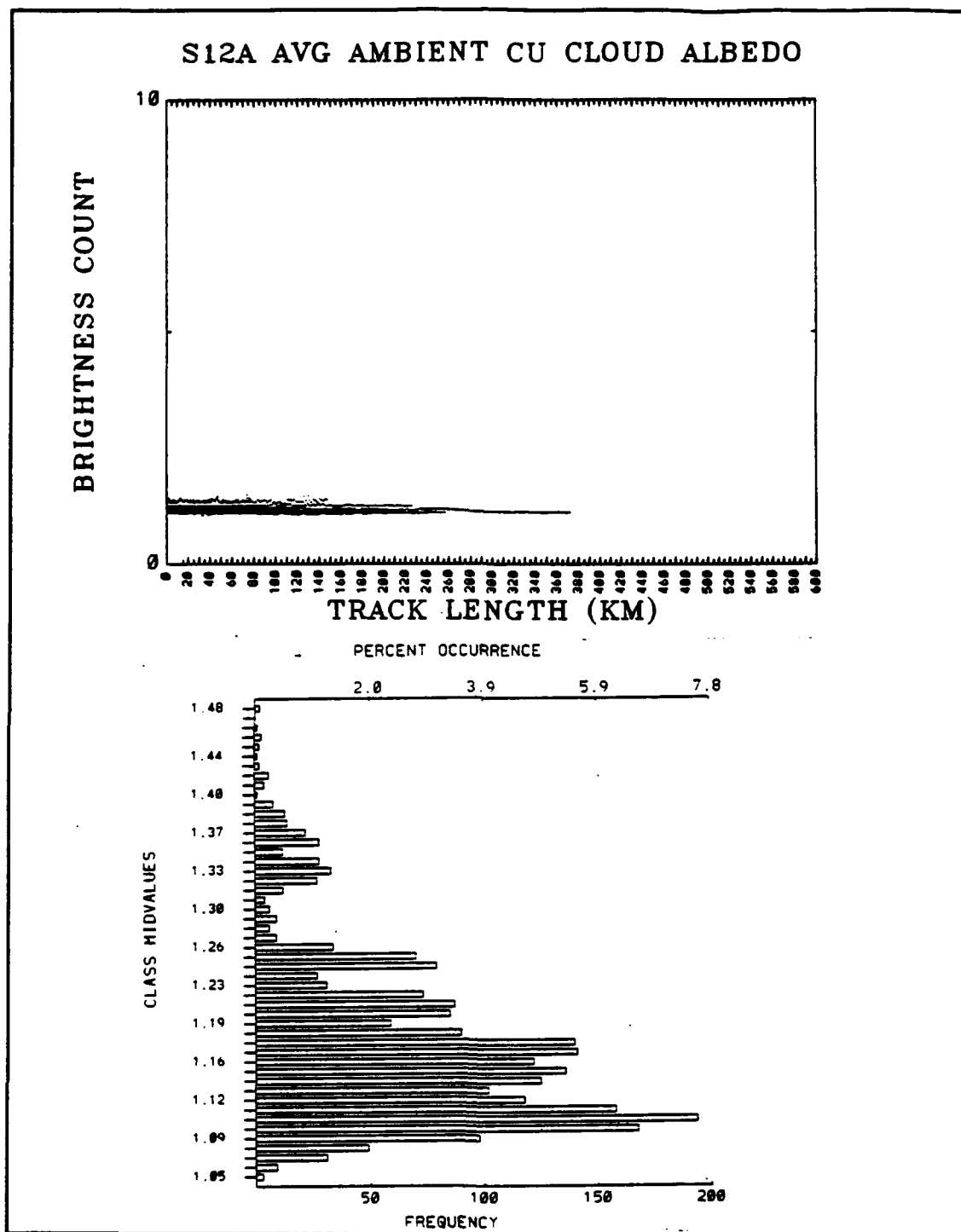


**Figure A7.** Scatterplot and Histogram for S12A Cumulus Cloud Regime.

# S12A AVG CU TRACK ALBEDO
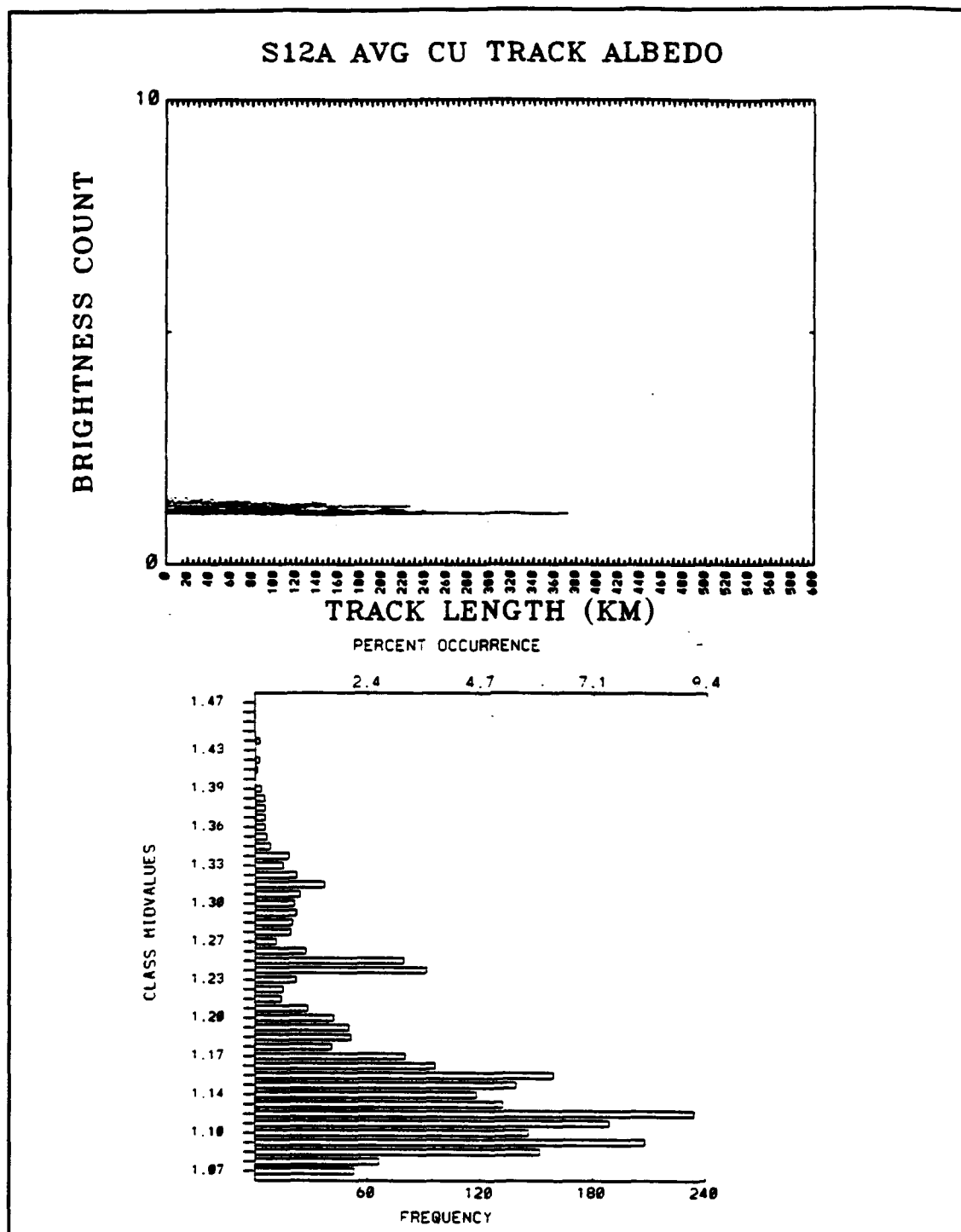


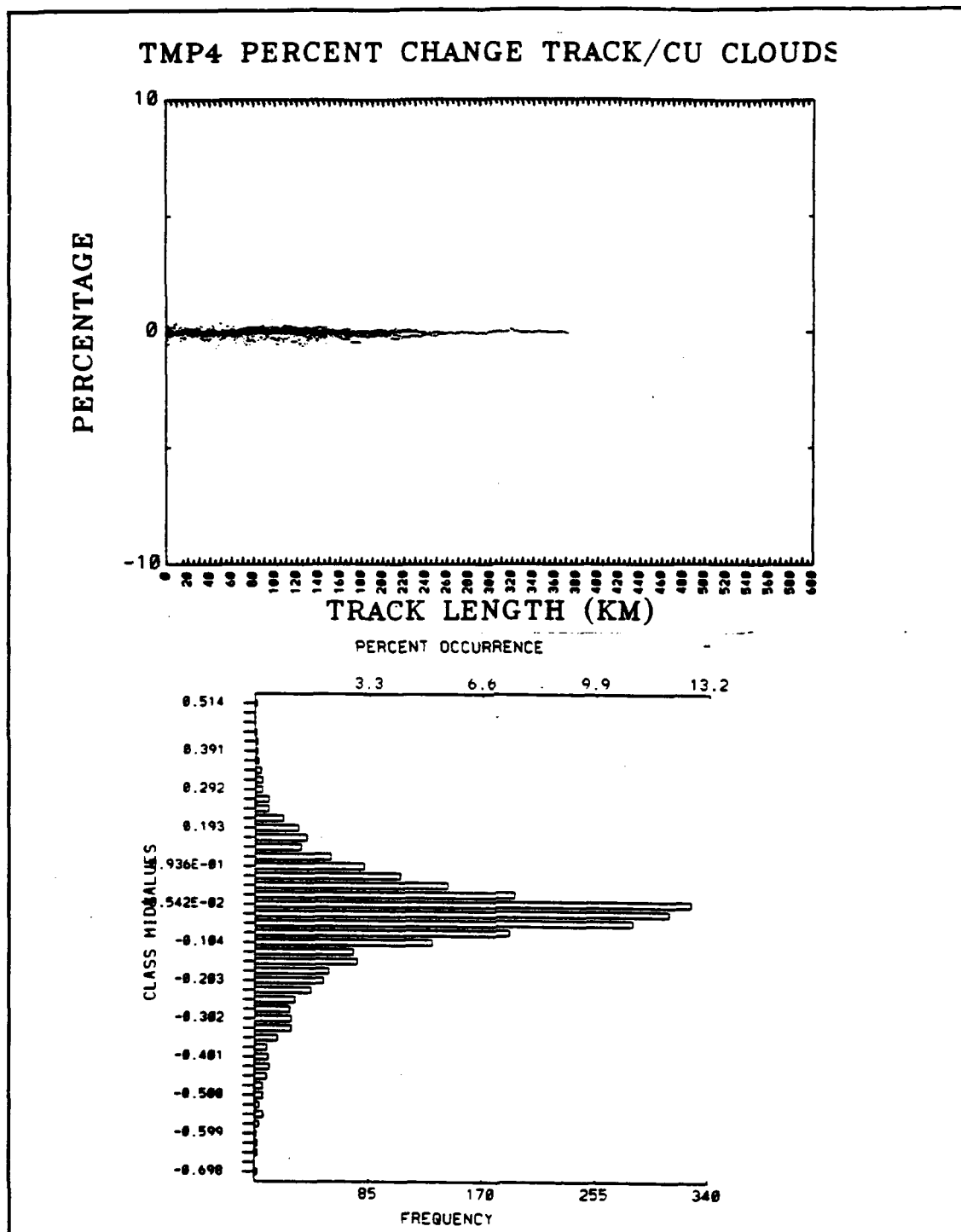**Figure A8.** Scatterplot and Histogram for S12A Cumulus Tracks.
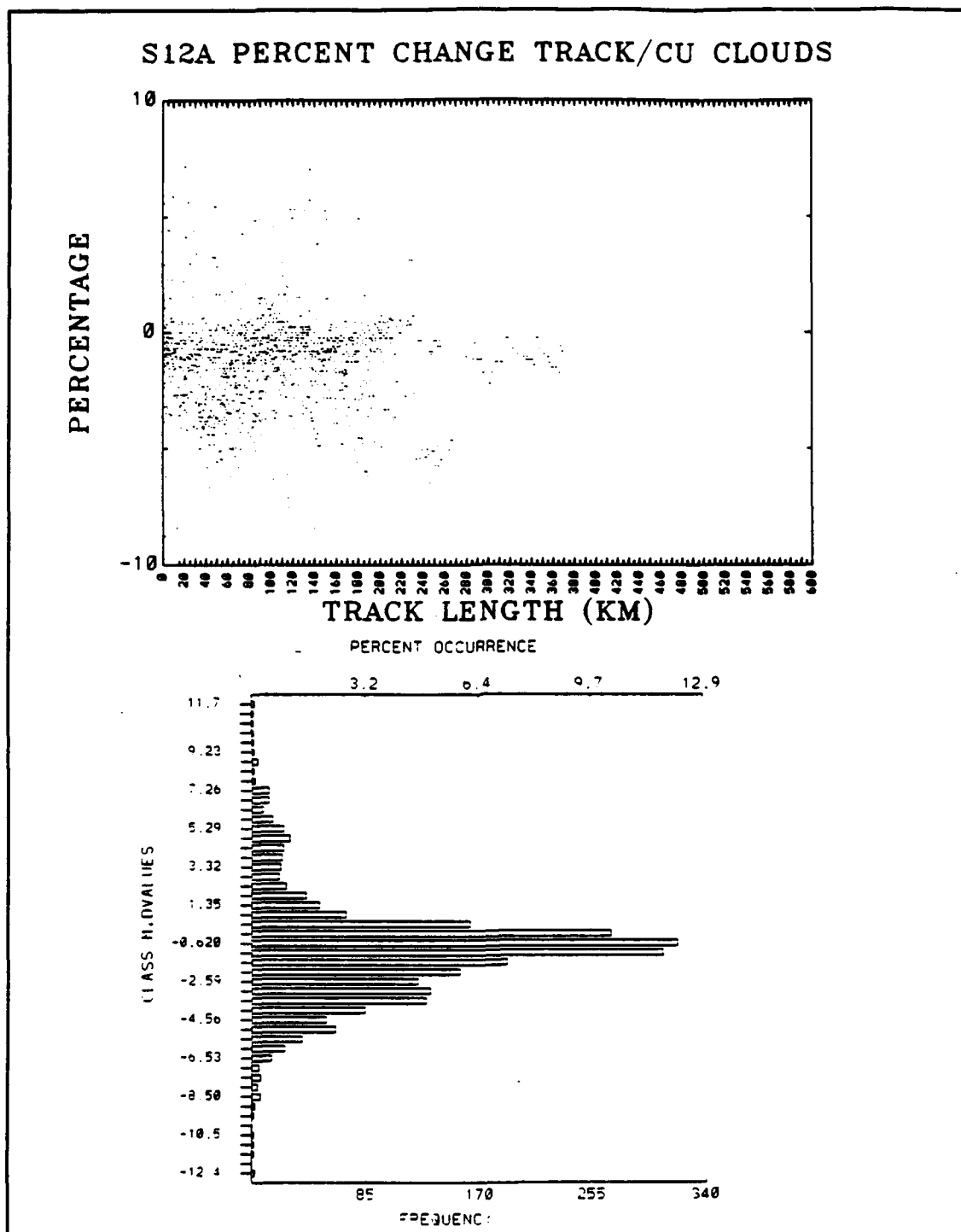
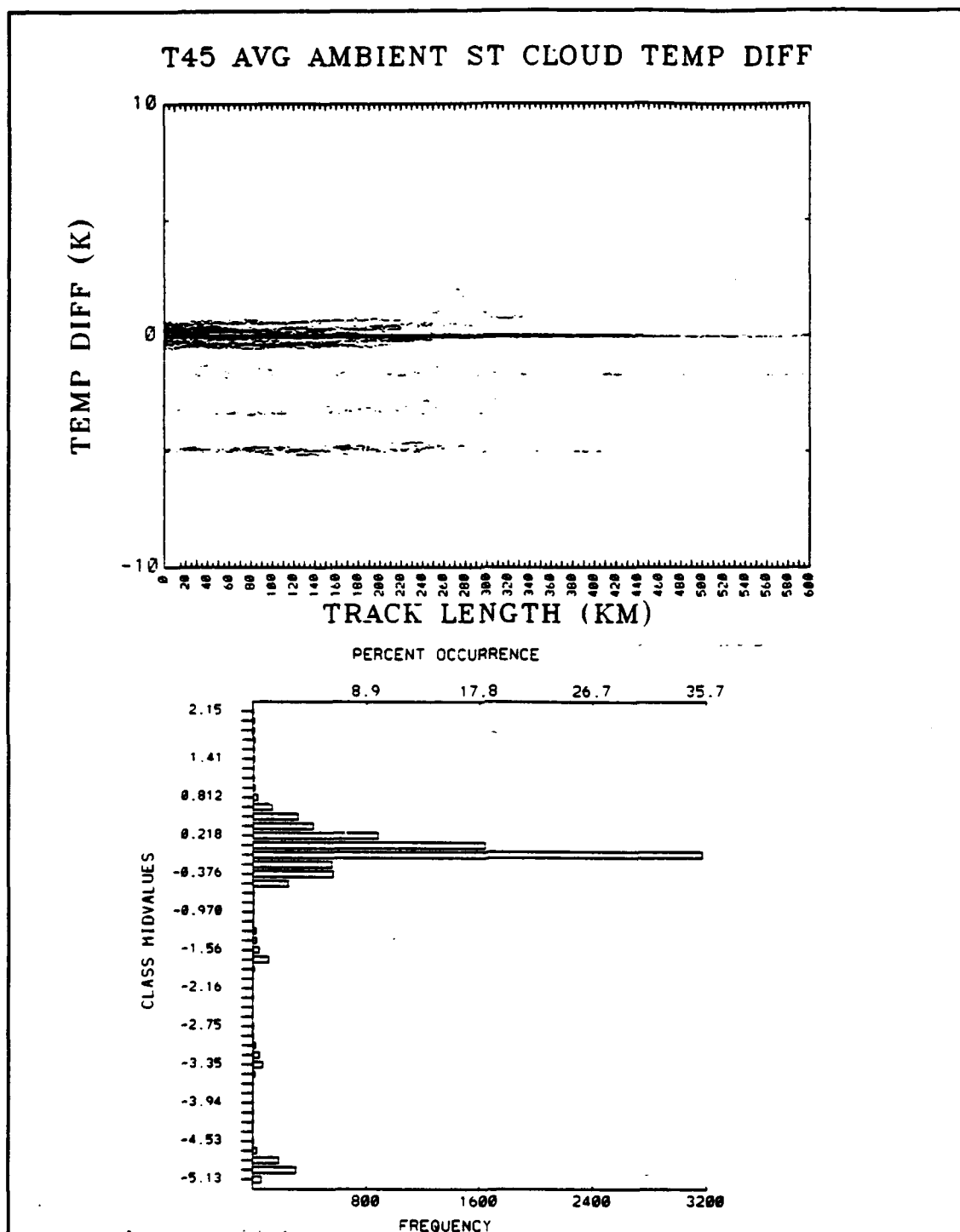**Figure A9.** Scatterplot and Histogram for DPC S12A Cumulus Track/Cloud.

71
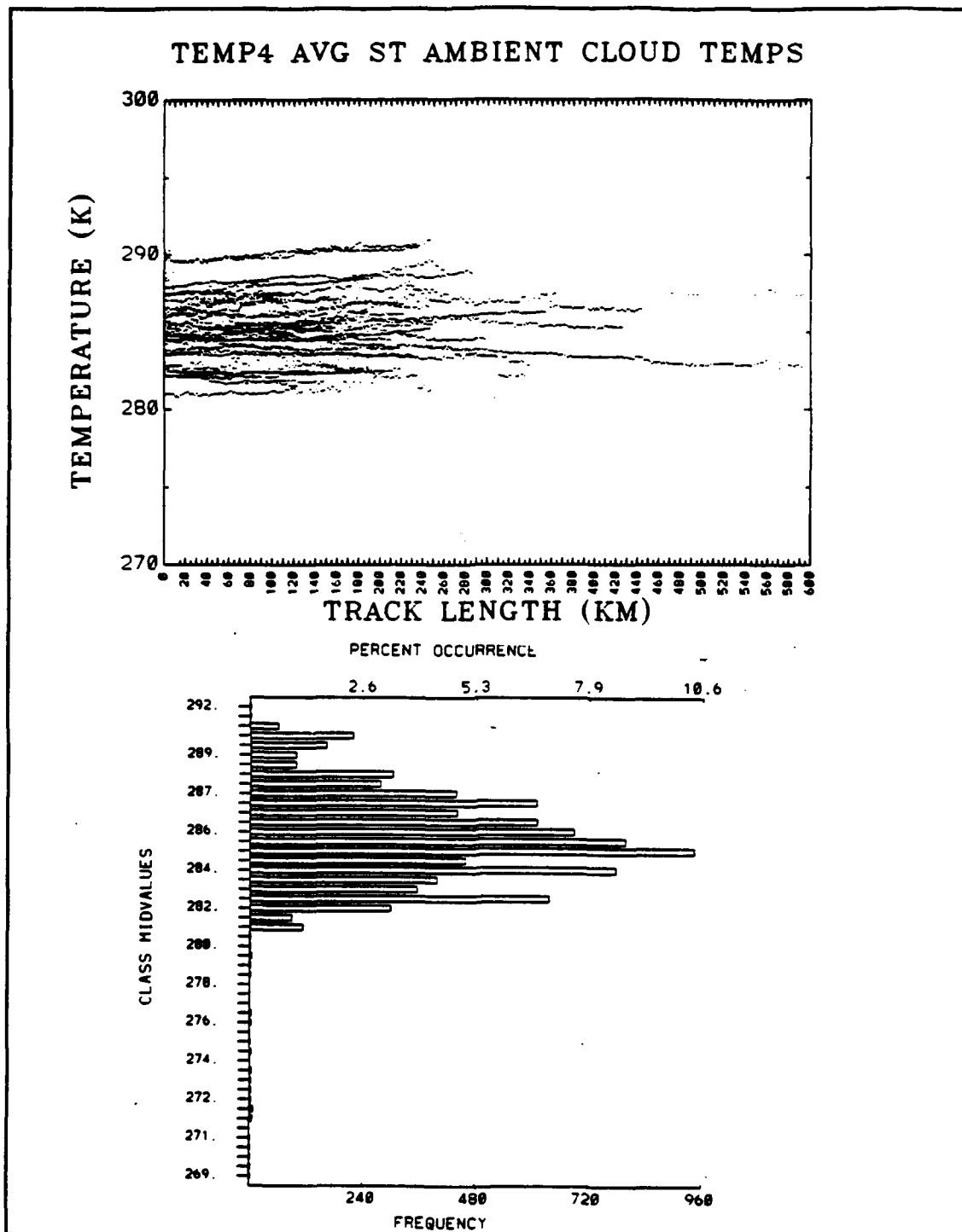
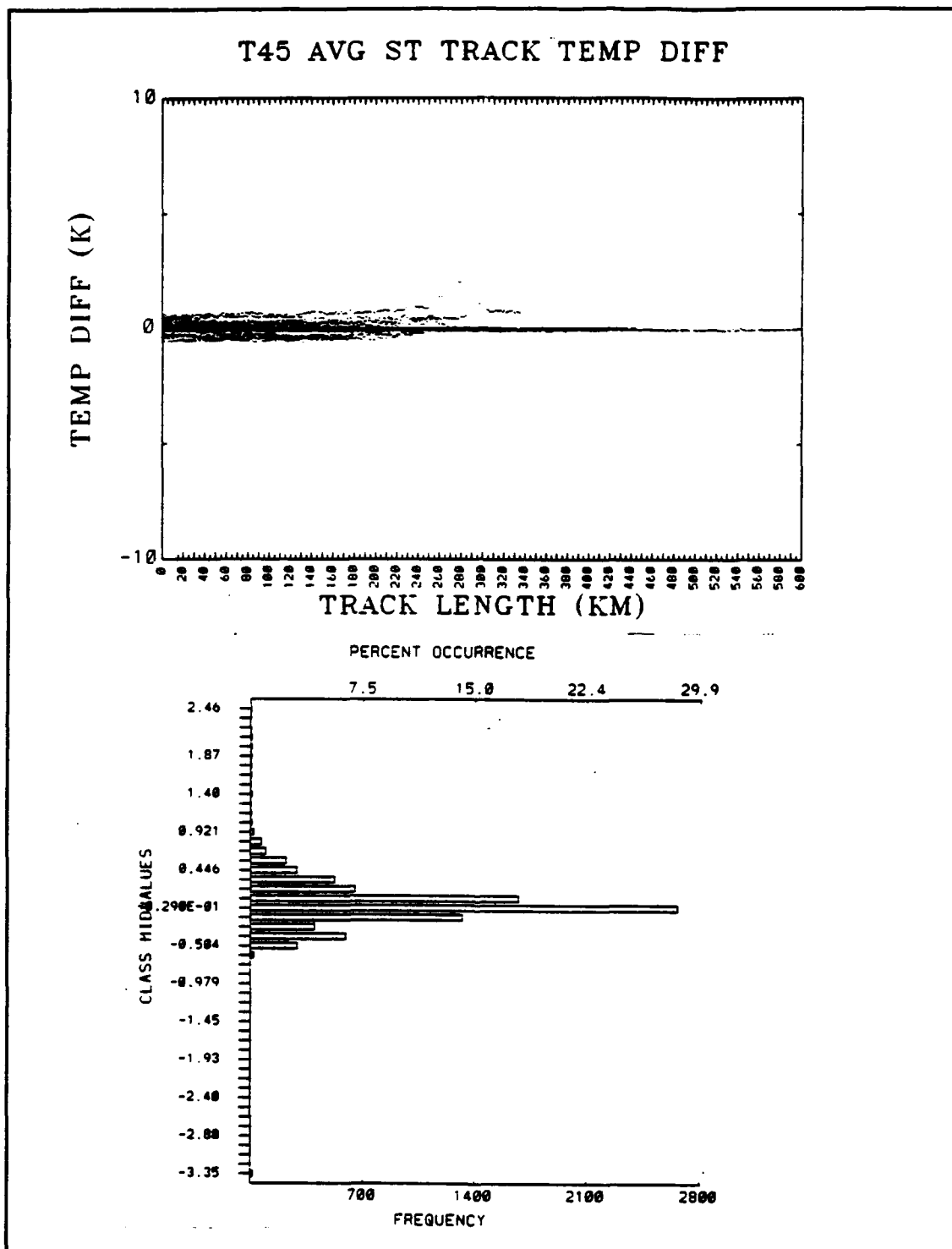**Figure A10.** Scatterplot and Histogram for TMP4 Stratus Cloud Regime.
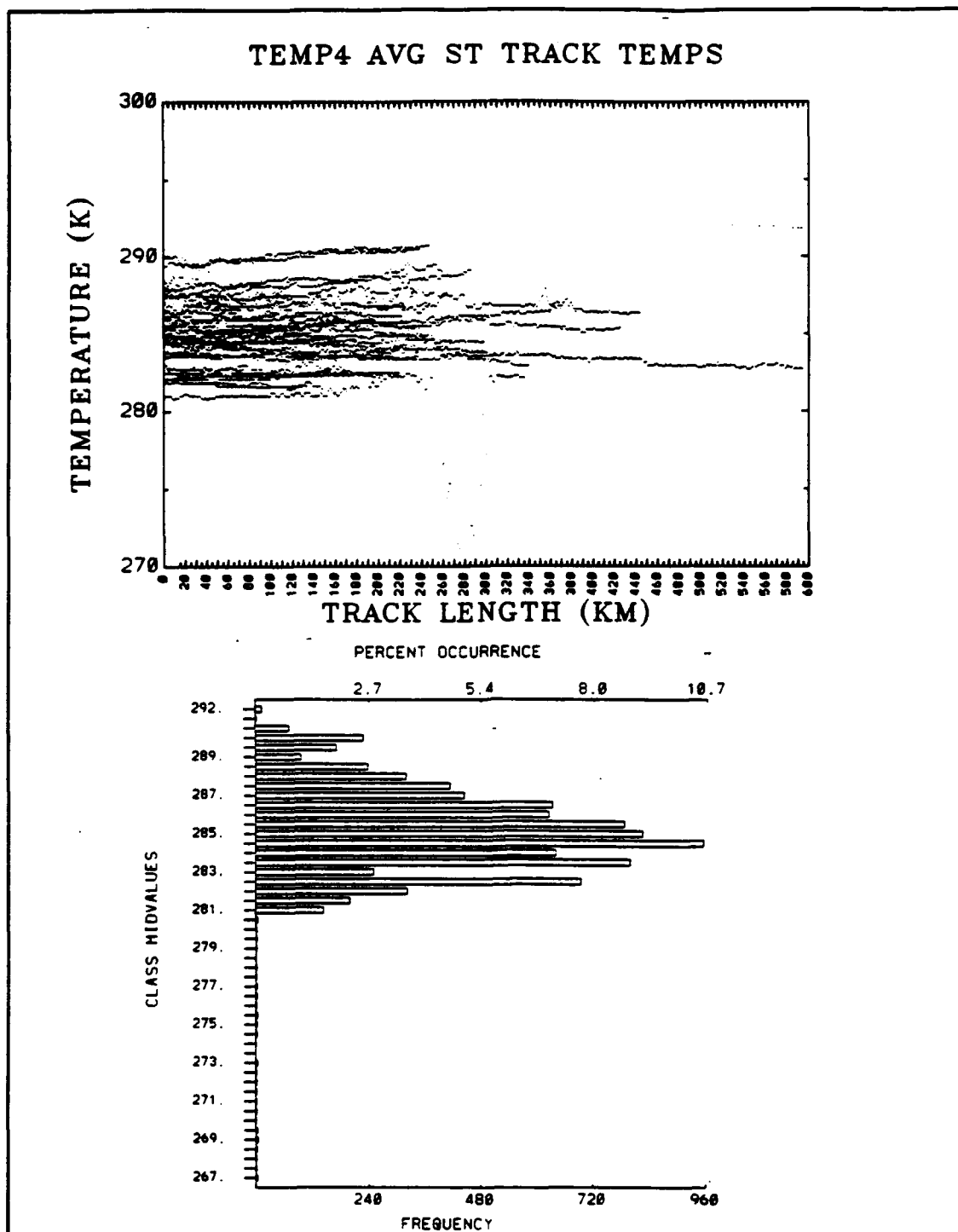
**Figure A11.** Scatterplot and Histogram for TMP4 Stratus Tracks.

# TMP4 PERCENT CHANGE TRACK/ST CLOUDS
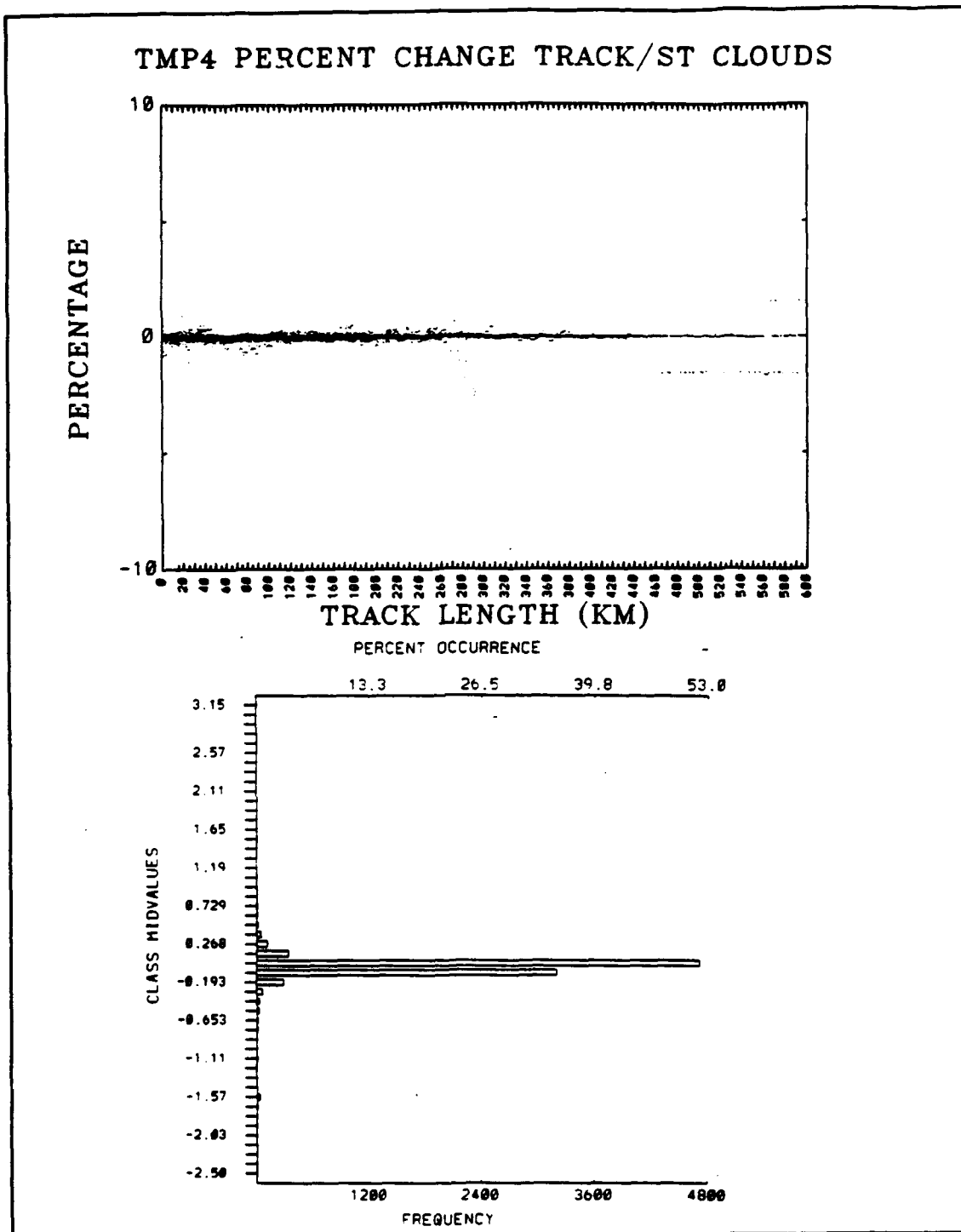


**Figure A12.** Scatterplot and Histogram for DPC TMP4 Track/Cloud.
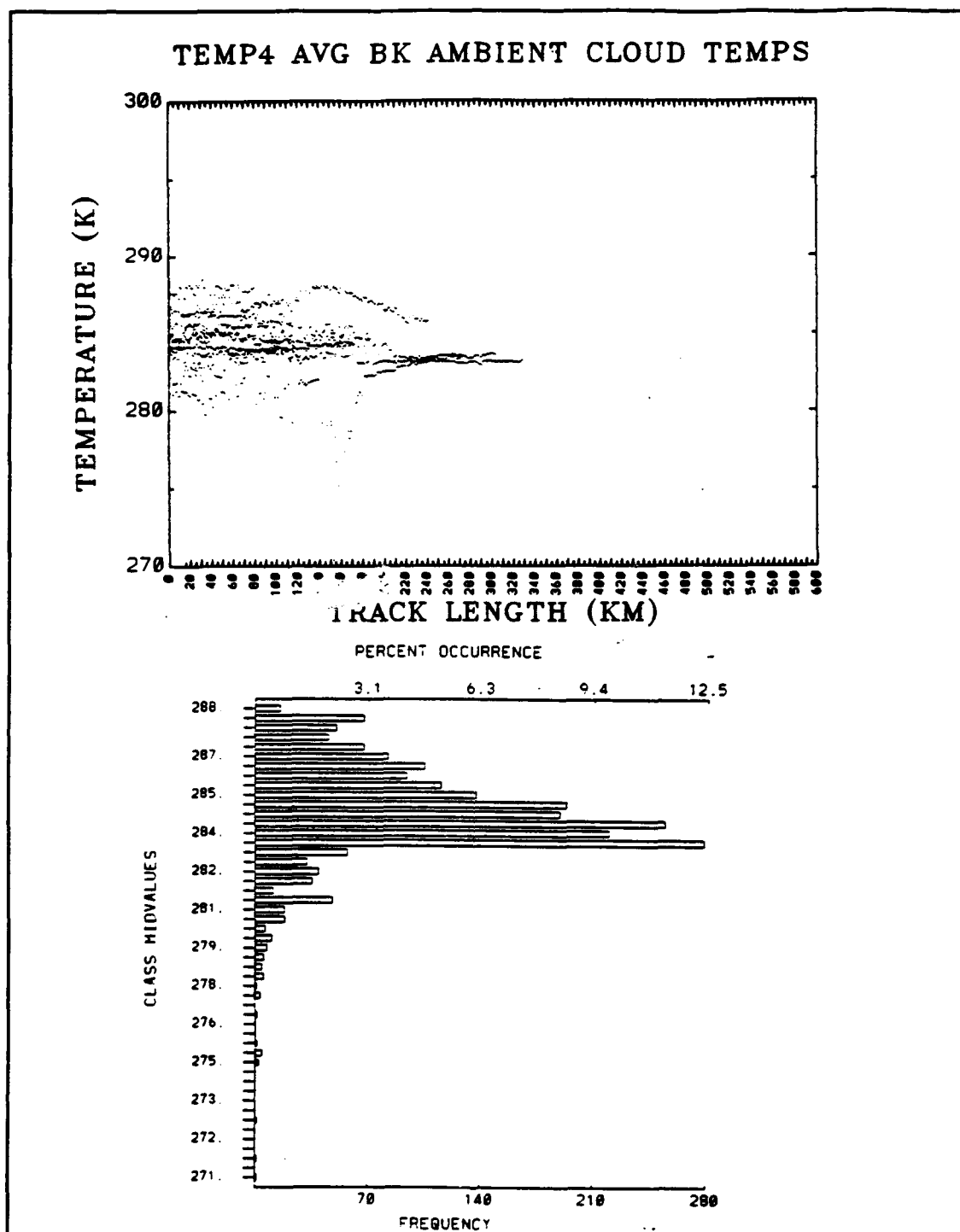
**Figure A13.** Scatterplot and Histogram for TMP4 Broken Stratus Clouds.
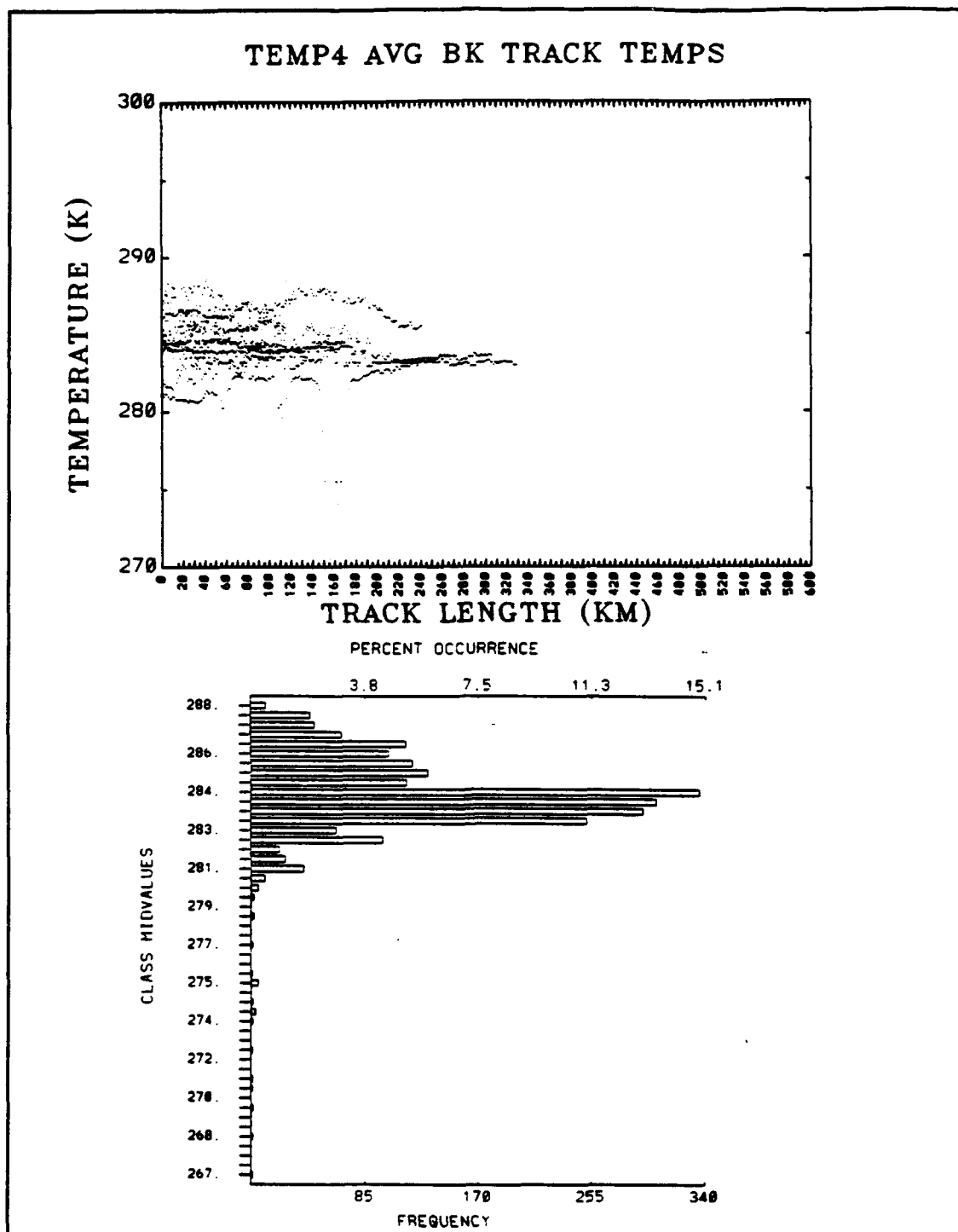
**Figure A14.** Scatterplot and Histogram for TMP4 Broken Stratus Tracks.
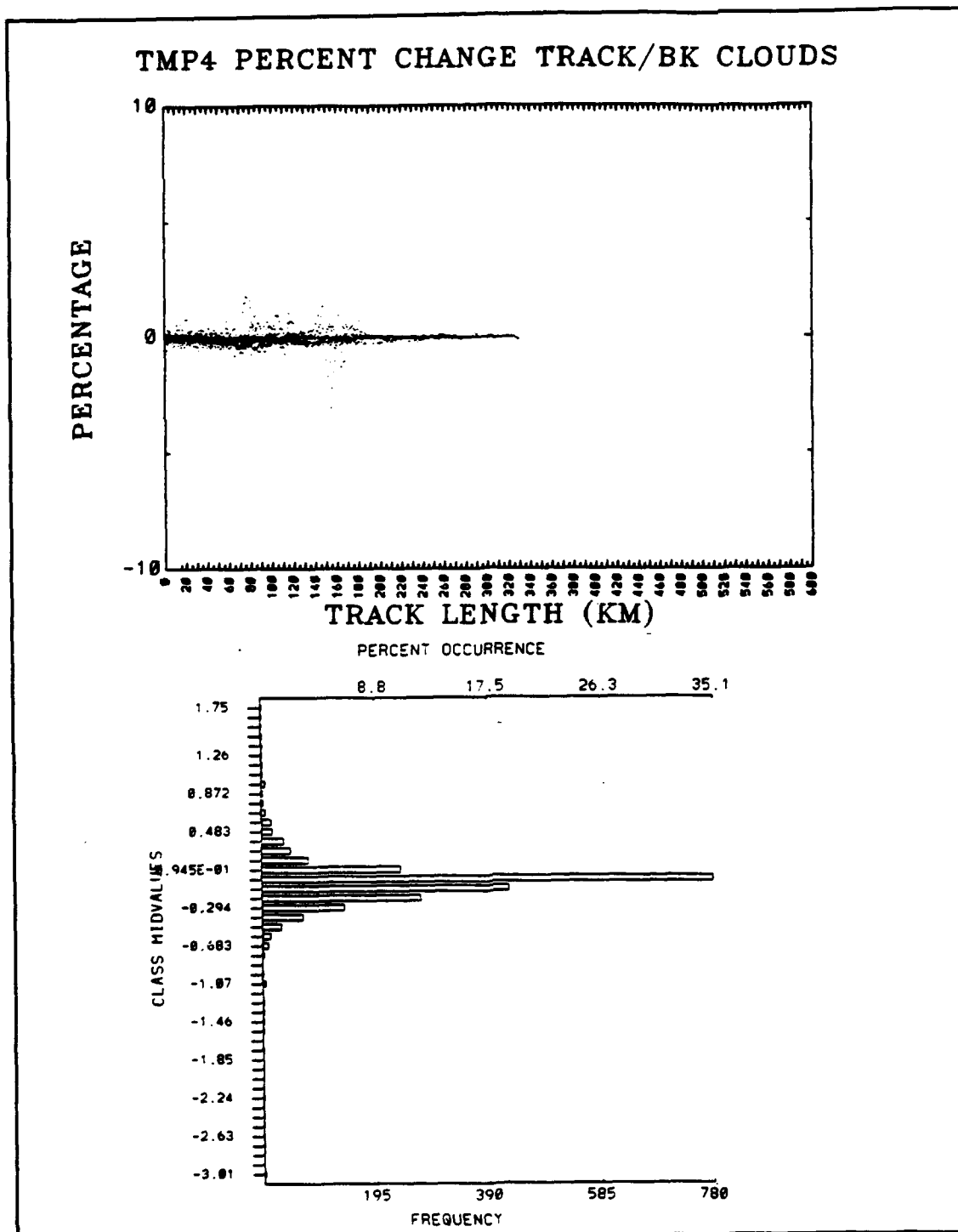
**Figure A15.** Scatterplot and Histogram DPC TMP4 Broken Stratus Track/Cloud.

77

# TEMP4 AVG CU AMBIENT CLOUD TEMPS
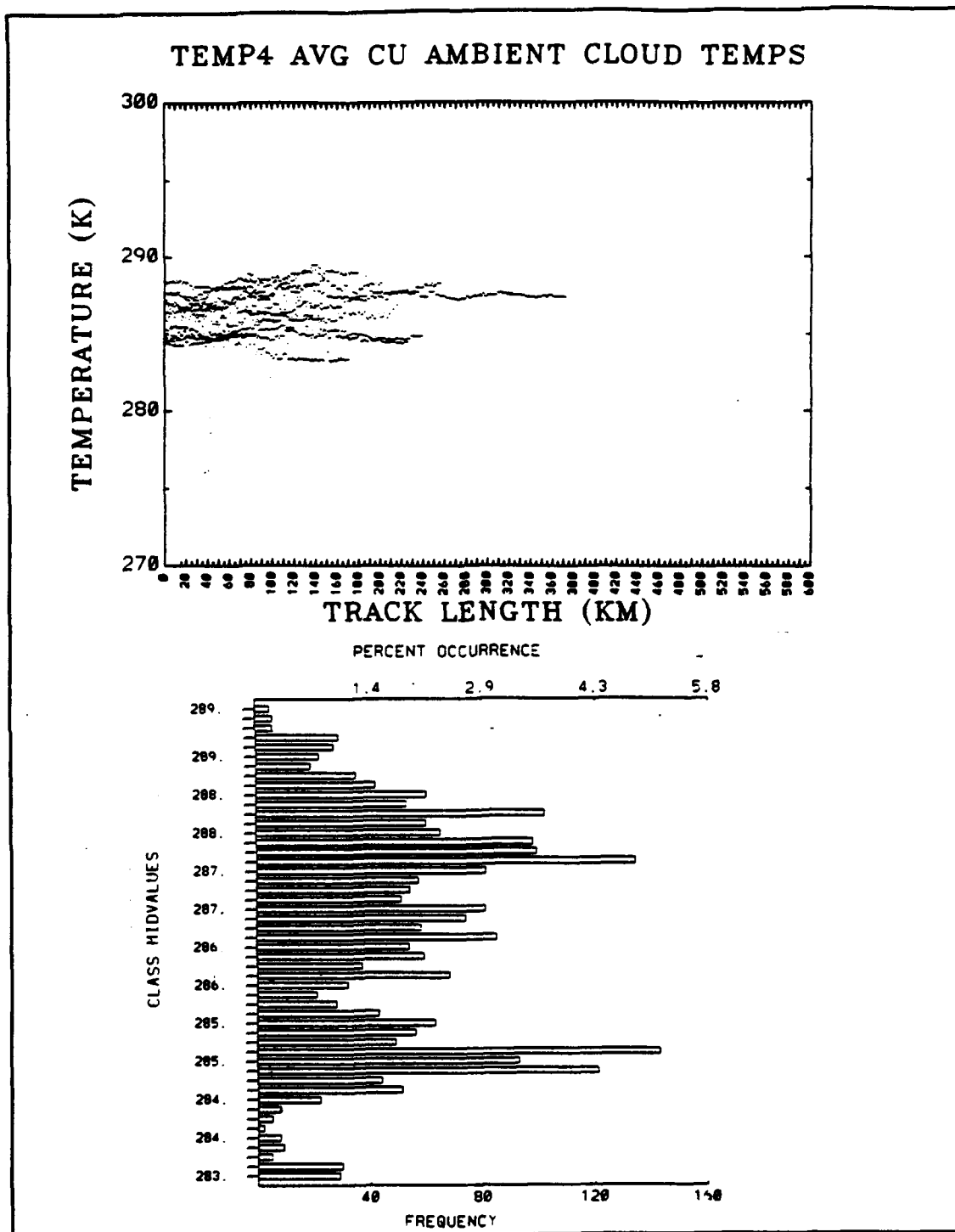


**Figure A16.** Scatterplot and Histogram for TMP4 Cumulus Cloud Regime.
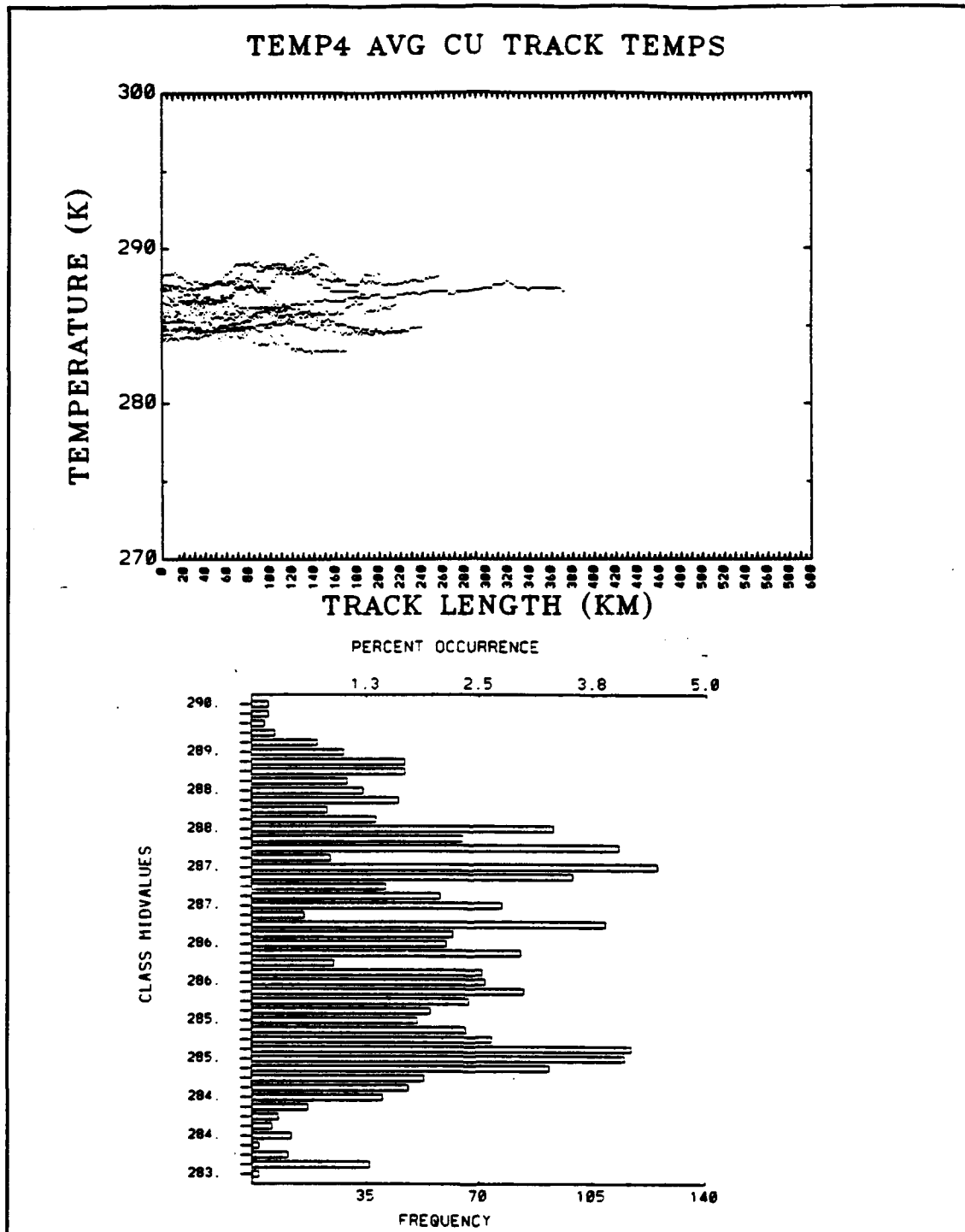
**Figure A17.** Scatterplot and Histogram for TMP4 Cumulus Tracks.

**Figure A18.** Scatterplot and Histogram for DPC TMP4 Cumulus Track/Cloud.

80

**Figure A19.** Scatterplot and Histogram for T45 Stratus Cloud Regime.

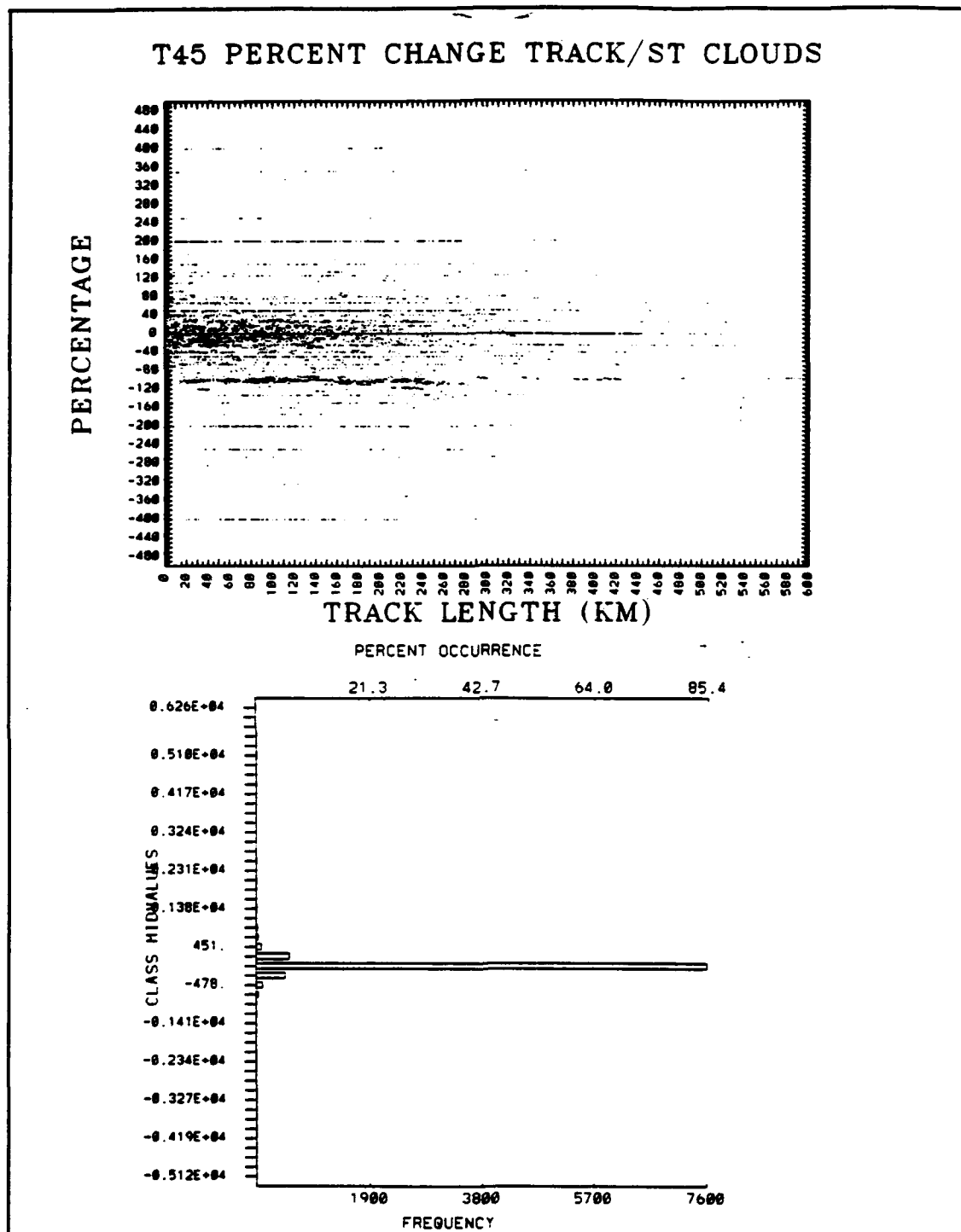**Figure A20.** Scatterplot and Histogram for T45 Stratus Track.

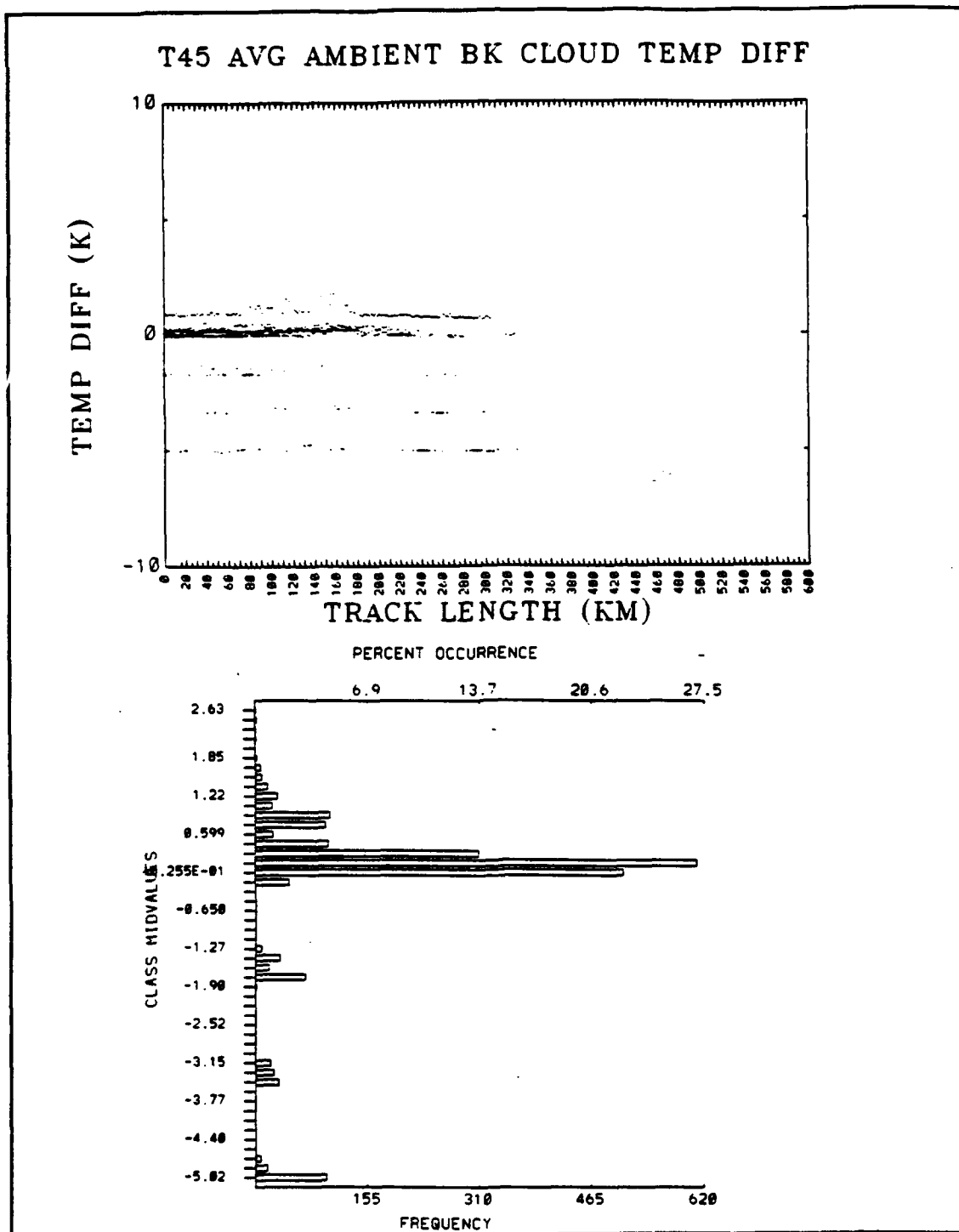**Figure A21.** Scatterplot and Histogram for DPC T45 Stratus Track/Cloud.

83

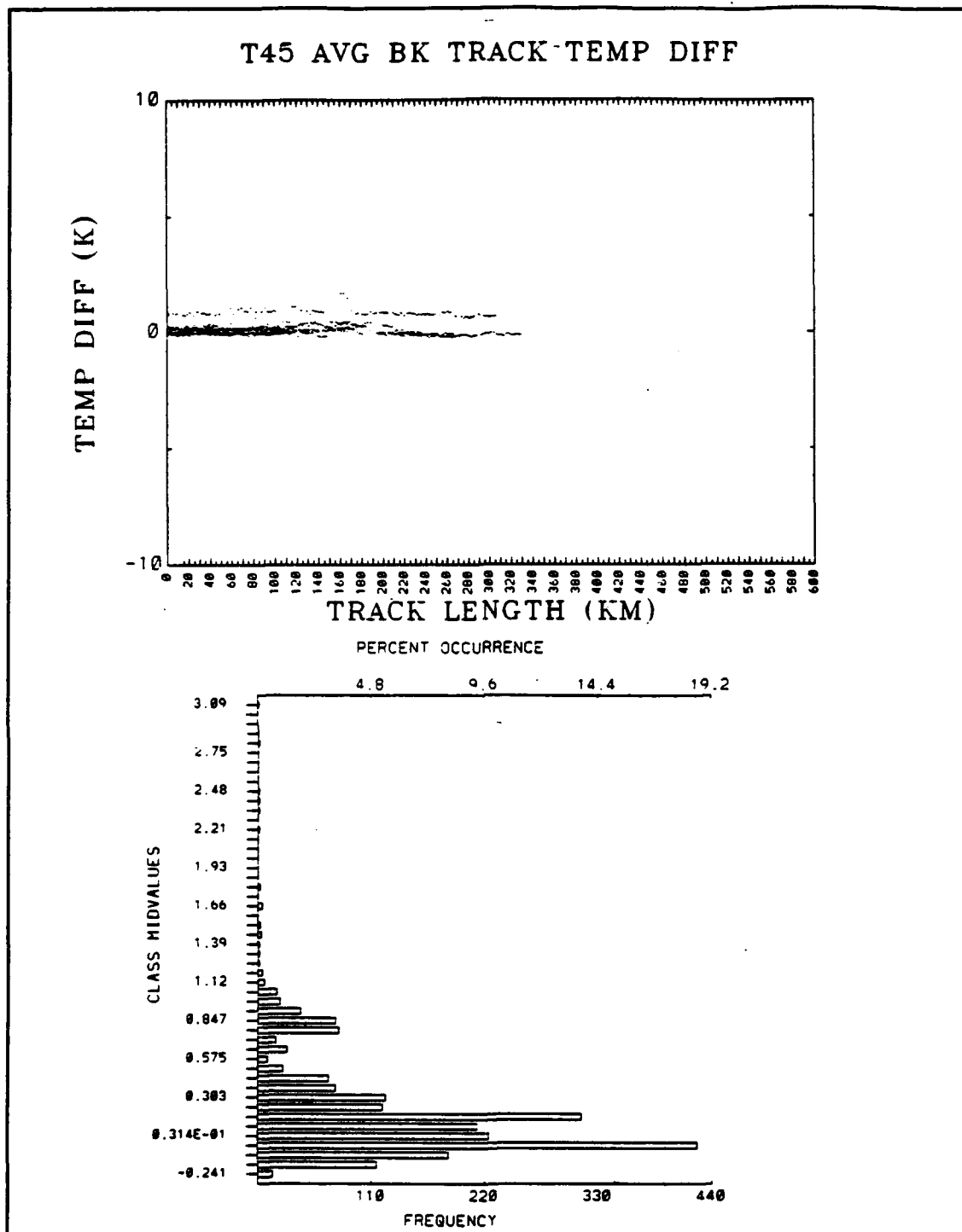**Figure A22.** Scatterplot and Histogram for T45 Broken Stratus Cloud Regime.

# T45 AVG BK TRACK TEMP DIFF



**Figure A23.** Scatterplot and Histogram for T45 Broken Stratus Tracks.
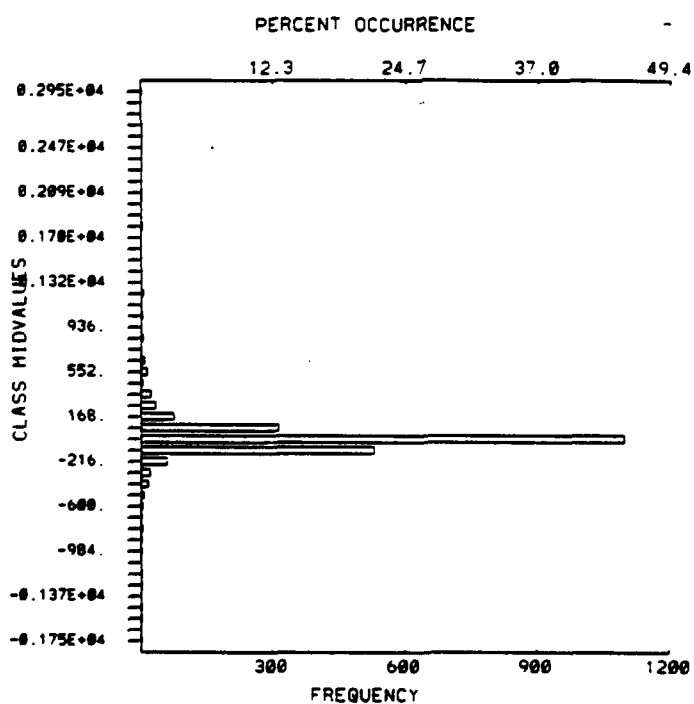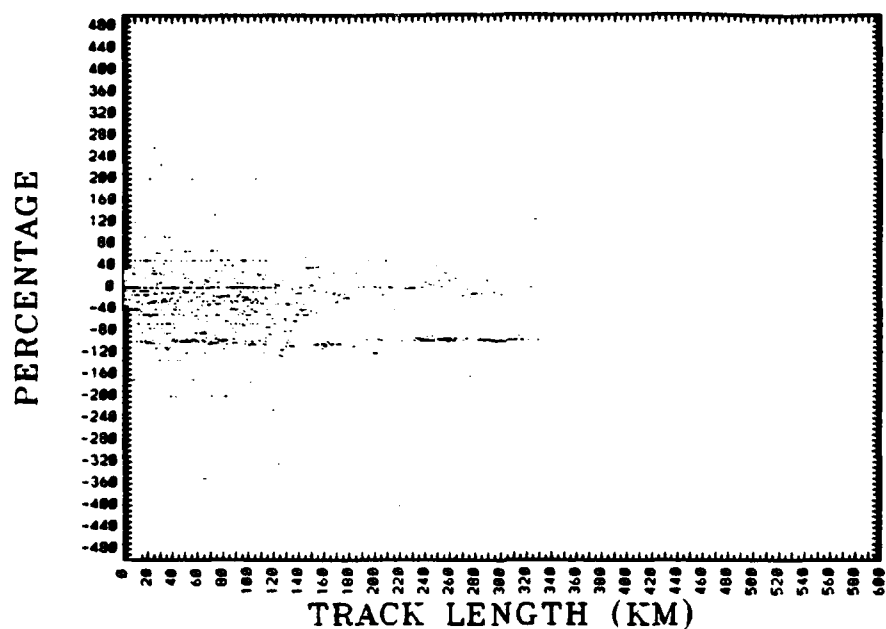
85

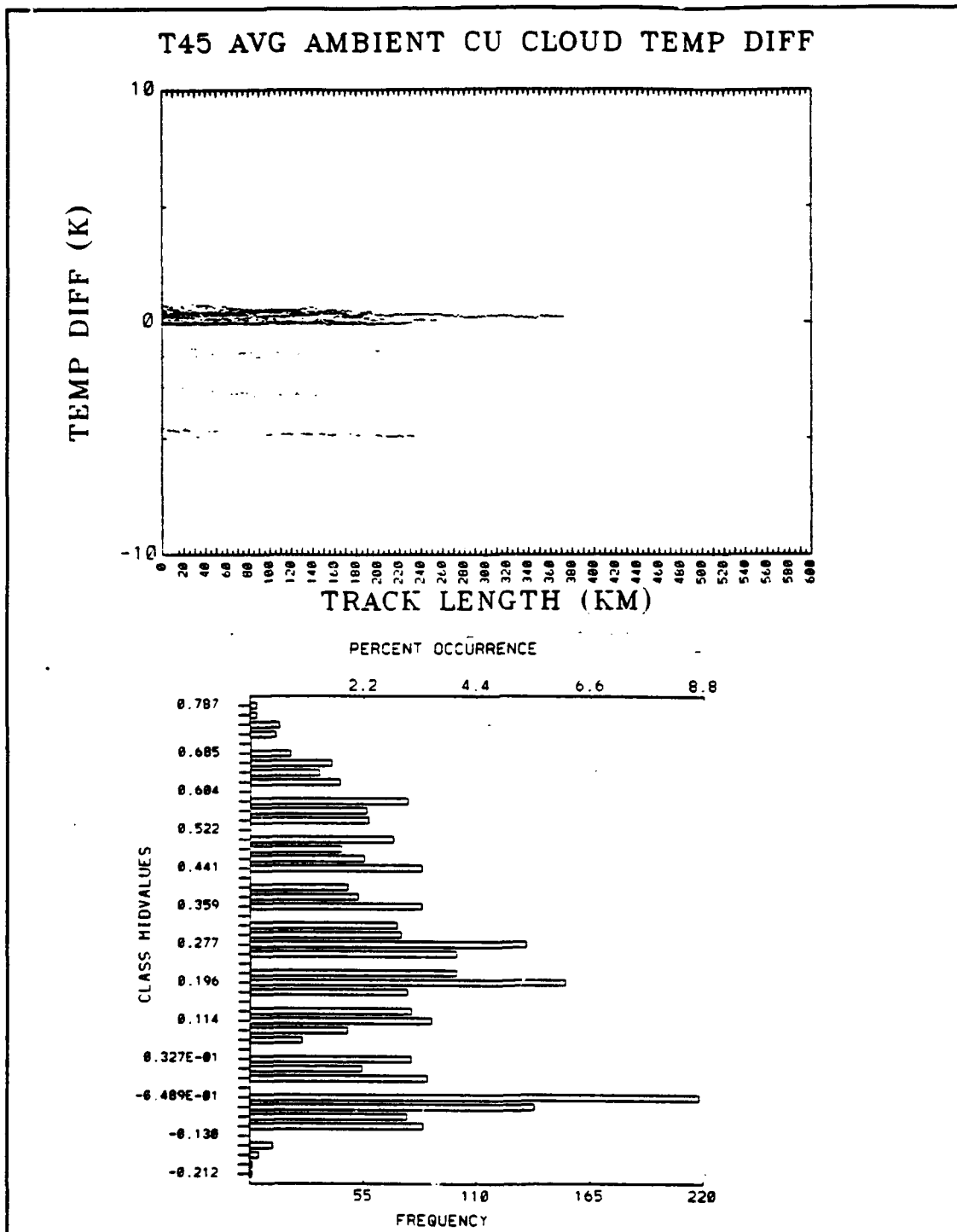**Figure A24.** Scatterplot and Histogram for DPC T45 Broken Stratus Track/Cloud.

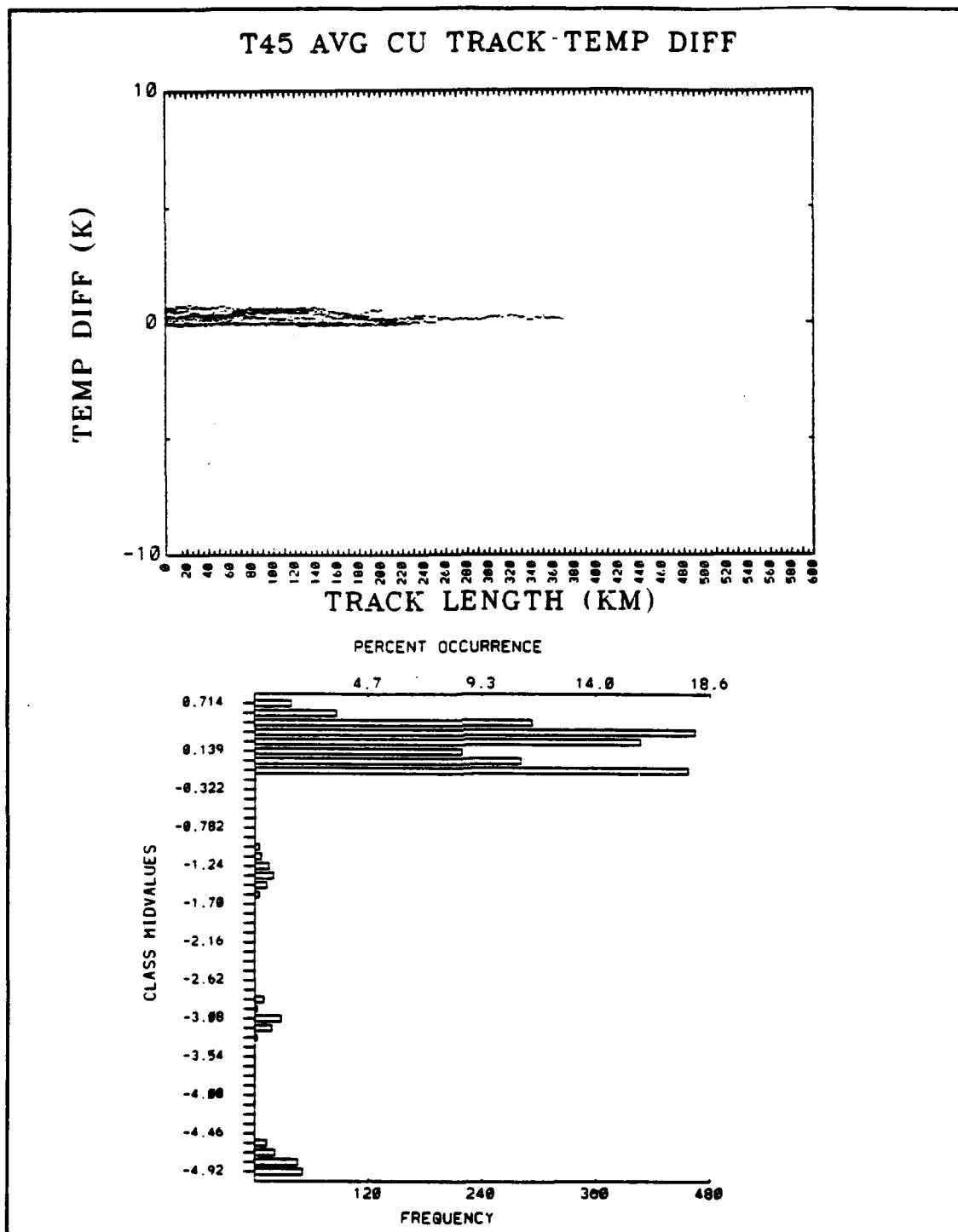**Figure A25.** Scatterplot and Histogram for T45 Cumulus Cloud Regime.

**Figure A26.** Scatterplot and Histogram for T45 Cumulus Tracks.
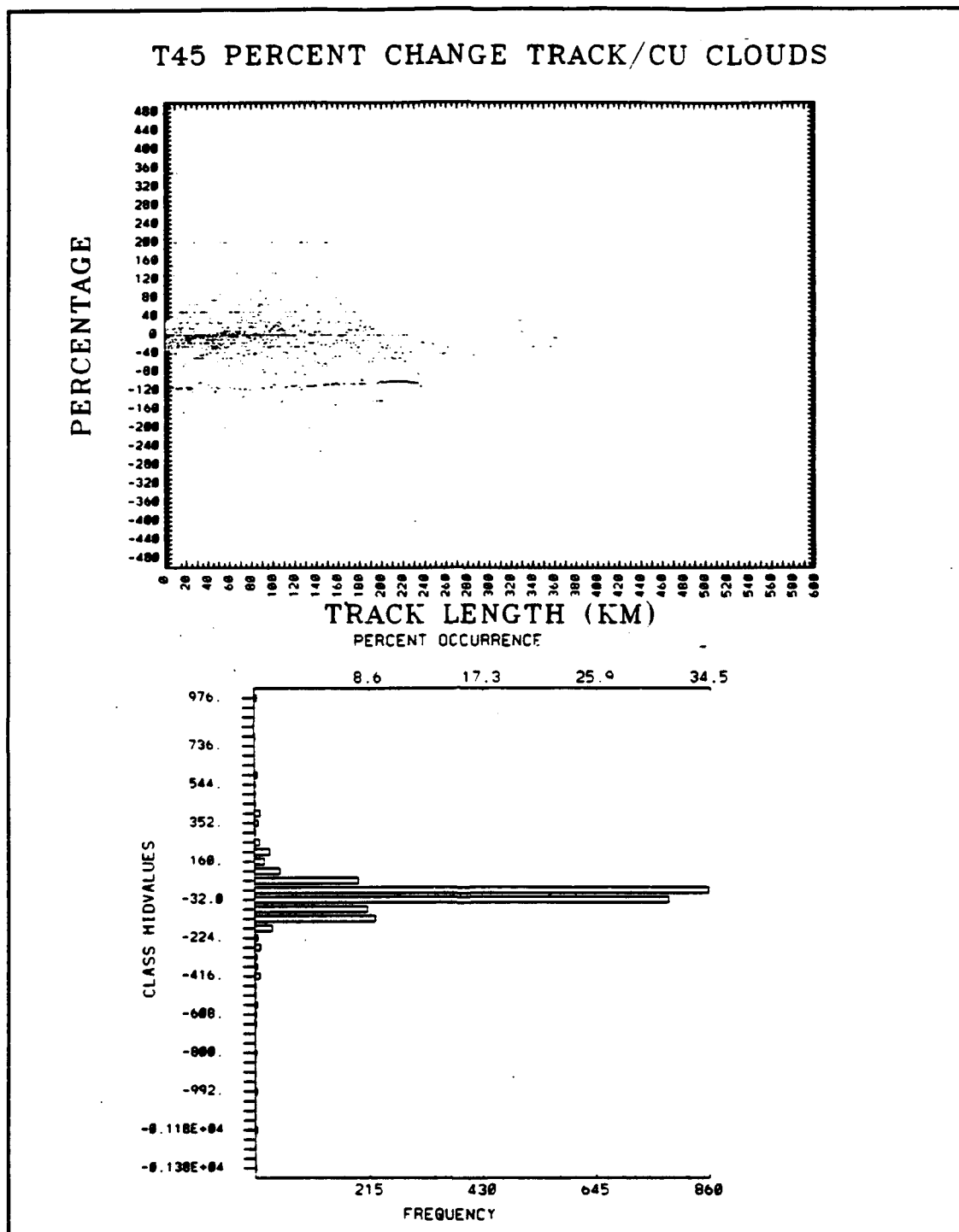
# T45 PERCENT CHANGE TRACK/CU CLOUDS



**Figure A27.** Scatterplot and Histogram for DPC T45 Cumulus Track/Cloud.

89

# LIST OF REFERENCES

Albrecht, B. A., D. A. Randall and S. Nicholls, 1988: Observations of marine stratocumulus during FIRE. *Bull. Amer. Meteor. Soc.*, **69**, 618-626.

Betts, A. K. and R. Boers, 1990: A cloudiness transition in a marine boundary layer, *J. Atmos. Sci.*, **47**, 1480-1497.

Brost, R. A., D. H. Lenschow and J. C. Wyngaard, 1982: Marine Stratocumulus layers. Part I: mean conditions. *J. Atmos. Science*, **39**, 800-817.

Calahan, R. F. and J. B. Snider, 1989 Marine stratocumulus structure, *Remote Sens. Environ.*, **28**, 95-107.

Coakley, J.A.Jr., R.L. Bernstein and P.A. Durkee, 1987: Effect ship-stack effuents on cloud reflectivity. *Science*, **237**, 1020-1022.

Hindman, E. E., 1990: Understanding ship-trail clouds. Preprints of 1990 Conference on Cloud Physics, July 23-27, 1990, San Francisco, Ca, A. M. S., Boston, Ma, 1990.

Hobbs, P. V., J. L. Stith and L. F. Radke, 1980: Cloud active nuclei from coal-fired power plants and their interaction with cloud. *J. Appl. Meteor*, **39**, 439-451.

Morehead, S. E., 1988: Ship track cloud analysis for the North Pacific area. M. S. Thesis, Naval Postgraduate School, Monterey, CA, September 1988, 57 pp.

Nielsen, K. E. and P. A. Durkee, 1992: A robust algorithm for locating ship track cloud features using 3.7 micron satellite data. Preprints of Sixth Conference on Satellite Meteorology and Oceanography, January 5-10, 1992, Atlanta, Ga, A. M. S. Boston, Ma, 1990

Paluch, I. R. and D. H. Lenschow, 1991: Stratiform cloud formation in the marine boundary layer, *J. Atmos. Sci.*, **48**, 2141-2158.

Radke, L. F., J. A. Coakley, Jr. and M. D. King, 1989: Direct and remote sensing observation of the effects of ship on clouds. *Science*, **246**, 1146-1149.

Snedecor, G. W. and W. G. Cochran; *Statistical Methods*, 6th ed., *Academic Press*, 1967.

# INITIAL DISTRIBUTION LIST

|  |  | No. Copies |
|---|---|---|
| 1. | Defense Technical Information Center<br>Cameron Station<br>Alexandria, VA 22304-6145 | 2 |
| 2. | Library, Code 0142<br>Naval Postgraduate School<br>Monterey, CA 93943-5002 | 2 |
| 3. | Chairman (Code 63Rd)<br>Department of Meteorology<br>Naval Postgraduate School<br>Monterey, CA 93943-5002 | 1 |
| 4. | Chairman (Code 68Co)<br>Department of Oceanography<br>Naval Postgraduate School<br>Monterey, CA 93943-5002 | 1 |
| 5. | Professor Philip A. Durkee (Code 63De)<br>Department of Meteorology<br>Naval Postgraduate School<br>Monterey, CA 93943-5002 | 2 |
| 6. | Professor Carlyle H. Wash (Code 63Wx)<br>Department of Meteorology<br>Naval Postgraduate School<br>Monterey, CA 93943-5002 | 1 |
| 7. | LT Michael E. Evans<br>NAVOCEANCOMDET NAS Memphis<br>Millington, TN 38053 | 3 |
| 8. | Director Naval Oceanography Division<br>Naval Observatory<br>34th and Massachusetts Avenue NW<br>Washington, DC 20390 | 1 |

9. Commander                                                      1
   Naval Oceanography Command
   NSTL Station
   Bay St. Louis, MS 39522

10. Chief of Naval Research                                        1
    800 North Quincy Street
    Arlington, VA 22217